

ฤทธิ์ทางชีวภาพของ 5-ไฮดรอกซี-3,7-ไดเมทอกซีฟลาโวน  
จาก *Kempferia parviflora* Wall. ex. Baker ใน *Saccharomyces cerevisiae*  
และเซลล์ไลน์มะเร็งตับของมนุษย์ HepG2

นางสาวณัฐนิช สนวนมะลิ

จุฬาลงกรณ์มหาวิทยาลัย  
CHULALONGKORN UNIVERSITY

บทคัดย่อและแฟ้มข้อมูลฉบับเต็มของวิทยานิพนธ์ตั้งแต่ปีการศึกษา 2554 ที่ให้บริการในคลังปัญญาจุฬาฯ (CUIR)  
เป็นแฟ้มข้อมูลของนิสิตเจ้าของวิทยานิพนธ์ ที่ส่งผ่านทางบัณฑิตวิทยาลัย

The abstract and full text of theses from the academic year 2011 in Chulalongkorn University Intellectual Repository (CUIR)  
are the thesis authors' files submitted through the University Graduate School.

วิทยานิพนธ์นี้เป็นส่วนหนึ่งของการศึกษาตามหลักสูตรปริญญาวิทยาศาสตรมหาบัณฑิต  
สาขาวิชาจุลชีววิทยาและเทคโนโลยีจุลินทรีย์ ภาควิชาจุลชีววิทยา  
คณะวิทยาศาสตร์ จุฬาลงกรณ์มหาวิทยาลัย  
ปีการศึกษา 2559  
ลิขสิทธิ์ของจุฬาลงกรณ์มหาวิทยาลัย

BIOLOGICAL ACTIVITY OF 5-HYDROXY-3,7-DIMETHOXYFLAVONE  
FROM *Kempferia parviflora* Wall. ex. Baker IN *Saccharomyces cerevisiae*  
AND HUMAN HEPATOMA CELL LINE HepG2

Miss Nattanich Suanmali



A Thesis Submitted in Partial Fulfillment of the Requirements  
for the Degree of Master of Science Program in Microbiology and Microbial  
Technology  
Department of Microbiology  
Faculty of Science  
Chulalongkorn University  
Academic Year 2016  
Copyright of Chulalongkorn University

Thesis Title	BIOLOGICAL ACTIVITY OF 5-HYDROXY-3,7-DIMETHOXYFLAVONE FROM <i>Kempferia parviflora</i> Wall. ex. Baker IN <i>Saccharomyces cerevisiae</i> AND HUMAN HEPATOMA CELL LINE HepG2
By	Miss Nattanich Suanmali
Field of Study	Microbiology and Microbial Technology
Thesis Advisor	Associate Professor Chulee Yompakdee, Ph.D.

---

Accepted by the Faculty of Science, Chulalongkorn University in Partial Fulfillment of the Requirements for the Master's Degree

..... Dean of the Faculty of Science  
(Associate Professor Polkit Sangvanich, Ph.D.)

THESIS COMMITTEE

..... Chairman  
(Assistant Professor Naraporn Somboonna, Ph.D.)

..... Thesis Advisor  
(Associate Professor Chulee Yompakdee, Ph.D.)

..... Examiner  
(Associate Professor Tanapat Palaga, Ph.D.)

..... External Examiner  
(Sittiruk Roytrakul, Ph.D.)

ณัฐนิช สวนมะลิ : ฤทธิ์ทางชีวภาพของ 5-ไฮดรอกซี-3,7-ไดเมทอกซีฟลาโวนจาก *Kempferia parviflora* Wall. ex. Baker ใน *Saccharomyces cerevisiae* และเซลล์ไลน์มะเร็งตับของมนุษย์ HepG2 (BIOLOGICAL ACTIVITY OF 5-HYDROXY-3,7-DIMETHOXYFLAVONE FROM *Kempferia parviflora* Wall. ex. Baker IN *Saccharomyces cerevisiae* AND HUMAN HEPATOMA CELL LINE HepG2) อ.ที่ปริกษาวิทยานิพนธ์หลัก: รศ. ดร.ชวลี ขมภักดี, 120 หน้า.

วิธีการส่งสัญญาณของแคลเซียมมีบทบาทสำคัญในการควบคุมกระบวนการทางชีวภาพต่างๆในสิ่งมีชีวิตชั้นสูง เนื่องจากขึ้นในยีสต์และมนุษย์มีการอนุรักษ์ที่สูง การค้นพบสารโมเลกุลขนาดเล็กที่ออกฤทธิ์ยับยั้งโปรตีนใดๆในยีสต์ จึงน่าที่จะออกฤทธิ์เช่นเดียวกันในมนุษย์ งานวิจัยก่อนหน้าได้ใช้ระบบคัดกรอง  $\Delta zds1$  yeast-based assay สามารถแยกได้สารบริสุทธิ์ 5-hydroxy-3,7-dimethoxyflavone (ในที่นี้ให้ชื่อว่า 5-OH-3,7-DMF) จากสารสกัดอย่างหยาบจากกระชายดำ ซึ่งมีฤทธิ์ยับยั้งวิธีการส่งสัญญาณแคลเซียมในยีสต์สายพันธุ์กลาย  $\Delta zds1$  (สายพันธุ์ YNS17) ในงานวิจัยนี้มุ่งหมายที่จะค้นหาฤทธิ์ทางชีวภาพที่เกี่ยวข้องในวิธีการส่งสัญญาณแคลเซียมของสาร 5-OH-3,7-DMF จากการใช้วิธีทางพันธุศาสตร์ในยีสต์สายพันธุ์กลายชนิดต่างๆ พบว่า *Mck1* เป็นโปรตีนโคเนสหนึ่งในวิธีการส่งสัญญาณแคลเซียม เป็นโมเลกุลเป้าหมายของสาร 5-OH-3,7-DMF ซึ่งยีน *MCK1* ในยีสต์มีความคล้ายคลึงกับยีนประมวลรหัสเอ็นไซม์ GSK-3 $\beta$  ในมนุษย์ ได้มีรายงานถึงความสัมพันธ์ระหว่างระดับ GSK-3 $\beta$  ที่สูงกับการเกิดพยาธิสภาพหลายประการ ได้แก่ โรคเบาหวานประเภท 2 และ โรคอัลไซเมอร์ เป็นต้น จากการทดสอบในหลอดทดลองพบว่า 5-OH-3,7-DMF มีฤทธิ์ยับยั้งแอกติวิตีของเอ็นไซม์ GSK-3 $\beta$  ที่ค่า  $IC_{50}$  เท่ากับ  $9.72 \pm 0.15$  ไมโครโมลาร์ คิดเป็น  $85.6 \pm 7.41$  เปอร์เซ็นต์การยับยั้งแอกติวิตีของเอ็นไซม์ จากการวาดกราฟ Dixon plot พบว่า สาร 5-OH-3,7-DMF ยับยั้งแอกติวิตีของเอ็นไซม์ GSK-3 $\beta$  ในรูปแบบ ATP-noncompetitive มีค่า  $K_i$  เท่ากับ 13.04 ไมโครโมลาร์ และในรูปแบบ Substrate competitive ด้วยค่า  $K_i$  เท่ากับ 53.92 ไมโครโมลาร์ จากการใช้เซลล์ไลน์มะเร็งตับชนิด HepG2 เป็นเซลล์ต้นแบบสำหรับภาวะการคือต่อฮอร์โมนอินซูลิน สารสกัดหยาบจากกระชายดำ และ 5-OH-3,7-DMF สามารถลดการแสดงออกของยีน *G6Pase* (ประมวลรหัสเอ็นไซม์กลูโคส 6 ฟอสฟาเทส) และ 5-OH-3,7-DMF สามารถทำให้เซลล์สังเคราะห์ไกลโคเจนได้สูงขึ้น โดยไปลดการเติมหมู่ฟอสเฟตให้กับโปรตีนไกลโคเจนซินเทส (GS) ส่งผลให้เกิดการสังเคราะห์ไกลโคเจนภายในเซลล์สูงขึ้น นอกจากนี้ยังพบว่า 5-OH-3,7-DMF สามารถลดระดับการเติมหมู่ฟอสเฟตที่ตำแหน่ง Tyr279/216 ของโปรตีน GSK3 ซึ่งเป็นการยับยั้งการกระตุ้นแอกติวิตีของโปรตีน GSK3 และ ยังไปเพิ่มระดับการเติมหมู่ฟอสเฟตที่ตำแหน่ง Ser21/9 ซึ่งเป็นการยับยั้งแอกติวิตีของโปรตีน GSK-3 ในการศึกษาี้แสดงให้เห็นว่าสาร 5-OH-3,7-DMF ที่มีอยู่ในส่วนสกัดหยาบจากกระชายดำ เป็นสารยับยั้งแอกติวิตีของเอ็นไซม์ GSK-3 ชนิดใหม่ โดยไปยับยั้งแอกติวิตีของเอ็นไซม์ GSK3 ส่งผลให้เพิ่มการสังเคราะห์ไกลโคเจนและอาจเป็นการรักษาระดับความสมดุลของน้ำตาลกลูโคสในร่างกาย ซึ่งสารมีความเป็นพิษต่ำ และมีศักยภาพนำไปพัฒนาเป็นยาเพื่อรักษาโรคเบาหวานประเภทที่ 2 ได้ในอนาคต

ภาควิชา จุลชีววิทยา ลายมือชื่อนิติติ .....

สาขาวิชา จุลชีววิทยาและเทคโนโลยีจุลินทรีย์ ลายมือชื่อ อ.ที่ปริกษาหลัก .....

# # 5771970423 : MAJOR MICROBIOLOGY AND MICROBIAL TECHNOLOGY

KEYWORDS: CALCIUM SIGNALING PATHWAYS / SACCHAROMYCES CEREVISIAE / KAEMPFERIA PARVIFLORA WALL. EX. BAKER / 5-HYDROXY-3,7-DIMETHOXYFLAVONE / MCK1 / INSULIN SIGNALING PATHWAY / HEPG2 CELLS / TYPE 2 DIABETES / GSK-3

NATTANICH SUANMALI: BIOLOGICAL ACTIVITY OF 5-HYDROXY-3,7-DIMETHOXYFLAVONE FROM *Kempferia parviflora* Wall. ex. Baker IN *Saccharomyces cerevisiae* AND HUMAN HEPATOMA CELL LINE HepG2. ADVISOR: ASSOC. PROF. CHULEE YOMPAKDEE, Ph.D., 120 pp.

Calcium signaling pathways play important roles in regulation of cellular processes in eukaryotes ranging from yeast to human. Because of the high degree in gene conservation from yeast to human, the small molecule inhibitors effectively function in yeast might exert their function in human as well. Our previous studies using a  $\Delta zds1$  yeast-based assay could identified a flavonoid 5-hydroxy-3,7-dimethoxyflavone (5-OH-3,7-DMF) from *Kaempferia parviflora* Wall. Ex. Baker showed inhibitory activity against the  $Ca^{2+}$ -signals in the mutant yeast YNS17 strain ( $\Delta zds1$ ). This study aimed to investigate biological activity of 5-OH-3,7-DMF related to calcium signaling pathways. Genetic analyses in several mutant yeast strains showed that Mck1, a protein kinase in the calcium signaling pathway, was the molecular target of the 5-OH-3,7-DMF. Yeast *MCK1* is an ortholog *GSK-3 $\beta$*  gene coding for glycogen synthase kinase-3 $\beta$  in human. There were many reports on the relationship between high expression level of GSK-3 $\beta$  and several pathogenesis including type 2 Diabetes and Alzheimer's disease. 5-OH-3,7-DMF showed *in vitro* inhibitory activity against GSK-3 $\beta$  with an  $IC_{50}$  values of  $9.72 \pm 0.15 \mu M$  with  $85.6 \pm 7.41 \%$  of inhibition. Interestingly, 5-OH-3,7-DMF showed ATP non-competitive binding mode to GSK-3 $\beta$  by Dixon plot ( $K_i = 13.04 \mu M$ ) and substrate competitive binding mode to GSK-3 $\beta$  by Dixon plot ( $K_i = 53.92 \mu M$ ). The treatment of insulin-resistant HepG2 cells model with crude extracted of *K. parviflora* (CE) or 5-OH-3,7-DMF caused a decrease in *G6Pase* gene expression and only 5-OH-3,7-DMF could recover glycogen levels through decreasing phosphorylation of glycogen synthase (GS) protein. Moreover, when the cells grown in high glucose-high insulin (HGHI) medium treated with 5-OH-37-DMF, phosphorylation of GSK-3 was abolished as comparable values to those of controls (LiCl and GSK-3 $\beta$  inhibitor I). These findings indicated that 5-OH-3,7-DMF might be a potential GSK-3 inhibitor that modulates the glucose homeostasis and might be potential for type II diabetes drug development.

Department: Microbiology Student's Signature .....

Field of Study: Microbiology and Microbial Technology Advisor's Signature .....

Academic Year: 2016

## ACKNOWLEDGEMENTS

I felt grateful appreciation to my thesis advisor, Associate Professor Chulee Yompakdee, Ph.D. for her helpful suggestion, guidance, with great kindness throughout my research study. In addition, I also express my appreciation to all thesis committee, Assistant Professor Naraporn Somboonna, Ph.D., Associate Professor Tanapat Palaga, Ph.D. and Sittiruk Roytrakul, Ph.D. for their helpful suggestion, comments, and correction as thesis examiners.

I thanked Emeritus Professor Tokichi Miyakawa, Department of Molecular Biotechnology, Hiroshima University for his kind help, suggestions and encouragement throughout my research. Furthermore, I would like to thank Ms. Anyaporn Sangkaew, Ms. Orrarat Sangkaew and Mr. Jumpol Sopanaporn for their constructive advice and encouragement. I would like to thank all of 2017 laboratory members for their suggestion and Department of Microbiology, Faculty of Science, Chulalongkorn University. Thai Government Annual Budget Fund for fiscal year 2015, Ratchadaphiseksomphot Endowment Fund of Chulalongkorn University (NRU59-058-AS) and the 90th Anniversary of Chulalongkorn University Fund for were grateful thank financial support on my research.

Finally, I was thankful to my families, who have shown the great patience, moral support, financial support and encouragement in every way possible to enable me to succeed in the education.

## CONTENTS

	Page
THAI ABSTRACT .....	iv
ENGLISH ABSTRACT.....	v
ACKNOWLEDGEMENTS .....	vi
CONTENTS.....	vii
LIST OF TABLES .....	xi
LIST OF FIGURES .....	xii
CHAPTER I INTRODUCTION.....	14
1.1 Research methodologies .....	17
1.2 Expected outcomes .....	18
CHAPTER II LITERATURE REVIEWS .....	19
2.1 Literature reviews of <i>Kaempferia parviflora</i> Wall. ex Baker.....	19
2.2 Calcium signaling pathways in <i>S. cerevisiae</i> .....	23
2.3 Yeast <i>MCK1</i> , a human ortholog <i>GSK-3</i> gene which encodes glycogen synthase kinase-3 family protein kinase.....	27
2.4 Role of GSK-3 in insulin resistance and type 2 diabetes.....	30
2.5 GSK-3 inhibitors: Therapeutic targets for type 2 diabetes Mellitus.....	33
CHAPTER III RESEARCH METHODOLOGY .....	37
3.1 Instruments used in this thesis .....	37
3.2 Chemicals .....	39
3.3 Primer sequences and conditions used in real-time PCR (RT-PCR).....	42
3.4 Antibody for Western blot analysis .....	42
3.5 Yeast strains and cultivation .....	43
3.6 Source of 5-hydroxy-3,7-dimethoxyflavone .....	44
3.6 Effect of 5-OH-3,7-DMF on growth of $\Delta zds1$ cells (YNS17 strain).....	44
3.7 Effect of 5-OH-3,7-DMF on $\Delta zds1$ cells overexpressed calcineurin (YRC1 strain).....	44
3.8 Effect of 5-OH-3,7-DMF on $\Delta zds1$ cells overexpressed Swe1 (YRC2 strain) .	45
3.9 Effect of 5-OH-3,7-DMF on $\Delta zds1$ cells overexpressed Mpk1 (NSC1 strain) .	45

	Page
3.10 Effect of 5-OH-3,7-DMF on $\Delta zds1$ cells overexpressed Mck1 (NSC2 strain).....	45
3.11 <i>In vitro</i> GSK-3 $\beta$ activity assay .....	46
3.11.1 Kinase-Glo <sup>®</sup> luminescent kinase assay platform.....	46
3.12 Optimization of GSK-3 $\beta$ kinase Reaction Conditions.....	46
3.12.1 ATP standard curve .....	47
3.12.2 Determination of optimal substrate concentration .....	47
3.13 Determination of the GSK-3 $\beta$ enzyme activity .....	48
3.14 Determination of the $K_m$ and $V_{max}$ of GSK-3 $\beta$ enzyme .....	48
3.15 Determination of $IC_{50}$ value and percentage of inhibition of 5-OH-3,7-DMF in inhibitory activity of human GSK-3 $\beta$ .....	49
3.16 Determination of the inhibition pattern of 5-OH-3,7-DMF on human GSK-3 $\beta$ protein.....	50
3.17 Human cancer cell line .....	50
3.18 Cell culture.....	50
3.19 Cell subculturing of HepG2 (adherent cells) .....	51
3.20 Cryopreservation procedure.....	51
3.21 Recovery of cryopreserved cells.....	51
3.22 Trypan blue dye exclusion test .....	52
3.23 MTT viability assay .....	52
3.24 Insulin-resistant HepG2 cell model (IRM) .....	53
3.25 Effect of 5-OH-3,7-DMF on insulin-resistant HepG2 cell model.....	53
3.26 Determination of glycogen content .....	54
3.27 Western blot analysis .....	55
3.27.1 Preparation of protein extract from HepG2 cells .....	55
3.27.2 Protein determination by BCA assay .....	55
3.27.3 SDS-polyacrylamide gel electrophoresis (SDS-PAGE).....	55
3.27.4 Western Blot Analysis.....	56
3.28 Determination of G6Pase expression by real-time PCR.....	56



	Page
3.28.1 RNA extraction.....	56
3.28.2 Generate complementary DNA (cDNA) by reverse transcriptase .....	57
3.28.3 One-step real time polymerase chain reaction (RT-PCR).....	57
3.29 Statistical analysis.....	58
CHAPTER IV RESULTS.....	59
4.1 5-OH-3,7-DMF could restore growth defect and abnormal bud morphology of on growth of $\Delta zds1$ cells (YNS17 strain).....	59
4.2 5-OH-3,7-DMF targeted MPK1 MAPK cascade of the $Ca^{2+}$ -signaling pathways due to restored growth defect and abnormal bud morphology of $\Delta zds1$ cells overexpressed <i>MPK1</i> gene (NSC1 strain) but did not inhibit the pathways via calcineurin pathway.....	61
4.3 Mck1, human ortholog GSK3, a potential molecular target of 5-OH-3,7- DMF in the $Ca^{2+}$ -signaling pathways.....	64
4.4 5-OH-3,7-DMF could not restore the growth defect of $\Delta zds1$ cells overexpressed <i>SWE1</i> of the $Ca^{2+}$ -signaling pathway.....	66
4.5 Kinase-Glo <sup>®</sup> Luminescent Kinase Assay Platform .....	68
4.5.1 Optimizing kinase reaction conditions .....	69
ATP standard curve .....	69
Optimized substrate concentration .....	70
Optimized amount of kinase.....	71
Determining the enzyme activity .....	72
The $K_m$ and $V_{max}$ of enzyme kinase .....	73
4.5.2 <i>In vitro</i> GSK-3 $\beta$ activity assay of 5-OH-3,7-DMF .....	74
4.5.3 5-OH-3,7-DMF is an ATP non-competitive but substrate competitive GSK-3 $\beta$ inhibitor.....	75
4.6 Study of cytotoxic effect of crude extracted of <i>K. parviflora</i> and 5-OH-3,7- DMF in HepG2 cell lines.....	77
4.7 Study on insulin-resistant condition induced hepatic gluconeogenesis on the expression of Glucose-6-phosphatase.....	79
4.8 5-OH-3,7-DMF could recover glycogen level in insulin-resistant HepG2 cells through inhibition phosphorylation of glycogen synthase protein (GS)....	81

	Page
4.9 5-OH-3,7-DMF abolished the impairment of insulin signaling in insulin-resistant HepG2 cells model via down regulation of GSK-3. ....	84
CHAPTER V DISCUSSION AND CONCLUSION .....	88
5.1 Discussion.....	88
5.2 Conclusion .....	93
REFERENCES .....	95
APPENDIX.....	109
APPENDIX A Media preparation .....	110
APPENDIX B The chemical preparation .....	114
APPENDIX C THE GLYCOGEN STANDARD CURVE.....	119
VITA.....	120



## LIST OF TABLES

	Page
<b>Table 2.1</b> GSK-3 $\beta$ Inhibitors under clinical Investigation .....	34
<b>Table 3.1</b> Primer sequences and conditions used in real-time PCR (RT-PCR) .....	42
<b>Table 3.2</b> Antibody for Western blot analysis.....	42
<b>Table 3.3</b> <i>S. cerevisiae</i> strains used in this study .....	43
<b>Table 3.4</b> Components and reagents for real time polymerase chain reaction (RT-PCR).....	58



## LIST OF FIGURES

	Page
<b>Figure 1.1</b> The outline of the signaling pathway by which insulin inhibits GSK-3 and stimulates glycogen synthase (Cohen and Goedert 2004). .....	15
<b>Figure 2.1</b> The characteristics of <i>Kaempferia Parviflora</i> Wall. Ex. Baker .....	19
<b>Figure 2.2</b> Chemical structures of the 11 <i>Kaempferia Parviflora</i> flavonoids.....	22
<b>Figure 2.3</b> Model for the Ca <sup>2+</sup> -activated signaling pathways .....	26
<b>Figure 2.4</b> Model structure of GSK-3 $\beta$ and schematic representations of mammalian GSK-3 $\alpha$ and GSK-3 $\beta$ . .....	28
<b>Figure 2.5</b> The insulin signaling pathway .....	31
<b>Figure 2.6</b> The reaction catalyzed by protein kinases and the general principle of ATP-competitive inhibitors and ATP-noncompetitive inhibitors of protein kinases. .	33
<b>Figure 2.7</b> The chemical structures of SB-216763 and SB-415286 .....	36
<b>Figure 3. 1</b> The Kinase-Glo® Assay reactions .....	46
<b>Figure 4.1</b> The effect of 5-OH-3,7-DMF on the growth of $\Delta zds1$ mutant yeast YNS17 cells. ....	60
<b>Figure 4.2</b> The effect of 5-OH-3,7-DMF on the growth of $\Delta zds1$ cells overexpressed <i>CMP2<math>\Delta</math>C</i> .....	62
<b>Figure 4.3</b> The effect of 5-OH-3,7-DMF on the growth of $\Delta zds1$ cells overexpressed <i>MPK1</i> . ....	63
<b>Figure 4.4</b> The effect of 5-OH-3,7-DMF on the growth of $\Delta zds1$ cells overexpressed <i>MCK1</i> . ....	65
<b>Figure 4.5</b> The effect of 5-OH-3,7-DMF on the growth of $\Delta zds1$ cells overexpressed <i>SWE1</i> .....	67
<b>Figure 4.6</b> A linear relationship exists between the luminescent signal measured and the ATP concentration.....	69
<b>Figure 4.7</b> A curve of enzyme activity relationship exists between the relative luminescent signal measured and the peptide kinase substrate concentration.....	70
<b>Figure 4.8</b> A curve of enzyme activity relationship exists between the relative luminescent signal measured and the human GSK-3 $\beta$ active enzyme concentration.....	71

<b>Figure 4.9</b> A curve of enzyme activity relationship exists between the relative luminescent signals measured and times .....	72
<b>Figure 4.10</b> A linear curve fitted of enzyme activity relationship exists between the relative luminescent signals. ....	72
<b>Figure 4.11</b> A curve of Michaelis-Menten and Lineweaver-Burk .....	73
<b>Figure 4.12</b> IC <sub>50</sub> determination of <i>in vitro</i> GSK-3 $\beta$ activity inhibition of 5-OH-3,7-DMF and GSK-3 $\beta$ inhibitor I .....	74
<b>Figure 4.13</b> Percentage inhibition of GSK-3 $\beta$ enzyme activity by 5-OH-3,7-DMF. .	75
<b>Figure 4.14</b> Dixon plot of 5-OH-3,7-DMF against human GSK-3 $\beta$ activity.....	76
<b>Figure 4.15</b> Cytotoxicity of CE, 5-OH-3,7-DMF, GSK-3 $\beta$ Inhibitor I and LiCl on human hepatoma HepG2 cell lines. ....	78
<b>Figure 4.16</b> Effect of CE and 5-OH-3,7-DMF on the expression of G6Pase. ....	80
<b>Figure 4.17</b> Effect of CE and 5-OH-3,7-DMF on the expression of Glycogen synthase (GS) .....	82
<b>Figure 4.18</b> Effect of CE and 5-OH-3,7-DMF on recovery of glycogen synthesis ....	83
<b>Figure 4.19</b> Effect of CE and 5-OH-3,7-DMF on the phosphorylation of GSK-3 .....	87
<b>Figure 5.1</b> Proposed model on mechanism of 5-OH-3,7-DMF on inhibitory activity of GSK-3 in insulin-resistant HepG2 cell model .....	93

## CHAPTER I

### INTRODUCTION

Diabetes is one of the largest global health emergencies of the 21<sup>st</sup> century. Each year more and more people live with this condition, which occurred in developing countries due to rapid and ongoing socioeconomic transition in life-changing complications. In 2013, the International Diabetes Federation (IDF) estimated that 382 million people had diabetes worldwide, and by 2035, this was predicted to rise to 592 million. Eighty percent live in low- and middle-income countries, and of the total, more than 60% live in Asia, with almost one-third in China (Nanditha et al. 2016). In addition, the current status of diabetes was 78.3 million people in South East Asia as well as Thailand (~ 4 million people) by year 2015 (International Diabetes Federation, 2015). The prevalence of both type I (T1DM) and type 2 diabetes (T2DM) has increased significantly during recent decades. Although, T2DM being much more common, has been the main driver for the increase in global diabetes prevalence (Guariguata et al. 2014).

Type 2 or non-insulin-dependent diabetes mellitus (NIDDM), which accounts for ~90% of all cases of this disease, is characterized by insulin resistance. That is, an inability of the tissues to respond to the insulin hormone that higher-than-normal concentrations of insulin are required to maintain normoglycemia (DeFronzo et al. 2014). Insulin is a hormone produced in the pancreas. It is required to transport glucose from the bloodstream into the body's cells where it is used as energy. In this pathology, the liver plays an importance role in the control of the whole body metabolism of energy nutrients (Klover and Mooney 2004). The lack, or ineffectiveness, of insulin in a person with diabetes result in remained glucose circulating in the blood. Over time, this organ is not able to control glucose homeostasis. There is a miss-regulation of the insulin pathway resulting in high levels of glucose in the blood (known as hyperglycemia). The hyperglycemia causes damage to many tissues in the body, leading to the development of classical symptoms of polyuria (frequent urination), polydipsia (increased thirst) and polyphagia (increased hunger) (Gardner et al. 2011). At the cellular level, insulin binds and activates the insulin receptor (IR) by phosphorylating key tyrosine residues. This is followed by

tyrosine phosphorylation of insulin receptor substrates (IRS) and subsequent activation of the phosphatidylinositol 3-kinase (PI3K)/protein kinase B (PKB/AKT) pathway. AKT stimulation leads to the inhibition of glycogen synthase kinase-3 (GSK-3) by phosphorylation. This leads to dephosphorylation of substrates of GSK3 including glycogen synthase (GS) due to glycogen synthesis activation (**Figure 1.1**) (Cohen and Frame 2001). The insufficient strength of insulin signaling altered the final substrates of insulin action involved in multiple metabolic and mitogenic aspects of cellular function such as high activated glycogen synthase kinase 3 (GSK-3) protein (Ginsberg 2000).

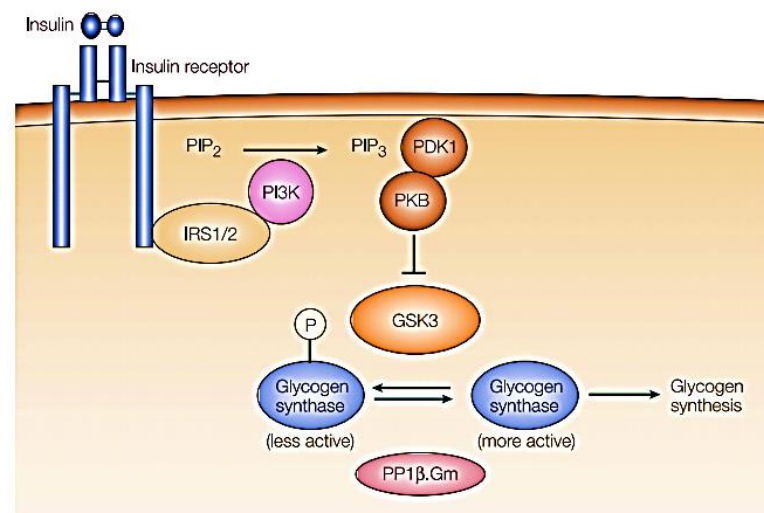


**Figure 1.1** The outline of the signaling pathway by which insulin inhibits GSK-3 and stimulates glycogen synthase (Cohen and Goedert 2004).

Interestingly, an elevated level of GSK-3 has been observed in diabetic and obese strains of mice (Eldar-Finkelman et al. 1999). GSK-3 is a serine-threonine protein kinase originally discovered in the context of its involvement in regulating glycogen synthase (Embi et al. 1980). GSK-3 is evolutionarily conserved and consists of 2 isoforms encoded by 2 different genes in mammals, GSK3 $\alpha$  (51 kDa) and GSK3 $\beta$  (46 kDa). They are 95% identical at the amino acid level, whereas the amino- and carboxy-termini are less conserved (Woodgett 2001). In addition to its role in regulating glycogen synthase, GSK-3 has been implicated in other aspects of glucose homeostasis, including the phosphorylation of insulin receptor IRS-1, a potential inhibitory mechanism for insulin resistance in type 2 diabetes (Lieberman and Eldar-

Finkelman 2005) and involves in activation of the hepatic gluconeogenesis through the modulation of the gluconeogenic enzymes, phosphoenolpyruvate carboxykinase (PEPCK) and glucose 6 phosphatase (G6Pase) (Lochhead et al. 2001).

As insulin induces the inhibition of GSK-3, small molecules that inhibit this protein kinase possibly expected to mimic some of the actions of insulin, such as its ability to activate glycogen synthase and stimulate the conversion of glucose to glycogen that lead to lower blood glucose by inhibiting the production of glucose by the liver and some GSK3 inhibitors have recently been reported to lower blood glucose levels *in vivo* (Norman 2001). Consequently, GSK-3 has recently emerged as one of the most attractive therapeutic targets for the development of selective inhibitors as promising new drugs for type 2 diabetes. Several potent GSK-3 $\beta$  inhibitors have been developed by pharmaceutical companies in preclinical models for diabetes treatment (Nakada et al. 2011).

In eukaryotes, *MCK1* in yeast *Saccharomyces cerevisiae* is an ortholog gene coding for glycogen synthase kinase 3 $\beta$  (*GSK-3 $\beta$* ) in human which has been implicated in many cellular functions. Mck1 protein promotes cell separation via controlling the fidelity of mitotic chromosome transmission and the induction of meiosis (Shero and Hieter 1991). Moreover, Mck1 involves in Ca<sup>2+</sup>-signaling pathway in yeast *S. cerevisiae* that play roles in the regulation of diverse cellular processes, such as T-cell activation, secretion, muscle contraction, neurotransmitter release and probably many more (Clapham 1995).

In the yeast, *S. cerevisiae*, calcium signaling pathways regulate G2/M cell cycle progression. Inappropriate activation of the Ca<sup>2+</sup>-signaling pathways in *S. cerevisiae* causes a deleterious physiological effect and various defects, including growth defects in the *zds1*-null mutant yeast (Mizunuma et al. 1998). Based on these observed phenotypes, and in particular the fact that the delayed G2 progression caused a loss of proliferation in the presence of calcium ions, a unique positive screening system utilizing the  $\Delta zds1$  yeast strain as indicator cells has been developed (Shitamukai et al. 2000). The  $\Delta zds1$  yeast- based assay is likely to detect inhibitors of the calcium dependent pathway targets. Small-molecule inhibitors of the Ca<sup>2+</sup> signaling in humans are of great medical importance, since Ca<sup>2+</sup> signaling in mammalian cells plays pivotal roles in the regulation of diverse cellular processes,



including T-cell activation, secretion, motility, and apoptosis (Foskett et al., 2007; Mizunuma et al., 1998) . Generally, small molecule inhibitors of  $\text{Ca}^{2+}$ -dependent signaling pathways exert their physiological effects by an evolutionary conserved manner throughout eukaryotes (Mager and Winderickx 2005). Consequentially, inhibitors found to be functional in yeast may well be active in relevance to human.

Boonkerd et al. (2011) reported the extensive screening study using  $\Delta zds1$  mutant yeast-based assay and found that the crude extract of *Kaempferia parviflora* Wall. Ex. Baker contained a potent inhibitory activity. *K. parviflora* is a member of Zingiberaceae (ginger) family, locally known in Thailand as Black Galingale or Kra-chai-dam. Members of this family, including *K. parviflora*, are traditionally very popular for health promotion (Putiyanan et al. 2008). The rhizomes of *K. parviflora* have been used as a traditional medicine for various purposes, including the treatment of leucorrhea, oral diseases (Chomchalow et al., 2003; Sudwan et al., 2005) , stomach ache, flatulence, digestive disorders, gastric ulcer as well as diuresis and tonic (Wattanapitayakul et al. 2007). Recently, Boonkerd et al. (2014) reported that a flavonoid 5-hydroxy-3,7-dimethoxyflavone or designated as 5-OH-3,7-DMF from *K. parviflora* exhibited an inhibitory activity against the  $\text{Ca}^{2+}$ -induced G2 cell-cycle arrest. Although, the molecular mechanism of 5-OH-3,7-DMF in yeast still unknown and needed to be investigated.

This research aimed to investigate the molecular target of 5-OH-3,7-DMF from *K. parviflora* in  $\text{Ca}^{2+}$ -signaling pathways in yeast and characterize the biochemical activity of 5-OH-3,7-DMF on inhibition of GSK-3 $\beta$  activity *in vitro*. Furthermore, the role of 5-OH-3,7-DMF and *K. parviflora* crude extract (CE) against insulin restraint HepG2 cell line as a type 2 diabetes cell model will be investigated.

## 1.1 Research methodologies

1.1.1 To investigate the molecular target of 5-OH-3,7-DMF in the  $\text{Ca}^{2+}$ -signaling pathways using yeast genetic method.

1.1.2 To characterize the biochemical activity of 5-OH-3,7-DMF *in vitro* in human GSK-3 $\beta$  inhibition and pattern of inhibition by Kinase Glo® Plus luminescent kinase assay platform.

1.1.3 To determine the cytotoxic effect of 5-OH-3,7-DMF on human hepatic HepG2 cell line by MTT Proliferation assay.

1.1.4 To establish insulin restraint HepG2 cell model and determine the toxicity of high glucose condition by MTT Proliferation assay. The effect of 5-OH-3,7-DMF in insulin restraint HepG2 cell model on the expression level of GSK-3 protein will be investigated by Western blot analysis and the expression level of G6Pase mRNA will be determined by RT-PCR.

1.1.5 To investigate the effect of 5-OH-3,7-DMF treatment in insulin restraint HepG2 cell model on the expression level of Glycogen synthase (GS) protein by Western blot analysis and glycogen content.

## 1.2 Expected outcomes

1.2.1 Understand the molecular target of 5-OH-3,7-DMF in the  $\text{Ca}^{2+}$ -signaling pathways (ortholog with *GSK-3 $\beta$* ) in yeast.

1.2.2 Understand the role of inhibition pattern of 5-OH-3,7-DMF as a GSK-3 $\beta$  inhibitor on human GSK-3 $\beta$  activity *in vitro*.

1.2.3 Understand the molecular mechanism of 5-OH-3,7-DMF in type 2 diabetes HepG2 cell line.

## CHAPTER II

### LITERATURE REVIEWS

#### 2.1 Literature reviews of *Kaempferia parviflora* Wall. ex Baker

*Kaempferia Parviflora* Wall. Ex. Baker (KP) is a member of Zingiberaceae family (ginger family), locally known in Thailand as Black Galingale or Kra-chai-dam (**Figure 2.1**). Members of this family, including KP, has been used in folk medicine reportedly for health promotion and stimulation (Putiyanan et al. 2008). Several pharmacological responses to the rhizomes of KP, locally known as Thai ginseng and its components have been claimed for various purposes, including the treatment of leucorrhea, oral diseases (Chomchalow et al., 2003; Sudwan et al., 2005), stomach ache, flatulence, digestive disorders, gastric ulcer as well as diuresis and tonic (Wattanapitayakul et al. 2007).

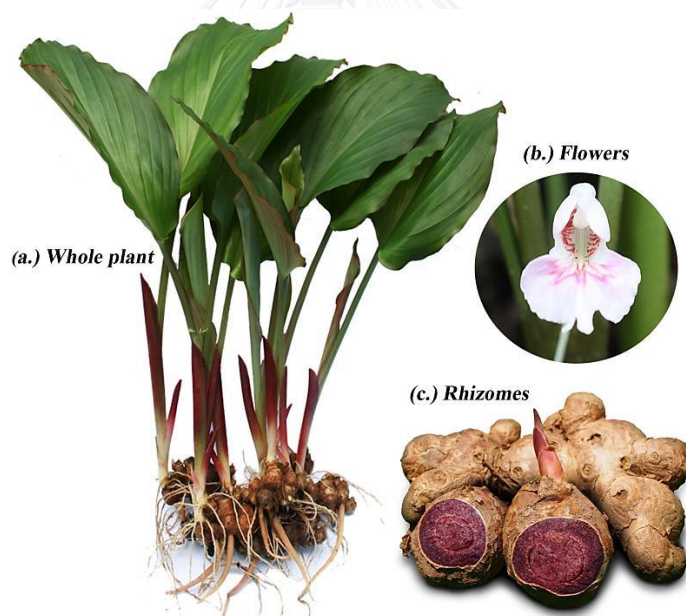


**Figure 2.1** The characteristics of *Kaempferia Parviflora* Wall. Ex. Baker, **(a.)**; A stemless, small, rhizomatous herb, up to 20 cm tall. Leaves 1-several, 8-16 cm long, obovate to elliptic, slightly unequal sided, acute or acuminate, base, subcordate, petiole short, channeled. **(b.)**; Flowers few in a sessile central tuft, corolla white, lip ovate-cuneate, emerginate, white with purple blotch at the middle. **(c.)**; Rhizome small, deep purple within (Modified from <http://www.kasetinfo.com>)

KP is a herb that has some historical and medicinal usage for treating metabolic ailments and improving vitality in Thailand as an aphrodisiac compound and physical enhancer. Currently, the research on Thai Ginseng appears to be a good source of a class of bioflavonoid compounds with methoxy groups, known as methoxyflavones. Flavonoids are demonstrated as the major constituents and proposed to contribute the biological effects. Phytochemical investigations have shown that the rhizome of KP contains the following: (1.) 5-hydroxy-7-methoxyflavone, (2.) 5-hydroxy-3,7-dimethoxyflavone, (3.) 5,7-dimethoxyflavone, (4.) 3,5,7-trimethoxyflavone, (5.) 5-hydroxy-3,7,4'-trimethoxyflavone, (6.) 5-hydroxy-7,4'-dimethoxyflavone, (7.) 5-hydroxy-3,7,3',4'-tetramethoxyflavone, (8.) 5,7,4'-trimethoxyflavone, (9.) 3,5,7,4'-tetramethoxyflavone, (10.) 5,7,3',4'-tetramethoxyflavone, (11.) 3,5,7,3',4'-pentamethoxyflavone (Sutthanut et al. 2007) (**Figure 2.2**).

Among these mentioned flavonoids, Azuma et al. (2011) reported that 5,7-dimethoxyflavone, flavonoid compounds from KP including 5,3'-dihydroxy-3,7,4'-trimethoxyflavone, 3,5,7-trimethoxyflavone and 5-hydroxy-7-methoxyflavone showed potent antimutagenic activity ( $IC_{50} = 0.40 - 0.47$  nmol/plate) and also showed  $\alpha$ -glucosidase inhibitory effect including 5,7,3',4'-tetramethoxyflavone exhibited the highest activity ( $IC_{50} = 20.4$   $\mu$ M), followed by 5,7,4'-trimethoxyflavone (54.3  $\mu$ M) and 3,5,7,3',4'-pentamethoxyflavone (64.3  $\mu$ M).

Moreover, flavonoid compounds 5,7,4'-trimethoxyflavone and 5,7,3',4'-tetramethoxyflavone exhibited antiplasmodial activity against *Plasmodium falciparum*, with  $IC_{50}$  values of 3.70 and 4.06 mg/mL, respectively. the compound 3,5,7,4'-tetramethoxyflavone and 5,7,4'-trimethoxyflavone possessed antifungal activity against *Candida albicans* with respective  $IC_{50}$  values of 39.71 and 17.63 mg/mL, and also showed mild anti-mycobacterial activity with the minimum inhibitory concentrations (MIC) of 200 and 50 mg/mL, respectively (Yenjai et al., 2004, 2007; Kumme et al., 2008).

Seven methoxyflavones were isolated from the hexane fraction of KP and were tested for their anti-inflammatory effects. Among those isolated compounds, 5-hydroxy-3,7,3',4'-tetramethoxyflavone exhibited the highest activity against nitric oxide (NO) release with an  $IC_{50}$  value of 16.1  $\mu$ M, followed by

5-hydroxy-7,4'-dimethoxyflavone (IC<sub>50</sub> 24.5 μM) and 5-hydroxy-3,7,4'-trimethoxyflavone (IC<sub>50</sub> 30.6 μM) (Tewtrakul et al. 2009).

Interestingly, 5-hydroxy-3,7,3',4'-tetramethoxyflavone was also tested on LPS-induced prostaglandin E<sub>2</sub> (PGE<sub>2</sub>) and tumor necrosis factor-alpha (TNF-α) release from RAW264.7 cells and revealed appreciable inhibitory effect on PGE<sub>2</sub> release (IC<sub>50</sub> = 16.3 μM), but inactive on TNF-α (IC<sub>50</sub> > 100 μM) (Tewtrakul et al. 2009). Furthermore, this compound showed the activity against inducible nitric oxide synthase (iNOS) and cyclooxygenase-2 (COX-2) mRNA expressions and also suppressed mRNA expression of iNOS in dose-dependent manners, whereas COX-2 mRNA expression was partly affected. According to the *in vivo* study, the chloroform and hexane fractions decreased rat paw edema greater than the ethanolic, ethyl acetate and water fractions (Sae-wong et al. 2009).

Not only the biological activity from pure compound of KP rhizomes but crude KP extract exhibited antidepressive (Wattanathorn et al. 2007), anticancer (Wen et al., 2005; Banjerdpongchai et al., 2008; Leardkamolkarn et al., 2009; Wudtiwai et al., 2011) cardioprotective (Tep-areenan et al., 2010; Malakul et al., 2011) and anti-obesity activity (Akase et al. 2011) in animal models. In addition, KP extract showed significant inhibitory acetylcholinesterase (AChE) and butyrylcholinesterase (BChE) activity activities *in vitro* (Sawasdee et al. 2009) and showed inhibition of P-glycoprotein function and multidrug resistance associated-proteins (MRP)-mediated transport in A549 cells (Patanasethanont et al. 2007).

A previous screening study using this  $\Delta zds1$  mutant yeast-based assay revealed that the crude extract of KP possessed a potent inhibitory activity against Ca<sup>2+</sup>-signaling in yeast (Boonkerd et al. 2011). In 2014, Boonkerd et al. reported that a 5-hydroxy-3,7-dimethoxyflavone designated as 5-OH-3,7-DMF from KP exhibited an inhibitory activity against the Ca<sup>2+</sup>-induced G2 cell-cycle arrest in *S. cerevisiae*.

Due to the flavonoid compounds of KP has a variety of mechanisms which indicates that KP is one of the potential plants for medical development.

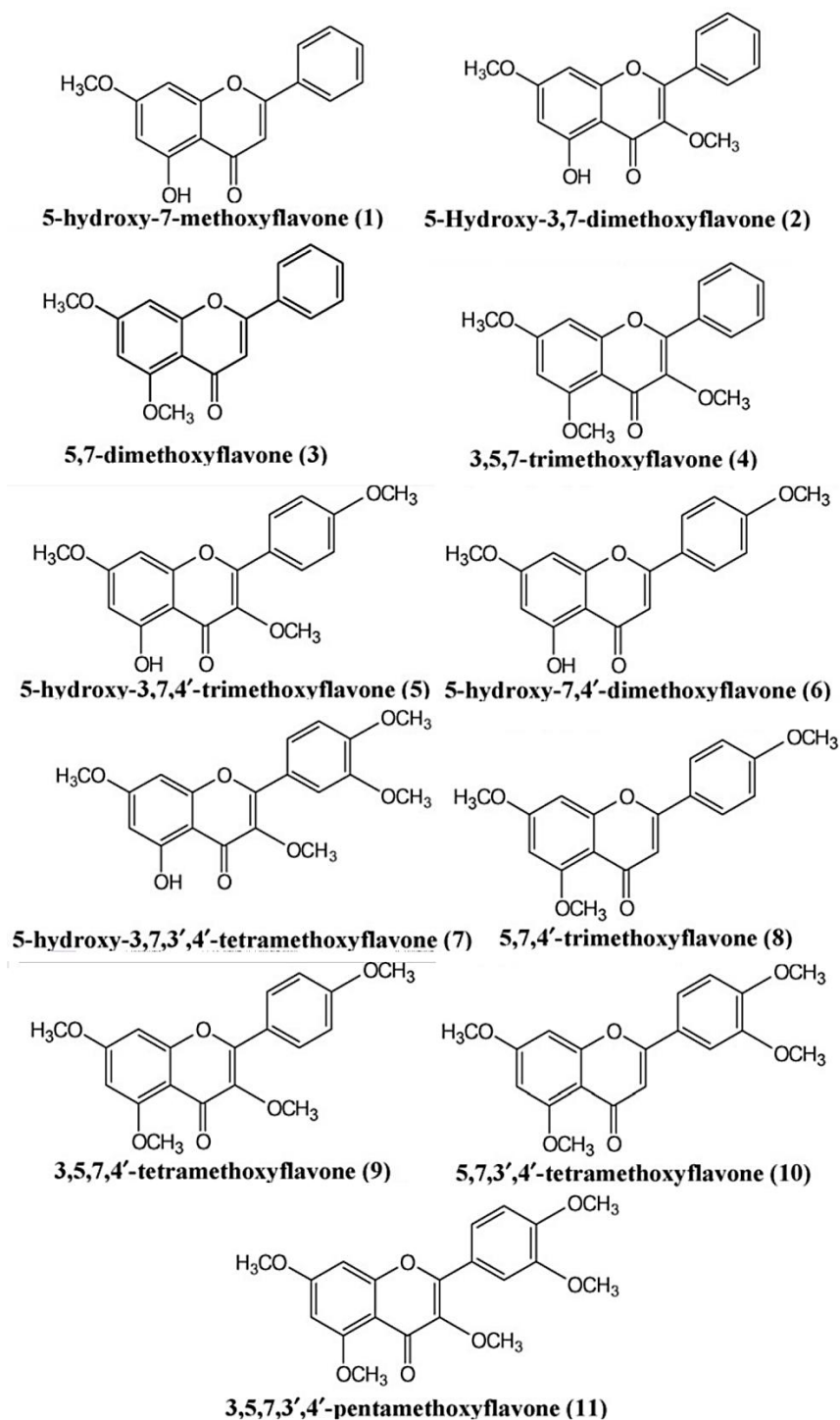


**Figure 2.2** Chemical structures of the 11 *Kaempferia Parviflora* flavonoids (modified from Sutthanut et al. (2007))

## 2.2 Calcium signaling pathways in *S. cerevisiae*

The search for novel drugs is still one of a major interest in the research especially in the health related area since infectious diseases are still a global problem. This is because of the development and spread of drug-resistant pathogens (Espinal et al. 2001) and the undesired side effects of the currently used drugs.

Intracellular calcium ion ( $\text{Ca}^{2+}$ ) concentration in eukaryotic organisms serves as a universal secondary messenger that helps translate extracellular stimuli to intracellular responses in numerous biological processes, including cell proliferation, membrane fusion, cytoskeleton organization, gene transcription, cell polarization, fertilization, development, motility, memory, and apoptosis (Clapham 1995). In *Saccharomyces cerevisiae*,  $\text{Ca}^{2+}$ -signaling pathways have been implicated in the regulation of G2/M cell-cycle progression as shown in **Figure 2.3**. The  $\text{Ca}^{2+}$  signal-dependent cell-cycle regulation in *S. cerevisiae* was identified by genetic investigations of the physiological effects of exogenous  $\text{CaCl}_2$  on mutant strains lacking the *ZDS1* gene (Shitamukai et al. 2000). The *ZDS1* gene is an enigmatic gene identified in numerous genetic screenings for its ability to suppress the phenotypes caused by defects in various genes when it is overexpressed on a high-copy vector, and it was so named for this capability call zillions of different screens. The genetic interactions of the *ZDS1* gene revealed by the screenings procedure including mutations in the *CDC42* gene encoding a GTPase involved in the regulation of cell polarity (Bi and Pringle 1996), a specific allele (*cdc28-1N*) of the *CDC28* gene encoding a protein kinase required for cell-cycle progression (Yu et al. 1996), the *hsl1* and *hsl7* mutations (Ma et al. 1996), and numerous other genes involved in multiple processes (Tsuchiya et al. 1996; Schwer et al. 1998; Roy and Runge 2000; Sekiya-Kawasaki et al. 2002). The function of *Zds1* is required for transcriptional repression of the *SWE1* gene, encoding a negative regulator of the Cdc28/Clb complex, and the *CLN2* gene, encoding a G2 cyclin, in the G2 phase (Ma et al. 1996). Swe1 kinase specifically inhibits a G2 form of Cdc28 by phosphorylating it at Tyr19 (Booher et al. 1993), and delays the onset of mitosis. Although *Zds1* (and its homolog *Zds2*) appears to be important in a wide range of cellular events, its biochemical function is still obscure. In the presence of high levels of exogenous  $\text{CaCl}_2$ , the cellular  $\text{Ca}^{2+}$  level is forced to rise due to the increased concentration of gradient across the plasma

membrane, resulting in hyperactivation of cellular  $\text{Ca}^{2+}$  signaling. Null alleles of the *ZDS1* gene on the W303 strain background exhibited a characteristic phenotype when cultivated in the presence of high external  $\text{CaCl}_2$ , showing a growth defect that was expressed by characteristic cellular changes, such as the formation of an elongated bud and the inhibition of the cell cycle in the G2 phase. Whereas the wild-type W303 strain did not show  $\text{Ca}^{2+}$ -sensitive phenotypes under similar conditions. The mutant strain exhibited no obvious phenotype in the presence of other solutes at concentrations that gave an osmolality equivalent to that of the high  $\text{CaCl}_2$  (Mizunuma et al. 1998). Because the  $\text{Ca}^{2+}$ -dependent phenotypes were canceled by deletion of the genes for calcineurin and Swe1 individually, the effect of  $\text{Ca}^{2+}$  must be exerted through the activation of calcineurin and Swe1. As mentioned above, calcineurin and the Mpk1 MAPK cascade cooperate in the regulation of various cellular events (Garrett-Engle et al. 1995; Nakamura et al. 1996; Nakamura et al. 1997). The  $\text{Ca}^{2+}$ -induced phenotypes were also suppressed by the deletion of a component of the MAPK cascade, such as Mpk1 (MAPK) or Bck1 (MAPK kinase), suggesting that calcineurin and the Mpk1 MAPK cascade collaborate in the  $\text{Ca}^{2+}$ -dependent regulation of the cell cycle and morphogenesis. Detailed genetic analysis of this mechanism has demonstrated that calcineurin elevates Swe1 (and Cln2) expression at the transcriptional level. Whereas the Mpk1 MAPK cascade activates Swe1 at the post-translational level. Both of these pathways are essential for the elevation and activation of Swe1 and Cln2, leading to the G2 cell-cycle inhibition and polarized bud growth (Mizunuma et al. 1998; Mizunuma et al. 2001; Mizunuma et al. 2004). Although, the mechanism of the calcineurin-dependent activation of *SWE1* and *CLN2* transcription is not well understood. The level of the *SWE1* transcript oscillates during the cell cycle. The calcineurin-dependent pathways are required to sustain a high *SWE1* mRNA level in the G2 phase, when its level normally (in the absence of  $\text{Ca}^{2+}$ ) declines to a low level. On the other hand, the Mpk1 pathway activates Swe1 by inhibiting Hsl1, a Nim1-related kinase that phosphorylates and negatively regulates Swe1, leading to inhibition of the cell-cycle entry into mitosis (Barral et al. 1999; Ma et al. 1996; Mizunuma et al. 1998; Tanaka and Nojima 1996).

The *MCK1* gene was genetically defined as a signaling component that acts in the downstream of the Mpk1 MAPK pathway. In accordance with this scheme, all of



the known  $\text{Ca}^{2+}$ -related phenotypes exhibited by the  $\Delta zds1$  strain were alleviated by the  $\Delta mck1$  mutation (Miyakawa and Mizunuma 2007). Further analyses have demonstrated that Mck1 promotes the  $\text{Ca}^{2+}$ -induced degradation of Hsl1, phosphorylated directly by Mck1 leading to an inhibitory kinase of Swe1. Induction of *MCK1* mRNA by  $\text{Ca}^{2+}$  occurs in a manner dependent on the Mpk1 pathway. However, elevation of the Mck1 level by  $\text{Ca}^{2+}$  was observed reproducibly, but only to a modest extent, suggesting that there are additional mechanisms of the regulation of Mck1 by  $\text{Ca}^{2+}$  signaling (Mizunuma, unpublished result; Miyakawa and Mizunuma 2007). The degradation of Hsl1 is rigorously regulated by  $\text{Ca}^{2+}$  signals, as suggested by the cooperative regulation of the degradation by calcineurin and the Mpk1-Mck1 pathway. Dephosphorylation of phospho-Hsl1 *in vivo* occurred in a calcineurin-dependent manner, and calcineurin and Hsl1 were co-precipitated in immunoprecipitation experiments (Mizunuma et al. 2001). Subsequent genetic and molecular analyses of this mechanism have demonstrated that Mck1 and calcineurin cooperatively regulate the delocalization of Hsl1 from the bud neck. The elaborate, calcineurin-dependent, mechanism of Hsl1 degradation appears to be required for the degradation of Hsl1 during the cell-cycle stages when the activity of the anaphase-promoting complex (APC) is low (during S, G2, and early M phases) (Miyakawa and Mizunuma 2007). In addition,  $\Delta mck1$  mutants do not eliminate Clb2-Cdk1 activity as efficiently as wild type cells at the end of mitosis. McQueen et al. (2012) demonstrated that Mck1 interacts with both Mih1 and Clb2 but does not promote degradation of these proteins and Clb2-Cdk1 activity is inhibited *in vitro* by the Mck1 kinase at the end of mitosis.

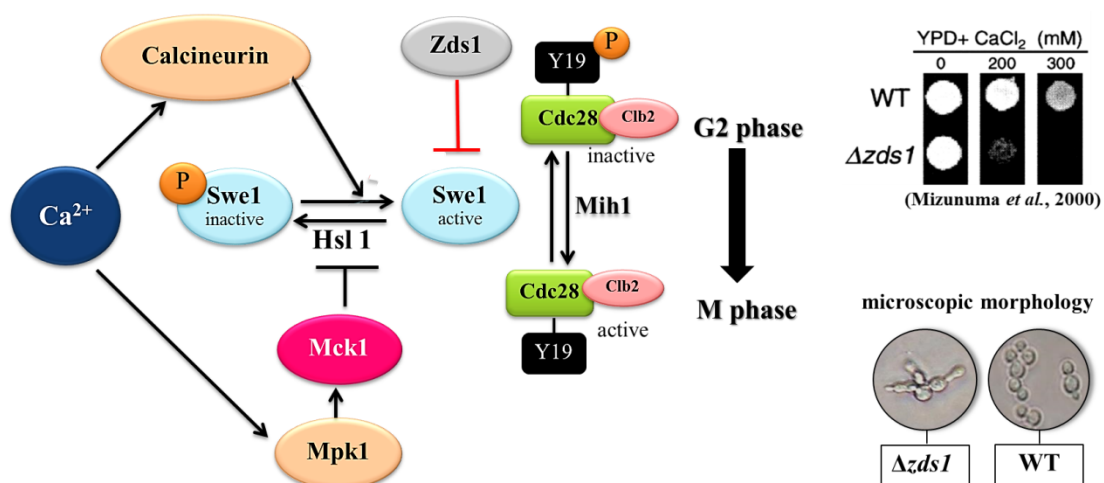


**Figure 2.3** Model for the Ca<sup>2+</sup>-signaling pathways that regulate G2/M cell cycle progression in *S. cerevisiae* represents potential target molecules of the drugs that are expected to be isolated by Δzds1 yeast-based screening system (modified from Shitamukai et al., 2000).

Because hyper-activated Ca<sup>2+</sup> signaling in yeast causes defective cell growth, it was assumed that exogenous inhibitors of the regulatory pathway could lead to the suppression of the deleterious effects of the Ca<sup>2+</sup> signaling, allowing the cells to resume growth. To apply this idea to drug screening based on the observation of phenotypes, and in particular the fact that the delayed G2 progression caused a loss of proliferation in the presence of calcium ions. The Δzds1 yeast-based assay is likely to detect inhibitors of the calcium dependent pathway targets. This unique positive screening system utilizing the Δzds1 yeast strain as indicator cells has been developed (Shitamukai et al. 2000). The inhibitory substances of this pathway can be detected positively by their ability to give rise to cell growth. Since small molecule inhibitors of Ca<sup>2+</sup>-dependent signaling pathways exert their physiological effects by an evolutionary conserved manner throughout eukaryotes (Mager and Winderickx 2005). Consequentially, inhibitors that are found to be functional in yeast may well be active in relevance to human, inhibiting target molecules that share common features structurally and functionally.

Therefore, the yeast-based procedures appear to provide a very convenient drug screening system. The unique features of this screening system may be summarized as follows (Miyakawa and Mizunuma 2007) :

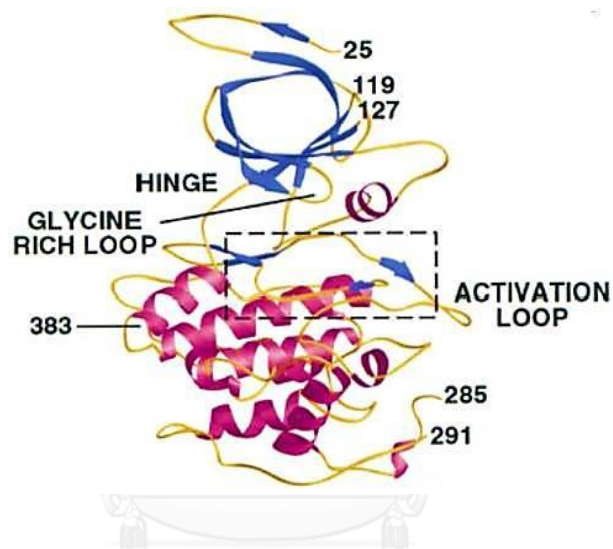
- 1) Because detection of the active substances is based on their positive effects on the growth of assay cells, cytotoxic compounds are not selected by the screening. Very crude samples, such as culture filtrates of microorganisms or plant extracts, are applicable for these screening.
- 2) Because the only cause for growth inhibition of the assay cells is the hyper-activation of  $\text{Ca}^{2+}$ -signaling, the molecules giving a restoration of growth are probably directed toward this pathway.
- 3) According to this procedure, potential targets as drugs of medical interest for the small molecule  $\text{Ca}^{2+}$ -signaling inhibitors are calcineurin (anti-inflammatory agents), GSK-3 family protein kinases (type 2 diabetes and Alzheimer's disease), protein kinase C and heat shock protein 90 or HSP90 (anti-cancer drugs) ((Boonkerd et al. 2011; Shitamukai et al. 2000).
- 4) Once the active substance is identified, the powerful genetic techniques available in the use of yeast provide valuable tools to identify the drug target of this pathway.

### **2.3 Yeast *MCK1*, a human ortholog *GSK-3* gene which encodes glycogen synthase kinase-3 family protein kinase**

The *MCK1* gene in yeast encodes a human glycogen synthase kinase-3 (GSK-3) family protein kinase (Andoh et al., 2000). Four of GSK-3 family protein kinase homologs identified in the yeast genome. The other kinases of this family (*MDS1*, *YGK3*, and *MRK1*) appear to contribute only trivially to this signaling pathway (Neigeborn and Mitchell 1991). Glycogen synthase kinase-3 (GSK-3) is expressed in all tissues and is a member of the protein kinase family, a group of enzymes that catalyze the transfer of a phosphate group from adenosine triphosphate (ATP) to target substrates.

Eukaryotic organisms contain homologous forms of GSK-3 with a high degree of similarity. In mammals, there are two isoforms of GSK-3, including GSK-3 $\alpha$  and GSK-3 $\beta$ , which are encoded by separate genes (Woodgett 1990). GSK-3 $\alpha$  (51 kDa) has a slightly higher molecular weight than that of GSK-3 $\beta$  (47 kDa). The extra length of GSK-3 $\alpha$  is due to the presence of an additional 63 amino acid residues at the N-terminus. Although both isoforms are structurally quite similar, they are functionally different (Hoeflich et al. 2000).

(a.)



(b.)

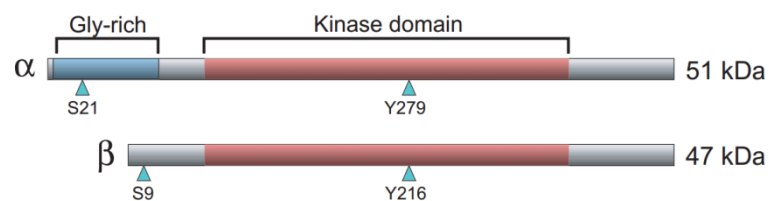


**Figure 2.4** (a.); Model structure of GSK-3 $\beta$  (Ter Haar et al. 2001), (b.); Schematic representations of mammalian GSK-3 $\alpha$  and GSK-3 $\beta$ . Sites of serine and tyrosine phosphorylation are indicated with blue arrowheads. The glycine-rich N-terminal domain unique to GSK-3 $\alpha$  and the conserved kinase domain shared by both isoforms are highlighted (Woodgett 2001).

A detailed structural and functional analysis of GSK-3 $\beta$  reported by Ter Haar et al. (2001) is depicted in **Figure 2.4 (a.)**. There are two major GSK-3 $\beta$  domains: a  $\beta$ -strand domain present at the N-terminus between amino acid residues 25-138 and  $\alpha$ -helical domain present at the C-terminus between amino acid residues 139-343. An ATP-binding site presents at the interface of the two domains that is adjoined by a glycine-rich loop and hinge region. The catalytic activity of GSK-3 $\beta$  is regulated by phosphorylation at two different sites. Phosphorylation of the Ser9 site inactivates GSK-3 $\beta$ , whereas phosphorylation at Tyr216 within the activation loop increases its catalytic activity. For GSK-3 $\alpha$ , phosphorylation at Ser21 renders it inactive and phosphorylation at Tyr279 increases its catalytic activity, **Figure 2.4 (b.)** (Woodgett 2001).

GSK-3 is a serine/threonine kinase, and thus transfers a phosphate group to either the serine or threonine residues of its substrates (Doble and Woodgett 2003). The mechanism of phosphorylation regulates various complex biological processes, including metabolism (glucose regulation) (Summers et al., 1999; Lochhead et al., 2001), cell signaling (Watkins et al., 2014; Maurer et al., 2014; Montori-Grau et al., 2013), cellular transport (Singh et al., 2014; Song et al., 2014; Yucel and Oro, 2011), apoptosis (Kuemmerle 2005), proliferation, and intracellular communication (Manning et al. 2002). Phosphorylation is a key regulatory step that initiates, enhances, or inhibits the function of a target substrate. GSK-3 has emerged as an important target for drug development and medical imaging in various diseases. Since the isolation of GSK-3 from rabbit skeletal muscle in 1980 (Embi et al. 1980), its role and participation in glucose metabolism has been extensively studied. A primary function of GSK-3 is the regulation of the activity of glycogen synthase (GS), an enzyme that mediates the conversion of glucose to glycogen (Woodgett and Cohen 1984). Elevated expression and over-activity of GSK-3 are associated with insulin resistance in type 2 diabetes (Pandey and DeGrado 2016). Therefore, GSK-3 inhibitors are under development for the treatment of type 2 diabetes (Nikoulina et al. 2000; Peat et al. 2004). GSK-3 $\beta$  associate in many neurodegenerative diseases (Eldar-Finkelman et al. 1999a) including Parkinson's disease (PD), Alzheimer's disease involve in the phosphorylation of tau protein (Llorens-Marín et al. 2014), and Huntington's disease (HD), Lim et al. (2014) observed higher levels of

phosphorylated GSK-3 in post-mortem human HD brain samples correlated with disrupted energy metabolism in two transgenic mouse models. The hypothesis that inhibition of GSK-3 $\beta$  activity may protect dopaminergic neurons (Li et al. 2014). GSK-3 regulatory activity is associated with acquired immunodeficiency syndrome (AIDS) (Dewhurst et al. 2007; Zhou et al. 2013), malaria (García et al. 2011), inflammation (Beurel and Jope 2010) and canonical Wnt/ $\beta$ -catenin pathways (Chen et al. 2014).

Clearly, GSK-3 is an important regulator of metabolic and signaling functions that are associated with a broad spectrum of disease areas, motivating extensive efforts on the GSK-3 inhibitor development.

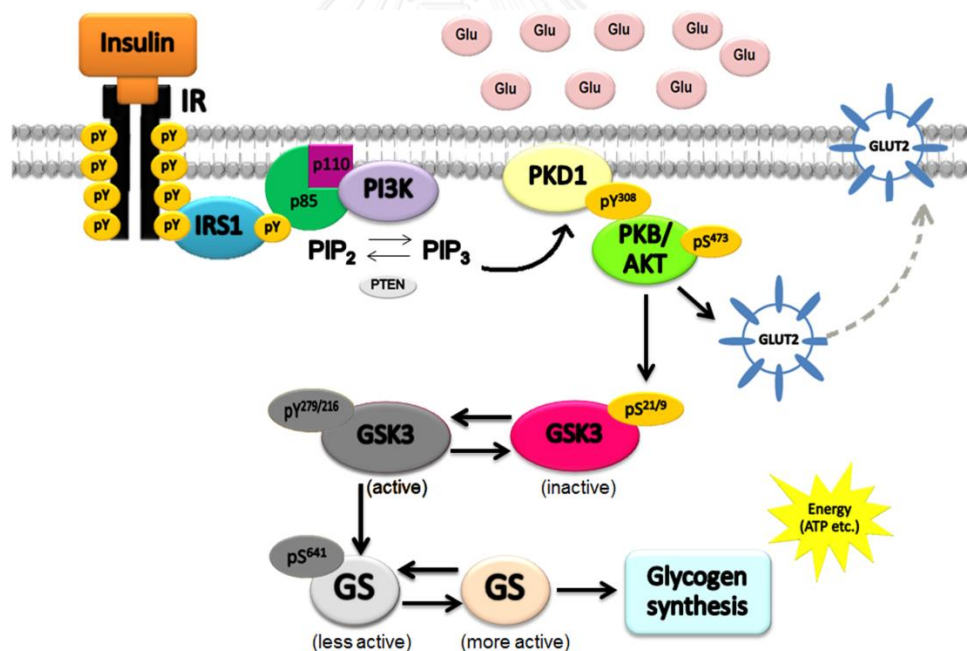
#### **2.4 Role of GSK-3 in insulin resistance and type 2 diabetes**

Diabetes is one of the largest global health emergencies of the 21<sup>st</sup> century. In 2013, the International Diabetes Federation (IDF) estimated that 382 million people had diabetes worldwide. By 2035, this was predicted to rise to 592 million. Eighty percent live in low- and middle-income countries; Of the total, more than 60% live in Asia, with almost one-third in China (Nanditha et al. 2016). In addition, the current status of diabetes was 78.3 million people in South East Asia as well as Thailand (~4 million people) by year 2015 (International Diabetes Federation, 2015). Although, Type 2 diabetes (T2DM) being much more common, has been the main driver for the increase in global diabetes prevalence (Guariguata et al. 2014).

T2DM or non-insulin-dependent diabetes mellitus (NIDDM), which accounts for ~90% of all cases of this disease, is characterized by insulin resistance. That is an inability of the tissues to respond to the insulin hormone that higher-than-normal concentrations of insulin are required to maintain normoglycemia (DeFronzo et al. 2014). Insulin is a hormone produced in the pancreas. It is required to transport glucose from the bloodstream into the body's cells where it is used as energy. In this pathology, the liver plays an importance role in the control of the whole body metabolism of energy nutrients (Klover and Mooney 2004). The lack or ineffectiveness of insulin in a person with diabetes cause remained glucose circulating in the blood. Over time, this organ is not able to control glucose homeostasis. There is a miss-regulation of the insulin pathway resulting high levels of glucose in the blood

(known as hyperglycemia) causes damage to many tissues in the body; As a consequence, the development of classical symptoms of polyuria (frequent urination), polydipsia (increased thirst) and polyphagia (increased hunger) (Gardner et al. 2011).

At the cellular level, insulin binds and activates the insulin receptor (IR) by phosphorylating key tyrosine residues. This is followed by tyrosine phosphorylation of insulin receptor substrates (IRS) and subsequent activation of the phosphatidylinositol 3-kinase (PI3K)/protein kinase B (PKB/AKT) pathway. AKT stimulation leads to the inhibition of glycogen synthase kinase-3 (GSK-3) by phosphorylation, resulting in the dephosphorylation of substrates of GSK3 including glycogen synthase (GS) cause glycogen synthesis activation (Cohen and Frame 2001) (**Figure 2.5**). The insufficient strength of insulin signaling altered the final substrates of insulin action involved in multiple metabolic and mitogenic aspects of cellular function such as high activated glycogen synthase kinase-3 (GSK-3) protein (Ginsberg 2000).



#### Normal liver cell

**Figure 2.5** The insulin signaling pathway by which inhibits GSK-3 and results in the stimulation of glycogen synthesis (modified from Cohen and Frame, 2001).

Interestingly, elevated level of GSK-3 has been observed in diabetic and obese strains of mice (Eldar-Finkelman et al. 1999). In addition to its role in regulating glycogen synthase, GSK-3 has been implicated in other aspects of glucose

homeostasis, including the phosphorylation of insulin receptor IRS-1, a potential inhibitory mechanism for insulin resistance in T2DM (Lieberman and Eldar-Finkelman 2005). In addition GSK-3 involves in activation of the hepatic gluconeogenesis through the modulation of the gluconeogenic enzymes, phosphoenolpyruvate carboxykinase (PEPCK) and glucose 6 phosphatase (G6Pase) (Lochhead et al. 2001). The involvement of GSK-3 in diabetes was further demonstrated in two model systems: First, in fat tissue of obese diabetic mice, where GSK-3 activity was found to be two fold higher than in control mice (Eldar-Finkelman et al. 1999). Second, in skeletal muscle of patients with T2DM, where GSK-3 activity and expression levels were significantly higher than in healthy individuals (Nikoulina et al. 2000). Thus, in insulin-sensitive tissue directly involved in the pathogenesis of T2DM, GSK-3 activity is higher than normal and seemingly contributes to impairment of insulin action.

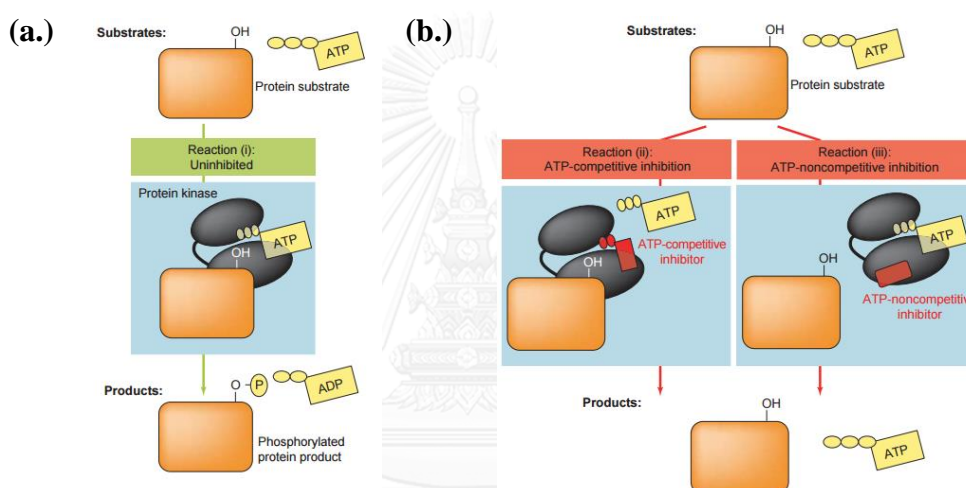
Eldar-Finkelman et al. (1999) reported that GSK-3 was shown to phosphorylate IRS-1, which impair the insulin signaling. IRS-1 is the immediate substrate of insulin receptor tyrosine kinase, which phosphorylates the protein on multiple tyrosine residues in response to insulin (Cohen and Frame 2001). This was demonstrated by Tanti et al. (1994), the treatment in 3T3-L1 adipocytes cells with okadaic, a protein phosphatase inhibitor, followed by hyperphosphorylation of IRS-1 on serine/threonine residues led to inhibition of the insulin signaling pathway. These data suggest that the serine/threonine phosphorylation of IRS-1 might represent a key regulatory mechanism of insulin action.

According to insulin induces the inhibition of GSK-3, small molecules that inhibit this protein kinase possibly expected to mimic some of the actions of insulin, such as its ability to activate glycogen synthase and stimulate the conversion of glucose to glycogen that lead to lower blood glucose by inhibiting the production of glucose by the liver. Some GSK-3 inhibitors have recently been reported to lower blood glucose levels *in vivo* (Norman 2001). Consequently, GSK-3 has recently emerged as one of the most attractive therapeutic targets for the development of selective inhibitors as promising new drugs for T2DM. Several potent GSK-3 $\beta$  inhibitors have been developed by pharmaceutical companies in preclinical models for diabetes treatment (Nakada et al. 2011).



## 2.5 GSK-3 inhibitors: Therapeutic targets for type 2 diabetes Mellitus

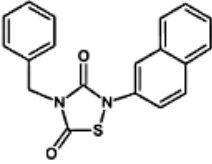
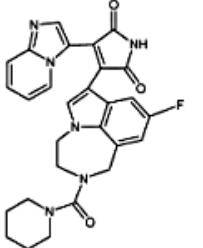
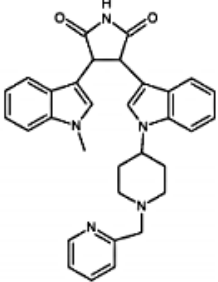
Inhibition of GSK-3 will have therapeutic benefit and intensive efforts have been made in the search for and design of selective GSK-3 inhibitors. The reported GSK-3 $\beta$  inhibitors are of diverse chemotypes and mechanisms of action. These include inhibitors isolated from natural sources, cations, and synthetic small molecules (Eldar-Finkelman and Martinez 2011). Regarding the mechanism of protein or enzyme inhibition that are ATP-competitive inhibitors, non-ATP-competitive inhibitors, and substrate-competitive inhibitors (Eldar-Finkelman and Martinez 2011) (**Figure 2.6**).



**Figure 2.6** The reaction catalyzed by protein kinases and the general principle of ATP-competitive inhibitors and ATP-noncompetitive inhibitors of protein kinases. (a.) The uninhibited reaction, protein kinases (black) catalyze the transfer of the phosphate group of ATP (yellow) to specific hydroxyl groups (-OH) of amino acids within their protein substrates (orange). The resulting products are ADP and the phosphorylated protein product. (b) Two different mechanisms of inhibition, ATP-competitive inhibition, in which the inhibitor (red, with some similarity to ATP) competes with ATP for the ATP-binding site of the kinase. For ATP-noncompetitive inhibition, in which the inhibitor competes with the protein substrate for the protein-substrate-binding site of the kinase. In both reactions, there is no phosphorylation of the hydroxyl group of the protein substrate, and thus no phosphorylated protein product is formed (modified from Bogoyevitch, 2005).

Clinical Prospects of GSK-3 in therapy, the involvement and association of GSK-3 in the pathogenesis of a wide variety of diseases makes it an important therapeutic and imaging target. The potential of GSK-3 $\beta$  inhibition in diabetes, bipolar disorder, and Alzheimer's disease has already been identified. Considerable progress has been made in the development of various GSK-3 $\beta$ -inhibitory molecules. Clinical Studies on GSK-3 Inhibitors of the developed GSK-3 inhibitors, only a few have reached clinical trials in human subjects. Clinical studies that have resulted in peer-reviewed articles along with studies listed on clinical trials.gov for GSK-3 inhibitors including; Tideglusib (Hicks et al. 2010), LY2090314 (Vasdev et al. 2005), Enzastaurin (Paquet et al. 2009) and lithium chloride (Cole et al. 2014) in **Table 2.1**.

**Table 2.1** GSK-3 $\beta$  Inhibitors under clinical Investigation

Compound No. (lit. com. No.)*	Structure of GSK-3 inhibitors tested clinically	IC <sub>50</sub> Value (nm)	Type of Disease(s)
94 (Tideglusib) (NP031112) (NP-12)		GSK-3 $\beta$ = 60	Alzheimer's disease, progressive supranuclear palsy
95 (LY2090314)		GSK-3 $\alpha$ = 1.5 GSK-3 $\beta$ = 0.9	Pancreatic cancer, leukemia
96 (Enzastaurin, LY317615)		PKC (protein Kinase C) $\beta$ = 0.6 nM also suppresses GSK- 3 $\beta$	Recurrent glioma, ovarian cancer,
97 (Lithium)	Lithium Chloride	GSK-3 $\beta$ = 2.0 mM (Ki)	Alzheimer's disease, bipolar disorder

(Modified from Pandey and DeGrado (2016))

According to T2DM also end up needing insulin to survive. Therefore, as in many other diseases, early diagnosis and treatment are the most important. Metformin is still the drug that is used most commonly to treat T2DM. The main effect of this drug from the biguanide family is to acutely decrease hepatic glucose production, mostly through a mild and transient inhibition of the mitochondrial respiratory chain complex I. In addition, the resulting decrease in hepatic energy status activates AMPK (AMP-activated protein kinase), a cellular metabolic sensor, providing a generally accepted mechanism for the action of metformin on hepatic gluconeogenesis. The demonstration that respiratory chain complex I, but not AMPK, is the primary target of metformin was recently strengthened by showing that the metabolic effect of the drug is preserved in liver-specific AMPK-deficient mice. Beyond its effect on glucose metabolism, metformin has been reported to restore ovarian function in PCOS (polycystic ovary syndrome), reduce fatty liver, and to lower microvascular and macrovascular complications associated with T2DM (Viollet et al. 2012). Also, as discussed later, metformin does not exert its effect by switching on the insulin signaling pathway; it is therefore unlikely to alleviate all the long-term effects of the disease. Therefore, improved drugs to treat diabetes are needed urgently.

The level of blood glucose is largely determined by the rate at which glucose is taken up by skeletal muscle and liver and converted into glycogen, and by the rate at which it is produced by the liver, these seem that GSK-3 inhibitors might be beneficial for the treatment of diabetes. Therefore, drugs that inhibit GSK-3 could mimic the ability of insulin to promote the conversion of glucose to glycogen, overcoming the resistance to insulin, which seems to be caused by blockade of the pathway at the level of the insulin receptor (IRS) proteins. Indeed, lithium ions, which inhibit GSK-3 relatively specifically *in vitro* (Davies et al. 2000; Klein and Melton 1996; Stambolic et al. 1996) were shown many years ago to activate glycogen synthase and to stimulate the synthesis of glycogen in muscle (Cheng et al. 1983).

GSK-3 inhibitors, SB 216763 and SB 415286 (**Figure 2.7**) inhibited GSK-3 much more potently than lithium, like lithium ions, activated glycogen synthase and accelerated the conversion of glucose to glycogen in a human liver cell line (Coghlan et al. 2000). Other members of this compound class were subsequently reported to normalize blood glucose levels *in vivo* (Norman 2001).

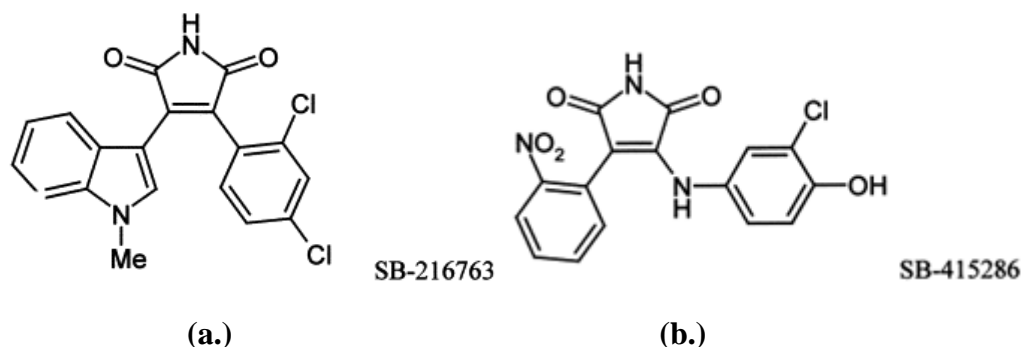


**Figure 2.7** The chemical structures of (a.); SB-216763 is 3-(2,4-dichlorophenyl)-4-(1-methyl-1H-indol-3-yl)-1H-pyrrole-2,5-dione. (b.); SB-415286 is 3-(3-chloro-4-hydroxyphenylamino)-4-(2-nitrophenyl)-1H-pyrrole-2,5-dione (Coghlan et al. 2000).

Interestingly, SB 216763, SB 415286 and lithium ions were found to mimic another action to suppress transcription of phosphoenolpyruvate carboxykinase (PEPCK) and glucose 6-phosphatase (G6Pase) (Lochhead and Thompson 2001), the key rate-limiting enzymes of gluconeogenesis. These data suggested that GSK-3 inhibitors might be able to suppress the production of glucose by the liver, as well as enhance its conversion into glycogen. Moreover, a number of other potent inhibitors of GSK-3 such as indirubins (Leclerc et al. 2001; Meijer et al. 2003; Polychronopoulos et al. 2004), paullones (Leost et al. 2000) and hymenialdisine (Meijer et al. 2000), inhibited some other protein kinases (Polychronopoulos et al. 2004), including the cyclin-dependent protein kinases (CDKs), which GSK-3 is most closely related in sequence. Whereas, lithium ions do not inhibit CDKs, but also inhibit some non-kinase targets, such as inositol monophosphatase and histone deacetylase (Phiel and Klein 2001). Lithium ions is ATP-noncompetitive inhibitors, in contrast to all the other compounds mentioned above that are ATP-competitive.

Finally, the interested GSK-3 inhibitors are effectively lowering blood glucose level in rodent models of T2DM; Their effects occurred primarily through an increase in hepatic glycogen synthesis and a decrease in hepatic gluconeogenesis.

## CHAPTER III

### RESEARCH METHODOLOGY

#### 3.1 Instruments used in this thesis

1. CO<sub>2</sub> incubator (Thermo Scientific, USA)
2. Incubator (Thermo Scientific, USA)
3. Amersham Hyperfilm<sup>TM</sup> ECL (GE healthcare, Sweden)
4. Amersham<sup>TM</sup> Hybond<sup>TM</sup> 0.45 (GE healthcare, Sweden)
5. Autoclave MLS 3020 (Sanyo, Japan)
6. Balance AG285 PG2002-S and PB3002 (Mettler Toledo, Switzerland)
7. Beaker (Pyrex, USA)
8. Bench-top centrifuge 2600 (Denville, Germany)
9. Bottle for culture media (tissue culture) 100 mL (Corning Incorporation, USA)
10. Centrifuge tubes 15 and 50 mL (Corning Incorporation, USA)
11. Cover slips (Nissho Nipro, Japan)
12. Cryotube (NUNCT<sup>TM</sup>, Denmark)
13. Deep freezer -80°C ULT1786 (Forma Scientific, USA)
14. Deep freezer -20°C MDF-U332 (Sanyo Electric, Japan)
15. Disposable syringe (Nissho Nipro, Japan)
16. DNA Thermal Cycle T100<sup>TM</sup> (Bio-Rad, USA)
17. Filter paper (Whatman, England)
18. Gel Documentation and Quantity One version 4.4.1 (Bio-Rad, USA)
19. Haemocytometer (Mettler Toledo, Switzerland)
20. Hot air oven UE (Mettmert, Germany)
21. Hypercassette<sup>TM</sup> (Amersham biosciences, UK)
22. Invert microscope (Olympus, USA)
23. Laminar flow clean model V4 (LAB Service, Thailand)
24. Measuring cylinder (Pyrex, USA)

25. Microcentrifuge tube 15 and 50 mL (Corning Incorporation, USA)
26. Microcentrifuge tube 1.5 mL (Axygen Scientific, USA)
27. Micropipette P10, P20, P100, P200 and P1000 (Gilson, France)
28. Microplate reader Elx 800 (Bio-tek instrument, USA)
29. Microwave oven (Samsung, Korea)
30. Optizen Nano Q (KAIA Bio-Ingenieria, Korea)
31. Parafilm (Parafilm®M, USA)
32. PCR tube 200 µl (Corning Incorporation, USA)
33. pH meter S-20K (Mettler-Toledo, Switzerland)
34. Pipette aid (Drummond, USA)
35. Polyvinylidene fluoride (PVDF) membrane 0.45 µm (GE healthcare, Sweden)
36. Power supply for electrophoresis (Bio-Rad, USA)
37. Refrigerator Tiara (Mitsubishi electric)
38. Seropipette 5 and 10 mL (Pyrex, USA)
39. Synergy™ HT Multi-Detection Microplate Reader (Bio-tek, USA)
40. SDS-polyacrylamide gel electrophoresis, Protein 2I System (Bio-Rad, USA)
41. Semi-dry electrophoretic transfer cell, Trans-Blot® SD (Bio-Rad, USA)
42. Sonicator RK100 (BANDELIN, Germany)
43. Stainless Alcohol burner
44. Syringe filter CA-CN 13 mm 0.45 µm (Restek, Thailand)
45. Thermo-block MylabTH Thermo-Block SLTDB-120 (Seoul in Bioscience, Korea)
46. Tissue culture Flask 25 and 75 cm<sup>3</sup> (Corning Incorporation, USA)
47. Tissue culture plate 6, 12, 24 and 96 well (NUNCTM, Denmark)
48. Vortex mixer Genie 2 G-560E (Scientific Industries, USA)
49. Water bath (Mettmert, USA)

### 3.2 Chemicals

1. Absolute ethanol (Lab Scan analytical science, USA)
2. Absolute methanol (Merck, Germany)
3. Acetic acid (Lab Scan analytical science, USA)
4. Acrylamide-solution (40%) Mix 37.5:1 (Sigma, USA)
5. Ammonium bicarbonate (Sigma, USA)
6. Ammonium persulfate (Bio Basic inc, Canada)
7. Anti-rabbit IgG, HRP-linked antibody; catalog#7074S (Cell signaling, USA)
8. BCA<sup>TM</sup> protein assay (Thermo Scientific, USA)
9.  $\beta$ -mercapto-ethanol (Sigma, USA)
10. Bromophenol blue (Sigma, USA)
11. Clarity<sup>TM</sup> Western ECL substrate (Bio-Rad, USA)
12. Chloroform (Lab Scan analytical science, USA)
13. Copper sulfate (Fisher Scientific, UK)
14. Developer (Carestream Health Inc, USA)
15. DNA ladder 100 bp (Fermentas, Canada)
16. Diethylpyrocarbonate (DEPC) (Sigma, USA)
17. Dimethyl sulfoxide (DMSO) (Amesco, USA)
18. dNTPs mix (Fermentas, Canada)
19. Fetal Bovine Serum (FBS) (Hyclone, UK)
20. Fixer (Kodak, USA)
21. FK506; catalog #445643 (Abcam, USA)
22. Goat Anti-Mouse IgG Antibody, Peroxidase Conjugated, H+L; catalog #AP124P (Merck, Germany)
23. Glycerol (Carlo ERBA, France)
24. Glycogen assay kit; catalog #MAK016 (Sigma, USA)
25. GSK-3 $\beta$  Inhibitor I; catalog #361540 (Merck, USA)
26. GSK3 substrate peptide; catalog #12-533 (Merck, Germany)
27. GSK-3 $\beta$  Protein active enzyme; catalog #14-306(Merck, Germany)

28. HEPES (4-(2-hydroxyethyl)-1-piperazineethanesulfonic acid) (Hyclone, UK)
29. Hydrochloric acid (HCl) (LAB-SCAN, Ireland)
30. Isopropanol (Merck, Germany)
31. Kinase-Glo® Luminescent Kinase Assay (Promega, USA)
32. Magnesium chloride (MgCl<sub>2</sub>) (Merck, Germany)
33. Magnesium sulfate (MgSO<sub>4</sub>) (Merck, Germany)
34. Mouse anti-phospho-GSK-3 $\beta$  (Ser9); catalog #05-643 (Merck, Germany)
35. Mouse anti-GSK3 ( $\alpha/\beta$ ); catalog #05-412 (Merck, Germany)
36. Mouse anti-phospho-GSK3 (Tyr279/Tyr216); catalog #05-413 (Merck, Germany)
37. Mouse anti-Actin, clone C4; catalog #MAB1501 (Merck, Germany)
38. MTT (3-(4,5-dimethylthiazol-2-yl)-2,5-diphenyltetrazolium bromide) (Bio Basic inc, Canada)
39. Nonidet P-40 (Bio Basic inc, Canada)
40. Penicillin (General Drugs House, Thailand)
41. Phosphatase inhibitor cocktail 2 (Sigma, USA)
42. Potassium chloride (KCl) (Merck, Germany)
43. Protease inhibitor (Sigma, USA)
44. Rabbit anti-Phospho-GSK3 (Ser21); catalog#3886 (Cell signaling, USA)
45. Rabbit anti-Phospho-GS (Ser641); catalog#3891 (Cell signaling, USA)
46. Random hexamer (Fermentas, Canada)
47. Reverse transcriptase (Fermentas, Canada)
48. Ribonuclease inhibitor (Fermentas, Canada)
49. RPMI 1640 (Hyclone, UK)
50. Streptomycin (AppliChem, USA)
51. SDS (sodium dodecyl sulfate) (C<sub>12</sub>H<sub>25</sub>OSO<sub>3</sub>) (Sigma, USA)
52. Sodium di-hydrogen phosphate (Na<sub>2</sub>HPO<sub>4</sub>) (Merck, Germany)
53. Sodium hydroxide (NaOH) (Merck, Germany)
54. Sodium pyruvate (Hyclone, UK)



55. Taq DNA polymerase (Fermentas, Canada)
56. TEMED (N, N, N, N-Tetramethylethylenediamide) (Bio Basic inc, Canada)
57. Tris buffer pH 6.8 (Preparation is described in appendix)
58. Tris buffer pH 7.5 (Preparation is described in appendix)
59. Tris buffer pH 8.8 (Preparation is described in appendix)
60. TriZol reagent (Invitrogen, USA)
61. Trypan blue 0.5% w/v (Hyclone, UK)
62. Tween 20 (Sigma, USA)



### 3.3 Primer sequences and conditions used in real-time PCR (RT-PCR)

**Table 3.1** Primer sequences and conditions used in real-time PCR (RT-PCR)

Gene	Nucleotide sequence	Annealing temp.(°C)	Product size (bp)	Reference
<i>G6Pase</i>	Fwd: 5'-TCATCTTGGTGT CCGTGATCG-3'	57	220	(Kang et al. 2010)
	Rev: 5'-TTTATCAGGGGC ACGGAAGTG-3'			
<i>β-actin</i>	Fwd: 5'-TTCCTTCCTGG GCATGGAGT-3'	55	180	(Kang et al. 2010)
	Rev: 5'- CCAGGGCAGTG ATCTCCTTC-3'			

### 3.4 Antibody for Western blot analysis

**Table 3.2** Antibody for Western blot analysis

Antigen	Ratio (1°antibody:bloking solution)	Ratio (2°antibody:bloking solution)
GSK3	Mouse anti-GSK3 1:2,000	Anti-mouse IgG-H+L 1:4,000
P-GSK3β	Mouse anti-P-GSK3β (ser9) 1:500	Anti-mouse IgG-H+L 1:2,000
P-GSK3α	Rabbit anti-P-GSK3β (ser21) 1:500	Anti-rabbit IgG-HRP 1:4,000
P-GSK3α/β	Mouse anti-P-GSK3α/β (Tyr279/Tyr216) 1:500	Anti-mouse IgG-H+L 1:2,000
GS	Rabbit anti-GS 1:2000	Anti-rabbit IgG-HRP 1:4,000
P-GS	Rabbit anti-P-GS (Ser641) 1:1,000	Anti-rabbit IgG-HRP 1:4,000
β-actin	Mouse anti-β-actin 1:4,000	Anti-mouse IgG-H+L 1:4,000

### 3.5 Yeast strains and cultivation

All mutant strains of *S. cerevisiae* were obtained from Prof. Tokichi Miyakawa, Hiroshima University. Details of the strains were listed in Table 3.3.

**Table 3.3** *S. cerevisiae* strains used in this study

Strain	Genotype	Source of reference
YNS17	<i>MAT a trp1 leu2 ade2 ura3 his3 can1-1 zds1::TRP1 syr1::HIS3 pdr1::hisG-URA3-hisG pdr3::hisG-URA3-hisG</i>	Miyakawa T, Hiroshima University (Chanklan et al. 2008)
YRC1	<i>MAT a ade2-1 can1-100 his3-11,15 leu2-3,112 trp1-1 ura3-1 zds1::TRP erg3::HIS3 pdr1::hisG pdr3::hisG GAL1-CMP2ΔC::URA3</i>	Miyakawa T, Hiroshima University (Chanklan et al. 2008)
YRC2	<i>MAT a trp1 leu2 ade2 ura3 his3 can1-1 swe1::GALp-SWE1-HA::LEU2 syr1::HIS3 pdr1::hisG-ura3-hisG pdr3::hisG-URA3-hisG</i>	Miyakawa T, Hiroshima University (Chanklan et al. 2008)
NSC1	<i>MATa ade2-1 can1-100 his3-11,15 leu2-3,112 trp1-1 ura3-1 zds1::TRP erg3::HIS3 pdr1::hisG pdr3::hisG pYES2::GAL1p-MPK1</i>	Wangkangwan et al., 2009
NSC2	<i>MAT a ade2-1 can1-100 his3-11,15 leu2-3,112 trp1-1 ura3-1 zds1::TRP erg3::HIS3 pdr1::hisG pdr3::hisG pYES2::GAL1p-MCK1</i>	Wangkangwan et al., 2009

*S. cerevisiae* mutant cells were cultivated on YPAUD (yeast extract peptone dextrose supplemented with adenine and uracil) or YPR (yeast extract peptone raffinose) medium at 30°C with shaking at 200 rpm for 2 d. For yeast transformants bearing plasmid with *URA3* marker, the cells were cultivated in SR-Ura (synthetic complete uracil drop out medium with 2% raffinose).

### 3.6 Source of 5-hydroxy-3,7-dimethoxyflavone

5-hydroxy-3,7-dimethoxyflavone or 5-OH-3,7-DMF from *K. parviflora* was previously isolated, identified and reported in Boonkerd et al., 2014.

### 3.6 Effect of 5-OH-3,7-DMF on growth of $\Delta zds1$ cells (YNS17 strain)

To see whether 5-OH-3,7-DMF inhibited the  $\text{Ca}^{2+}$ -signaling pathways or not, phenotype of  $\Delta zds1$  cells was observed. If 5-OH-3,7-DMF could inhibit the  $\text{Ca}^{2+}$ -signaling pathways, then the growth defect phenotypes should be alleviated. In the experiment, yeast YNS17 cells were seeded at  $5 \times 10^6$  cells/mL in YPAUD broth either in the presence or absence of 5-OH-3,7-DMF including 500, 250 and 125  $\mu\text{M}$  (250 nM FK506 or 1.5% DMSO as positive and negative controls) at 30 °C for 30 min before the addition 100 mM  $\text{CaCl}_2$  in YPAUD medium and cultured at 30°C. The growth of  $\Delta zds1$  cells was monitored. Samples were taken every 4 h until 20 h for measurement of the cell density with a hemocytometer under light microscopy with appropriate dilution.

### 3.7 Effect of 5-OH-3,7-DMF on $\Delta zds1$ cells overexpressed calcineurin (YRC1 strain)

The growth-promoting effect of 5-OH-3,7-DMF in the YRC1 strain was evaluated in liquid culture in YPG (yeast extract peptone raffinose supplemented with 2% galactose) medium. YRC1 cells were seeded at  $5 \times 10^6$  cells/mL in YPR broth and cultured at 30°C with various concentrations of 5-OH-3,7-DMF including 500, 250 and 125  $\mu\text{M}$  (250 nM FK506 or 1.5% DMSO as positive and negative controls) for 30 min before the addition of 2% galactose in YPR medium and cultured at 30°C. Samples were taken every 12 h until 48 h for measurement of the cell density with a hemocytometer under light microscopy with appropriate dilution.

### **3.8 Effect of 5-OH-3,7-DMF on $\Delta zds1$ cells overexpressed Swe1 (YRC2 strain)**

The growth-promoting effect of 5-OH-3,7-DMF in the YRC2 strain was observed in liquid culture in YPG medium. YRC2 cells were seeded at  $5 \times 10^6$  cells/mL in YPR broth and cultured at 30°C with various concentrations of 5-OH-3,7-DMF including 500, 250 and 125  $\mu$ M (10  $\mu$ M radicicol or DMSO as positive and negative controls) for 30 min before the addition of 2% galactose in YPR medium and cultured at 30°C. Samples were taken every 12 h until 48 h for measurement of the cell density with a hemocytometer under light microscopy with appropriated dilution.

### **3.9 Effect of 5-OH-3,7-DMF on $\Delta zds1$ cells overexpressed Mpk1 (NSC1 strain)**

The growth-promoting effect of 5-OH-3,7-DMF in the NSC1 strain was studied in liquid culture in SR-Ura medium. NSC1 cells were seeded at  $5 \times 10^6$  cells/mL in YPR broth and cultured at 30°C with various concentrations of 5-OH-3,7-DMF including 500, 250 and 125  $\mu$ M (DMSO as negative controls) for 30 min before the addition of 2% galactose in YPR medium and cultured at 30°C. Samples were taken every 12 h until 48 h for measurement of the cell density with a hemocytometer under light microscopy with appropriated dilution.

### **3.10 Effect of 5-OH-3,7-DMF on $\Delta zds1$ cells overexpressed Mck1 (NSC2 strain)**

The growth-promoting effect of 5-OH-3,7-DMF in the NSC2 strain was monitored in liquid culture in SR-Ura medium. NSC2 cells were seeded at  $5 \times 10^6$  cells/mL in YPR broth and cultured at 30°C with various concentrations of 5-OH-3,7-DMF including 500, 250 and 125  $\mu$ M (10  $\mu$ M GSK-3 $\beta$  inhibitor I or DMSO as positive and negative controls) for 30 min before the addition of 2% galactose in YPR medium and cultured at 30°C. Samples were taken every 12 h until 48 h for measurement of the cell density with a hemocytometer under light microscopy with appropriated dilution.

### 3.11 *In vitro* GSK-3 $\beta$ activity assay

#### 3.11.1 Kinase-Glo<sup>®</sup> luminescent kinase assay platform

The Kinase-Glo<sup>®</sup> luminescent kinase assay platform provided a homogeneous, high-throughput screening method for measuring kinase activity by quantitating the amount of ATP remaining in solution following a kinase reaction. The Kinase-Glo<sup>®</sup> Assays were performed in a single well of a multiwell plate by adding a volume of Kinase-Glo<sup>®</sup> Reagent equal to the volume of a complete kinase reaction and measuring luminescence (Figures 3.1). The luminescent signals were correlated with the amount of ATP present and were inversely correlated with the amount of kinase activity.

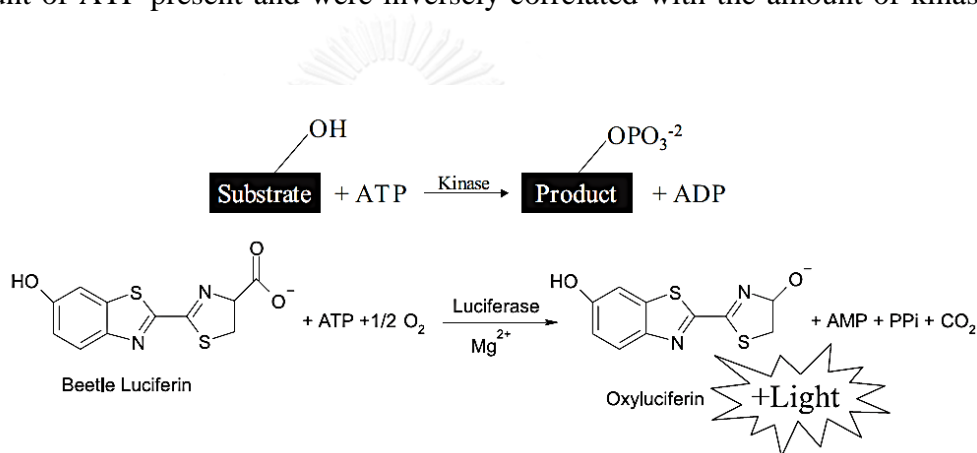


**Figure 3. 1** The Kinase-Glo<sup>®</sup> Assay reactions modified from [www.promega.com](http://www.promega.com). The kinase reaction is conducted under the appropriate conditions. ATP remaining at the time that the reagent is added is used as a substrate by the Ultra-Glo<sup>™</sup> Luciferase to catalyze the mono-oxygenation of luciferin. The luciferase reaction produces one photon of light per turnover. Luminescence is inversely related to kinase activity (Promega, USA).

### 3.12 Optimization of GSK-3 $\beta$ kinase Reaction Conditions

Kinase-Glo<sup>®</sup> plus assays were performed in assay buffer using white 96-well plates in total volume of 50  $\mu$ l per well and constant ATP concentrations at 100  $\mu$ M. The assay was optimized with regard to enzyme concentration, substrate and concentration and incubation time.

### 3.12.1 ATP standard curve

The ATP concentration was prepared in a serial dilutions across the plate using 140, 120, 100, 80, 60, 40, 20, 18, 16, 14, 12, 10, 8, 6, 4, 2, 0  $\mu\text{M}$  in the reaction buffer (40 mM Tris pH 7.5, 20 mM  $\text{MgCl}_2$  and 0.1 mg/mL BSA) in total volume of 50  $\mu\text{l}$  prior to addition of equal volume of reaction Kinase-Glo<sup>®</sup> plus reagent. The reaction solution mixed well and incubated at room temperature for 10 min to stabilize the luminescent signal. The reaction was measured the Glow-type luminescence signal using a Synergy HT Multi-Mode microplate reader (BioTek<sup>®</sup> Instruments Inc., Vermont, USA).

### 3.12.2 Determination of optimal substrate concentration

The peptide kinase substrate concentrations were prepared as a serial dilutions across the plate using 150, 100, 90, 80, 70, 60, 50, 25, 12.5, 0  $\mu\text{M}$  and were mixed with a constant concentration of GSK-3 $\beta$  active enzyme (100  $\mu\text{M}$ ) and ATP (100  $\mu\text{M}$ ) in the reaction buffer (40 mM Tris pH 7.5, 20 mM  $\text{MgCl}_2$  and 0.1 mg/mL BSA) in total volume of 50  $\mu\text{l}$ . For a control, the same titration without GSK-3 $\beta$  active enzyme was performed. The reaction were mixed well and incubated at room temperature for 180 min. Then, equal volume of reaction Kinase-Glo<sup>®</sup> plus reagent was added to stop enzyme reaction and incubated at room temperature for 10 min to stabilize the luminescent signal. The luminescence signal was measured using multimode microplate reader. The optimal kinase substrate concentration was obtained by comparing kinase reaction wells that having largest change in luminescence to wells that did not contain kinase or the enzyme reaction at the early stationary phase of enzyme reaction.

### 3.12.3 Determination of the optimal amount of GSK-3 $\beta$ kinase

The GSK-3 $\beta$  active enzyme concentrations were made as a serial dilutions across the plate using 150, 100, 50, 25, 12.5, 0  $\mu\text{M}$  and were mixed with a constant concentration of peptide kinase substrate (100  $\mu\text{M}$ ) and ATP (100  $\mu\text{M}$ ) in the reaction buffer (40 mM Tris pH 7.5, 20 mM  $\text{MgCl}_2$  and 0.1

mg/mL BSA) in total volume of 50  $\mu$ l. As a control, the same titration without peptide kinase substrate was performed. The reaction was mixed well and incubated at room temperature for 180 min. Equal volume of reaction Kinase-Glo<sup>®</sup> plus reagent was added to stop enzyme reaction and the plate was incubated at room temperature for 10 min to stabilize the luminescent signal. The luminescence signal was measured using multimode microplate reader. The kinase concentration which resulted in the largest change in luminescence when comparing kinase reaction wells to wells that did not contain kinase or the enzyme reaction at the early stationary phase of enzyme reaction was the optimal kinase concentration.

### **3.13 Determination of the GSK-3 $\beta$ enzyme activity**

GSK-3 $\beta$  assays were performed using the Kinase Glo<sup>®</sup> Plus luminescent kinase assay platform in a white flat bottom 96-well plate. The optimized peptide kinase substrate concentration (100  $\mu$ M) was mixed with recombinant human GSK-3 $\beta$  (100  $\mu$ M or 0.01098 unit) in a total volume of 50  $\mu$ l of assay buffer (40 mM Tris pH 7.5, 20 mM MgCl<sub>2</sub> and 0.1 mg/mL BSA) containing 100  $\mu$ M ATP. The reaction contents were mixed and incubated at room temperature. The reaction Kinase-Glo<sup>®</sup> plus reagent of 50  $\mu$ l was added and mixed well at 0, 30, 45, 60, 75, 90, 105 and 120 min of reaction time mixed well and incubated at room temperature for 10 min to stabilize the luminescent signal. Then, the plate was measured of the luminescence signal using multimode microplate reader.

### **3.14 Determination of the Km and Vmax of GSK-3 $\beta$ enzyme**

The peptide kinase substrate concentrations were made in a serial dilutions across the plate using 0, 10, 25, 50, 80, 100  $\mu$ M with a constant concentration of human GSK-3 $\beta$  (0.01098 unit) and ATP (100  $\mu$ M) in the reaction buffer (40 mM Tris pH 7.5, 20 mM MgCl<sub>2</sub> and 0.1 mg/mL BSA) in total volume of 50  $\mu$ l. The reaction contents were mixed and incubated at room temperature. The reaction Kinase-Glo<sup>®</sup> plus reagent of 50  $\mu$ l was added at 0, 30, 45, 60, 75, 90, 105 and 120 min of reaction time in each peptide kinase substrate concentration. The reaction were mixed well



and incubated at room temperature for 10 min to stabilize the luminescent signal and was measured of the luminescence signal using multimode microplate reader. The  $K_m$  and  $V_{max}$  values were measured using Michaelis-Menten kinetic and Lineweaver-Burk plotting using GraphPad Prism® software.

### **3.15 Determination of $IC_{50}$ value and percentage of inhibition of 5-OH-3,7-DMF in inhibitory activity of human GSK-3 $\beta$**

GSK-3 $\beta$  assays performed in a white flat bottom 96-well plate with peptide kinase substrate (100  $\mu$ M) were mixed with recombinant human GSK-3 $\beta$  (0.01098 unit) in a total volume of 50  $\mu$ l of assay buffer (40 mM Tris (pH 7.5), 20 mM MgCl<sub>2</sub> and 1.5  $\mu$ M BSA) containing 100  $\mu$ M ATP in the presence of inhibitor in varying concentrations of 0, 10, 20, 50  $\mu$ M of 5-OH-3,7-DMF or GSK-3 $\beta$  inhibitor I (a positive control) and DMSO (a negative control). The reaction contents were mixed well and incubated at room temperature for 2 h. The enzymatic reaction was stopped by addition of 50  $\mu$ l of reaction Kinase-Glo® plus reagent and incubated at room temperature for 10 min to stabilize the luminescent signal. Prior to measurement of the Glow-type luminescence signal using microplate reader. The  $IC_{50}$  of the inhibitor was analyzed using GraphPad Prism® sigmoidal dose-response (normalized response) software. The percentage of inhibition were performed in the same condition containing 100  $\mu$ M of 5-OH-3,7-DMF or 100  $\mu$ M GSK-3 $\beta$  inhibitor I (a positive control) and DMSO (a negative control). The percentage of inhibition was calculated as follows:

$$\text{Inhibition (\%)} = \frac{\text{sample} - \text{control 1 (with substrate)}}{\text{control 2 (without substrate)} - \text{control 1 (with substrate)}} \times 100$$

### **3.16 Determination of the inhibition pattern of 5-OH-3,7-DMF on human GSK-3 $\beta$ protein**

ATP-competitive analysis was performed with varying both ATP levels (20, 50 and 100  $\mu$ M) and 5-OH-3,7-DMF concentrations (0, 10, 20 and 50  $\mu$ M) with a constant concentration of peptide kinase substrate (100  $\mu$ M) and recombinant human GSK-3 $\beta$  (0.01098 unit) in 50  $\mu$ l of assay buffer (40 mM Tris (pH 7.5), 20 mM MgCl<sub>2</sub> and 1.5  $\mu$ M BSA). The reaction was mixed well and incubated at room temperature before adding of 50  $\mu$ l of reaction Kinase-Glo<sup>®</sup> plus reagent at 0, 30, 60, 90 and 120 mins of reaction time in each condition and incubated at room temperature for 10 mins to stabilize the luminescent signal. The luminescence signal was measured using multimode microplate reader. In substrate-competitive inhibition, both peptide kinase substrate (10, 25, 50 and 100  $\mu$ M) and 5-OH-3,7-DMF concentrations (0, 10, 20 and 50  $\mu$ M) were varied in their concentration with a constant concentration of recombinant human GSK-3 $\beta$  (0.011 unit) and ATP level (100  $\mu$ M). The K<sub>m</sub> and V<sub>max</sub> value were analyzed using Michaelis-Menten kinetic and Lineweaver-Burk plotting. The K<sub>i</sub> value was measured by Dixon plotting using GraphPad Prism<sup>®</sup> software.

### **3.17 Human cancer cell line**

Human hepatoma HepG2 cells ATCC number HB-8065 was obtained from the Institute of Biotechnology and Genetic Engineering, Chulalongkorn University.

### **3.18 Cell culture**

HepG2 cells were cultured in RPMI-1640 with L-Glutamine supplemented with 10% fetal bovine serum, 10<sup>6</sup> U/mL penicillin, 500 mg/mL streptomycin, sodium pyruvate and HEPES. The cells were maintained at 37°C in a humidified incubator in 5% CO<sub>2</sub> containing atmosphere. The cells were examined under microscope. The media was changed every 2 - 3 d.

### **3.19 Cell subculturing of HepG2 (adherent cells)**

The complete medium was brought to 37°C in the water bath. After removing and discarding the medium. The cells were gently washed with PBS (phosphate buffered saline). After removing the buffer the pre-warmed trypsin was added to cover the cell layer. The T-flask was gently rocked to get complete coverage of the cell layer. The cells were incubated at 37°C in 5% CO<sub>2</sub> for approximately 5-10 min. The cells were observed under microscope. Then, the complete medium (twice the volume used for the trypsin) was added to the flask containing detached cells, and the cells were dispersed by pipetting over the cell layer surface several times. The cells were transferred to centrifuge tube and centrifuged at 1000×g for 5 min then removing the supernatant. Cell pellet were resuspended in complete medium. The cells suspensions were transferred to complete medium by determining the total number of cells and percent viability. The cultures were incubated at 37°C in 5% CO<sub>2</sub> containing atmosphere.

### **3.20 Cryopreservation procedure**

The freezing medium (Appendix A) was prepared for cell culture. The cells were collected by centrifuged for 5 min at 1000 × g and resuspended in freezing medium. Then, 1 mL of the cell suspensions were added to each of the vial and sealed. The vial was placed into 4°C or on ice and quickly transferred to a liquid nitrogen tank or -80°C freezer.

### **3.21 Recovery of cryopreserved cells**

A complete medium was prepared in T-flask. The vial from liquid nitrogen or -80°C freezer was quickly removed and thawed by gentle agitation at 37°C. The cell suspensions were transfer to sterile centrifuge tube containing 5 mL of RPMI-1640 medium free serum and centrifuged at 1000× g for 5 min. The supernatant was discarded and resuspended in 1- 2 mL of complete medium. The cell pellets were gently mixed to loosen the pellet before transferring the cell suspension into the medium in T-flask the cell culture was checked for sterility and viability after 24 h.

### 3.22 Trypan blue dye exclusion test

Cells were trypsinized and transferred for centrifugation. The supernatant was discarded, then 1 mL complete media was added. Fourty microliter of the cell suspension was transferred to a new microcentrifuge tube. Equal volume of 0.5% (w/v) trypan blue was added and mixed. Then, 10  $\mu$ l of the cell suspensions were transferred to hemocytometer for counting. Finally, the unstained cells were counted under microscope and the cell viability was calculated using the formula as follow:

$$\text{Cell viability (cells/mL)} = (\text{unstained cells} / 4) \times 10^4 \times 2$$

### 3.23 MTT viability assay

MTT viability assay which is a modified colorimetric method (Mosmann, 1983). The HepG2 cells were seeded in 96-well plates at a concentration of  $5 \times 10^4$  cells/well in 100  $\mu$ l RPMI complete medium containing 10% fetal bovine serum (FBS). The culture was incubated at 37°C in humidified atmosphere of 5% CO<sub>2</sub>. The cells were allowed to attach to the surface of well for at least 24 h. After that, the medium was changed to 100  $\mu$ l RPMI complete medium; 10% FBS, One hundred microliter containing 0.5% DMSO and with or without varied concentrations of crude extracted of test samples and were incubated for 1 d. Subsequently, 10  $\mu$ l of 5 mg/mL MTT (3-(4,5-dimethylthiazol-2-yl)-2,5-diphenyltetrazolium bromide) was added to each well, and cells were incubated for an additional 4 h at 37 °C in a humidified atmosphere of 5% CO<sub>2</sub> . Finally, 100  $\mu$ l of isopropanol was added to each well. The optical density of the dissolved material was measured by a microplatereader at 540 nm. The cell survival was expressed as percentage of viable cells of treated samples to control samples. The test was performed in triplicates.

$$\% \text{Viability} = \frac{\text{OD test average} - \text{OD blank average}}{\text{OD control cell average} - \text{OD blank average}} \times 100$$

OD test average = The average value of optical density of treated cells

OD control cell average = The average value of optical density of cells in complete medium

OD blank average = The average value of optical density of medium

### **3.24 Insulin-resistant HepG2 cell model (IRM)**

Human HepG2 cells were grown in 2 mL RPMI medium supplemented with 10% FBS,  $10^6$  U/mL penicillin, 500 mg/mL streptomycin, sodium pyruvate and HEPES. Cells were maintained at 37 °C in a humidified atmosphere of 5% CO<sub>2</sub>. After plating in 6-well for 24 h at a concentration of  $1 \times 10^6$  cells/well, the medium was changed to 2 mL RPMI containing various concentrations of D-glucose (10, 20, 30, 40, 50 mM), FBS-free medium. Subsequently, the medium was exchanged with FBS-free medium containing 25 mM D-glucose with various concentration of insulin (100, 10, 1, 0.1, 0.01  $\mu$ M) also called “high glucose and high insulin medium” (HGHI). The incubation was conducted in this medium for 24 h.

### **3.25 Effect of 5-OH-3,7-DMF on insulin-resistant HepG2 cell model**

Human HepG2 cells were grown in 2 mL RPMI medium supplemented with 10% FBS,  $10^6$  U/mL penicillin, 500 mg/mL streptomycin, sodium pyruvate and HEPES. Cells were maintained at 37 °C in a humidified atmosphere of 5% CO<sub>2</sub>. The treatment group was separated into two groups. First, the cells were treated before IRM induction (pre-treatment) as follows; After plating in 6-well for 24 h at a concentration of  $1 \times 10^6$  cells/well, the medium was changed to 2 mL RPMI containing 25 mM D-glucose, 0.5% DMSO, FBS-free medium supplemented with or without various concentrations of CE (15, 10, 5  $\mu$ g/mL), 5-OH-3,7-DMF (62.5, 31.25, 15.625  $\mu$ M) compared to both of positive controls, GSK-3 $\beta$  Inhibitor I (20, 10  $\mu$ M) and LiCl (10, 1, 0.5 mM). Subsequently, the medium was exchanged with FBS-free medium 25 mM D-glucose containing 500 nM insulin (HGHI). Second, the cells were treated after IRM induction (post-treatment) as follows; After plating in 6-well for 24 h at a concentration of  $1 \times 10^6$  cells/well, the medium was changed to 2 mL RPMI containing 25 mM D-glucose, 0.5% DMSO, FBS-free medium. Subsequently, the medium was exchanged with FBS-free medium 25 mM D-glucose containing 500 nM insulin (HGHI) supplemented with CE (15  $\mu$ g/mL), 5-OH-3,7-DMF (62.5  $\mu$ M) compared to the both of positive controls, GSK-3 $\beta$  Inhibitor I (20  $\mu$ M) and LiCl (10 mM). The incubation was conducted in this medium for 24 h then the cells were harvested.

### 3.26 Determination of glycogen content

To measure the content of glycogen, Glycogen Assay Kit (Sigma, USA) was used. HepG2 cells were seeded in 6-well plates at a density of  $1 \times 10^6$  cells/well in 2 mL RPMI medium supplemented with 10% FBS,  $10^6$  U/mL penicillin, 500 mg/mL streptomycin, sodium pyruvate and HEPES. Following 24 h of stabilization, the cells were treated with or without sample as in previous described method in section 3.25. After harvesting, cells were washed twice with cold phosphate buffer saline (PBS) and resuspended in 200  $\mu$ l of double distilled water (ddH<sub>2</sub>O) on ice; The cells were homogenized quickly by pipetting up and down a few times. Then, the homogenates were boiled for 10 min to inactivate enzymes in the samples. The boiled samples were centrifuged at  $18,000 \times g$  for 10 min at 4°C to remove any insoluble materials. The supernatant were collected and transferred to new tubes. The samples were adjusted to a final volume of 50  $\mu$ l with the Hydrolysis Buffer in 96-well plate. Two microliter of the Hydrolysis Enzyme Mix was added, mixed well and incubated for 30 min at room temperature. Subsequently, Fifty microliter of the Master Reaction Mix (Development Buffer 46  $\mu$ l, Development Enzyme Mix 2  $\mu$ l, Fluorescent Peroxidase Substrate 2  $\mu$ l) was added to each of the wells, mixed well using a horizontal shaker or by pipetting. The reaction was incubated for 30 min at room temperature in dark. The absorbance was measured at 570 nm (A<sub>570</sub>). Calculation of the concentration of glycogen using the formula as follows:

$$S_a/S_v = C$$

$S_a$  = Amount of glycogen in unknown sample ( $\mu$ g) from standard curve

$S_v$  = Sample volume ( $\mu$ l) added into the wells

C = Concentration of glycogen in sample

### **3.27 Western blot analysis**

#### **3.27.1 Preparation of protein extract from HepG2 cells**

HepG2 cells were seeded on 6-well plates at a density of  $1 \times 10^6$  cells/well in 2 mL RPMI medium supplemented with 10% FBS,  $10^6$  U/mL penicillin, 500 mg/mL streptomycin, sodium pyruvate and HEPES at 37°C in a humidified atmosphere of 5% CO<sub>2</sub>. The cells were treated with or without sample as described in method in section 3.25. Cells were harvested by centrifugation at  $7500 \times g$  for 5 min at 4°C. The cell pellets were then washed with 1 mL of cold PBS and centrifuged at  $7500 \times g$  for 5 min. After that, the cell pellets were resuspended in 40 µl of cold LIPA buffer (the preparation is described in appendix B) for 30 min and centrifuged at  $12,000 \times g$  for 15 min. Finally, the supernatant was transferred into a new microcentrifuge tube and kept at -80°C.

#### **3.27.2 Protein determination by BCA assay**

The standard proteins BCA (2 mg/mL) were added as gradient volume to each well followed by adding of sample protein (1 µl/well). After that BCA reagent (Thermo Scientific, USA) was added and the plate was incubated at 37°C for 30 min in dark. The absorbance was measured at 540 nm by a microplate reader. Then, a standard curve was plotted using data of various concentration of standard protein and concentrations of protein samples were determined from the standard curve's equation.

#### **3.27.3 SDS-polyacrylamide gel electrophoresis (SDS-PAGE)**

Samples were mixed with sample buffer (loading buffer) and boiled in boiling water for 5 min. The prepared samples and protein marker were loaded into wells of 10% SDS-polyacrylamide by following the protocol as described in Laemmli et al. (1976). The Electrophoresis was performed with 80 voltages for 150 min.

### 3.27.4 Western Blot Analysis

Proteins were transferred onto PVDF membrane. The membrane was blocked in a blocking buffer (5% of skim milk in PBST (preparation is described in appendix B)) for 60 min. After that, the membrane was incubated with appropriate primary antibody in the blocking buffer at 4°C overnight, followed by incubation with appropriate secondary antibody for 1 h at room temperature. The bands were detected using chemiluminescent reagent (Bio-Rad, USA) and the membrane was exposed to autoradiographic film (GE healthcare, Sweden);  $\beta$ -actin expression level was used as a gel loading control.

## 3.28 Determination of G6Pase expression by real-time PCR

### 3.28.1 RNA extraction

HepG2 cells were seeded on 6-well plates at a density of  $1 \times 10^6$  cells/well in 2 mL RPMI medium supplemented with 10% FBS,  $10^6$  U/mL penicillin, 500 mg/mL streptomycin, sodium pyruvate and HEPES at 37°C in a humidified atmosphere of 5% CO<sub>2</sub>. The cells were treated with or without sample as described in method in section 3.25. The cells were harvested by centrifuged at  $4200 \times g$  for 5 min and the supernatant was discarded. The cell pellets were resuspended in 1 mL of TriZol reagent (Invitrogen, USA), incubated at room temperature for 5 min. After that, 200  $\mu$ l of chloroform was added; Tubes were vortexed and incubated at room temperature for a few minutes, and then centrifuged at  $12000 \times g$  for 15 min at 4°C. The supernatant was transferred into a new tube. Equal volume of isopropanol was added, follow by incubation at room temperature for 10 min. Then, tubes were subjected to centrifugation at  $12000 \times g$  for 10 min at 4°C. After discarding the supernatant, the RNA pellet was washed with 1 mL of 75% ethanol and dissolved in DEPC water (Sigma, USA). After centrifugation at  $7500 \times g$  for 5 min, supernatant was discarded and the RNA pellet was dried. RNA will then be dissolved in DEPC water and then incubated at 60°C for 10 min. The concentration of RNA was measured by NanoDrop™ spectrophotometers (KAIA Bio-Ingeneiria, Korea) at 260 nm and 280 nm compared to those of DEPC water.



### 3.28.2 Generate complementary DNA (cDNA) by reverse transcriptase

To generate complementary DNA (cDNA), the RNA from section 3.28.1 approximately 0.1-1 µg was added into PCR tube, then 1 µl of Random hexamer primer (Fermentas, Canada) 0.2 µg/µl were added to 12.5 µl by DEPC water. The tube was mixed and centrifuged about 2-3 second and transferred to DNA Thermal Cycle T100™ (Bio-Rad, USA) at 65°C for 5 min and 4°C for 5 min, respectively. Four µl of 5X Reverse Transcriptase buffer (Fermentas, Canada), 2 µl of dNTP Mix (Fermentas, Canada) at concentration 10 mM and 0.5 µl of Ribonuclease inhibitor (Fermentas, Canada) at concentration 40 units/µl were added and then mixed and centrifuged for 2-3 second. The tube was incubated at room temperature for 5 min. Then 1 µl of Reverse transcriptase (Fermentas, Canada) at concentration 200 units/µl was added and incubated at room temperature for 10 min. After that, the reaction was continued at 25°C for 10 min and 42°C for 60 mins on DNA Thermal Cycle T100™ respectively, Finally, the reaction was stopped by heating to 70°C for 10 min and the cDNA samples were kept at -20°C.

### 3.28.3 One-step real time polymerase chain reaction (RT-PCR)

The cDNA from section 3.28.2 was used as a template in the reaction and the specific primers for *G6Pase* were fwd: 5'-TCATCTTGGTGTCCGTGATCG-3' and rev: 5'-TTTATCAG GGGCACGGAAGTG-3' and the primer used to amplified *β-actin* were fwd: 5'-TTCCTTCCTGGGCATGGAGT-3' and rev: 5'- CCAGGGCAGT GATCTCCTTC-3' (Kang et al. 2010) at concentration of 10 µM. The reaction was performed using a DNA Thermal Cycle T100™ follow by adding the components listed in Table 3.4. The PCR condition was as follows: 95°C for 5 min, followed by 35 cycles of 94°C for 30 sec, 55°C for 30 sec and 72°C for 30 sec. and a final extension at 72°C for 5 min.

**Table 3. 4** Components and reagents for real time polymerase chain reaction (RT-PCR)

Component	Concentration	Volume	Final Concentration
<i>Taq</i> Reaction Buffer	10X	2.5 $\mu$ l	1X
dNTPs	10 mM	0.5 $\mu$ l	200 $\mu$ M
Forward Primer	10 $\mu$ M	0.5 $\mu$ l	0.2 $\mu$ M
Reverse Primer	10 $\mu$ M	0.5 $\mu$ l	0.2 $\mu$ M
cDNA	1 $\mu$ g	4 $\mu$ l	500 ng
<i>Taq</i> DNA Polymerase	25 units/mL	0.125 $\mu$ l	0.625 units/mL
Nuclease-free water		16.87 $\mu$ l	

### 3.29 Statistical analysis

The Tukey's multiple comparison test, one-way ANOVA were performed to determine statistical significance of the growth curve of yeast-based assays.

The Dunnett's Multiple Comparison test, one-way ANOVA were performed to determine statistical significance of percentage of GSK-3 $\beta$  enzyme inhibition, MTT assay, G6Pase expression, GS expression, GSK-3 expression and glycogen content assay.

Enzyme kinetic analysis were performed to determine statistical significance of enzyme kinase activity as follows; Michaelis-Menten analysis,  $K_i$  analysis, Competitive inhibitor and non-competitive inhibitor analysis, Normalized response (sigmoidal dose-response). All of these statistical analyses were performed by GraphPad Prism<sup>®</sup> 5, USA.

## CHAPTER IV

### RESULTS

#### **4.1 5-OH-3,7-DMF could restore growth defect and abnormal bud morphology of on growth of $\Delta zds1$ cells (YNS17 strain).**

To see whether 5-OH-3,7-DMF inhibited the  $\text{Ca}^{2+}$ -signals, phenotype of  $\Delta zds1$  cells was observed. The calcium hyperactivation caused growth defect (G2/M delay) in  $\Delta zds1$  cells (Mizunuma et al. 1998). If 5-OH-3,7-DMF could inhibit the  $\text{Ca}^{2+}$ -signals, then the growth defect phenotypes should be alleviated. In the experiment, yeast  $\Delta zds1$  cells were grown in YPAUD broth either in the presence or absence of 5-OH-3,7-DMF. The growth of  $\Delta zds1$  cells was monitored. It was found that the growth of the yeast  $\Delta zds1$  cells was severely defected when cultivated under induced condition (100 mM  $\text{CaCl}_2$ ). However, in the presence of 500, 250 and 125  $\mu\text{M}$  5-OH-3,7-DMF even cultivated in the induced condition, the growth defect could be restored to the similar extent as that of control (uninduced condition) in dose dependent manner and in the presence of 250 nM FK506 (Figure 4.1 (a.)) and restored the abnormal bud morphology (Figure 4.1 (b.)). The results confirmed that 5-OH-3,7-DMF has an inhibitory activity against the  $\text{Ca}^{2+}$ -induced G2 cell-cycle arrest.

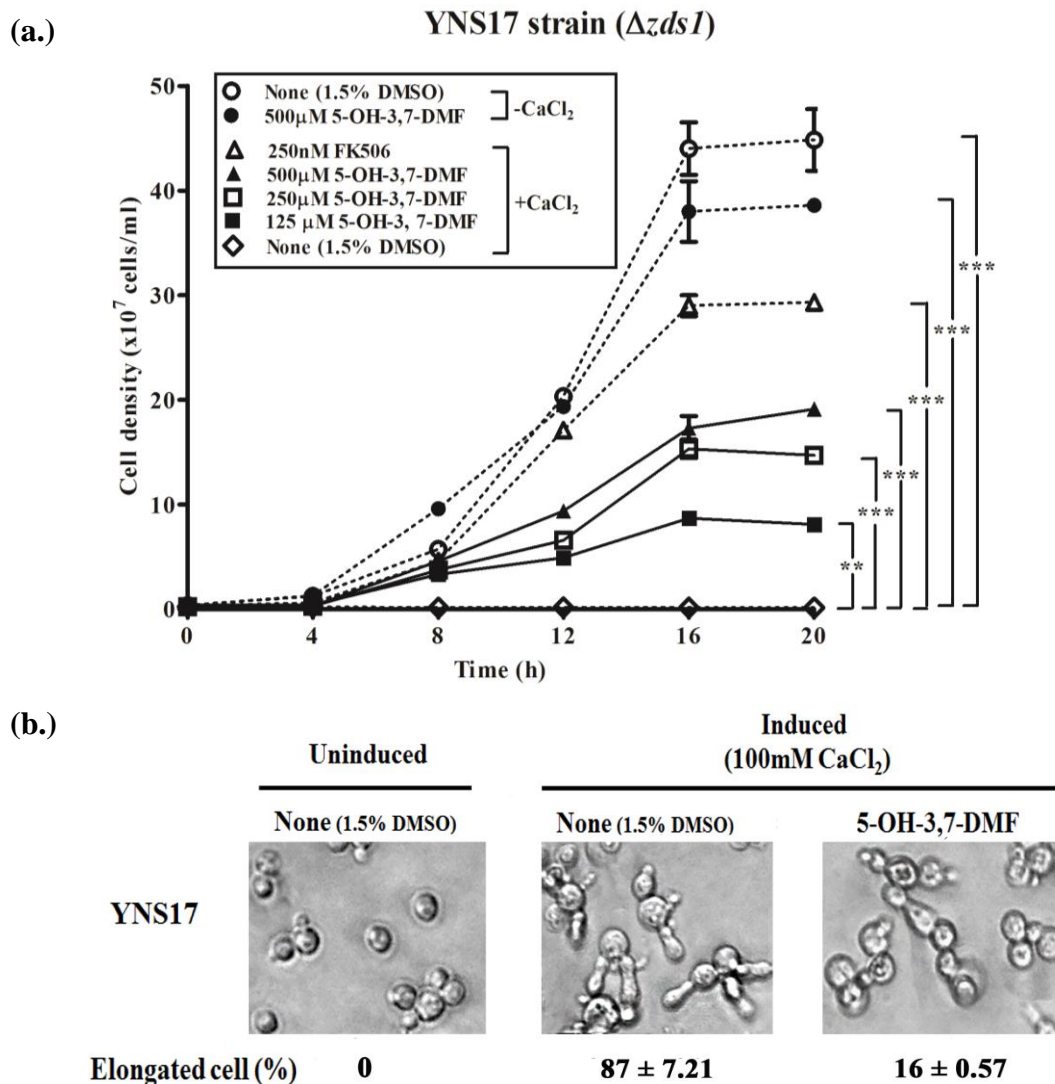
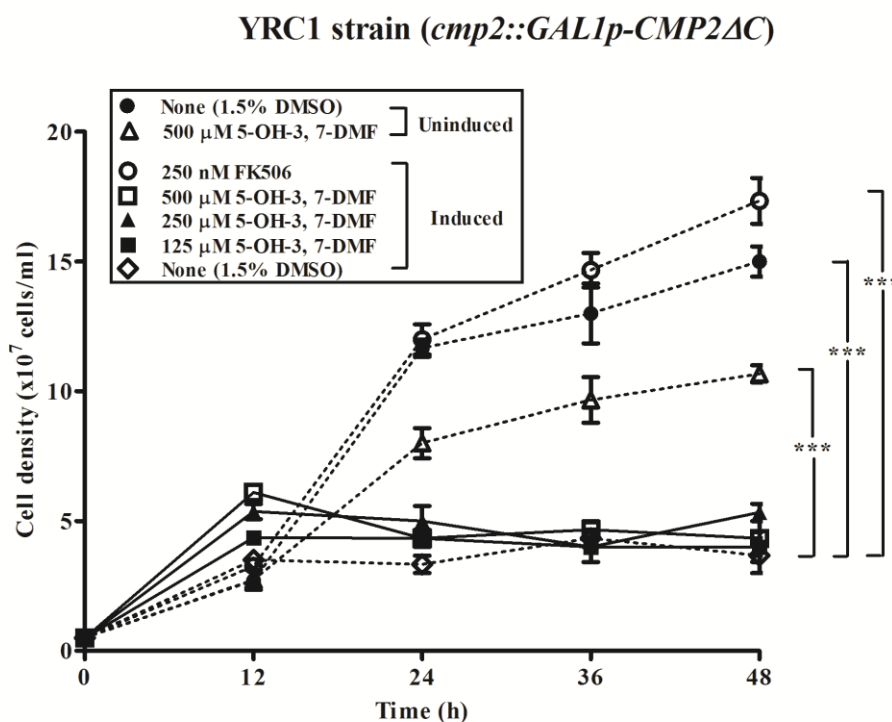


**Figure 4.1** The effect of 5-OH-3,7-DMF on the growth of  $\Delta zds1$  mutant yeast YNS17 cells. (a.); The mutant yeast  $5 \times 10^6$  cells/mL were cultivated under hyperactivation of  $\text{Ca}^{2+}$ -signals by 100 mM  $\text{CaCl}_2$  in YPAUD medium in either presence or absence of 5-OH-3,7-DMF at 30°C with shaking at 200 rpm. The cell density was measured using hemocytometer every 4 h until 20 h. The data showed values of mean  $\pm$  SD from the triplicate experiments. \*\*, \*\*\*Significant differences at  $p$ -value  $< 0.01$  and  $p$ -value  $< 0.001$ , respectively as compared with the control group using Tukey's multiple comparison test. (b.); The cell morphology of  $\Delta zds1$  mutant yeast cells under microscope (X400). The mutant yeast showed elongated cells under induced condition (100 mM  $\text{CaCl}_2$ ) and after treating with 5-OH-3,7-DMF the cells showed normal bud morphology. % elongated cell = number of elongated cells in 100 cells.

**4.2 5-OH-3,7-DMF targeted MPK1 MAPK cascade of the Ca<sup>2+</sup>-signaling pathways due to restored growth defect and abnormal bud morphology of  $\Delta zds1$  cells overexpressed *MPK1* gene (NSC1 strain) but did not inhibit the pathways via calcineurin pathway.**

The Ca<sup>2+</sup>-signals in yeast cells were transduced in two parallel pathways: calcineurin or MPK1 MAPK cascade (Nakamura et al. 1996). To see the effect of 5-OH-3,7-DMF on calcineurin or Mpk1 MAP kinase, the growth of cells overexpressed Mpk1 (the NSC1 strain) and overexpressed Calcineurin (the YRC1 strain) was observed in either presence or absence of 5-OH-3,7-DMF. To induce expression of *MPK1* or *CMP2 $\Delta$ C*, encoding catalytic subunit of calcineurin (Nakamura et al. 1997), under control of *GALI* promoter, the mutant yeast strains were cultivated in YPR medium containing 2% galactose in the presence or absence of 500, 250 or 125  $\mu$ M 5-OH-3,7-DMF having FK506, a potent calcineurin inhibitor as a positive control. The growths of the cultures were monitored for 48 h. The results showed that in the presence of 250 nM FK506, the growth defect could be partially alleviated. However, either in the absence or presence of 5-OH-3,7-DMF, the mutant cells overexpressed *CMP2 $\Delta$ C* (the YRC1 strain) showed severely growth defect (Figure 4.2 (a.) and (b.)). On the other hand, the mutant cells overexpressed *MPK1* (the NSC1 strain) showed the growth defect restoration to the similar extent as that of control (uninduced condition) (Figure 4.3 (a.) and (b.)). These results suggested that MPK1 MAPK cascade was the molecular target of 5-OH-3,7-DMF in the Ca<sup>2+</sup>-signaling pathways in yeast.

(a.)



(b.)

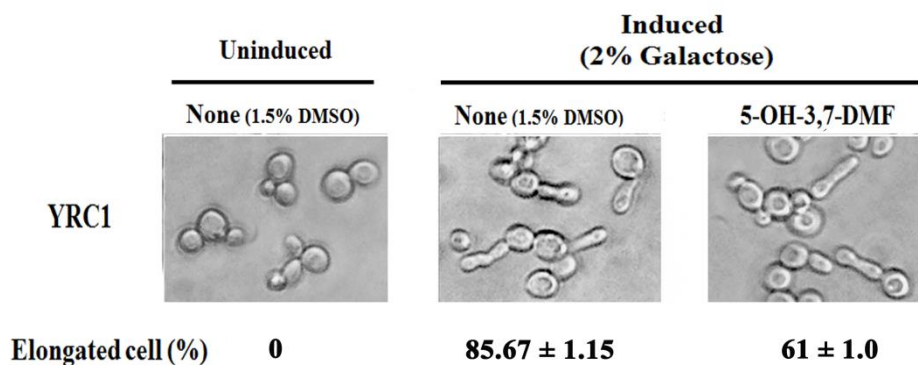
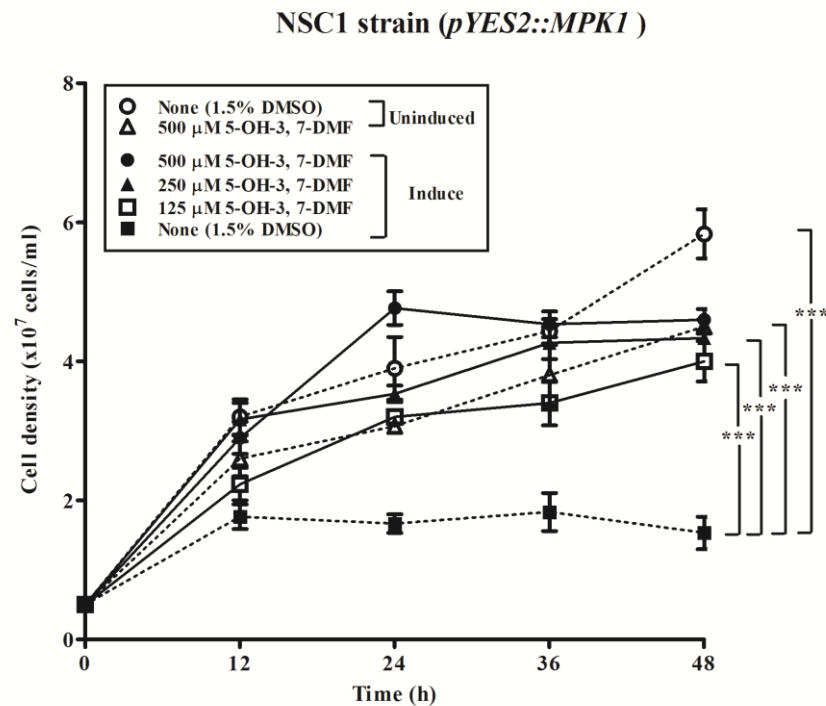


**Figure 4.2** The effect of 5-OH-3,7-DMF on the growth of  $\Delta zds1$  cells overexpressed *CMP2ΔC*. (a.); The YRC1 strain (*cmp2::GAL1p-CMP2ΔC*) of  $5 \times 10^6$  cells/mL were cultivated under induced condition in YPR+2% galactose medium in either presence or absence of 5-OH-3,7-DMF at 30°C with shaking at 200 rpm. The cell density was measured using hemocytometer every 12 h until 48 h. The data showed values of mean  $\pm$  SD from the triplicate experiments. \*\*\*Significant differences at  $p$ -value < 0.001 as compared with the control group using Tukey's multiple comparison test. (b.); The cell morphology of mutant yeast cells under microscope (X400). The mutant yeast showed elongated cells under induced condition (2% galactose) and after treating with 5-OH-3,7-DMF the cells showed abnormal elongated bud morphology. % elongated cell = number of elongated cells in 100 cells.

(a.)



(b.)

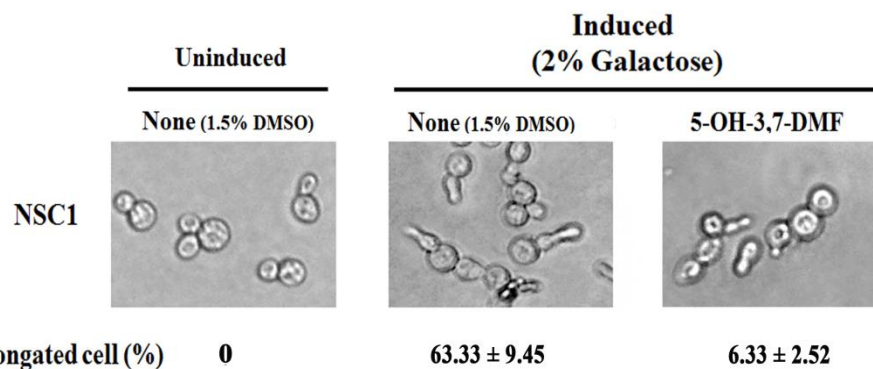


**Figure 4.3** The effect of 5-OH-3,7-DMF on the growth of  $\Delta zds1$  cells overexpressed *MPK1*. (a.); The NSC1 strain bearing *pYES2::MPK1* of  $5 \times 10^6$  cells/mL were cultivated under induced condition in SR-Ura + 2% galactose medium in either presence or absence of 5-OH-3,7-DMF at 30°C with shaking at 200 rpm. The cell density was measured using hemocytometer every 12 h until 48 h. The data showed values of mean  $\pm$  SD from the triplicate experiments. \*\*\*Significant differences at  $p$ -value < 0.001 as compared with the control group using Tukey's multiple comparison test. (b.); The cell morphology of mutant yeast cells under microscope (X400). The mutant yeast showed elongated cells under induced condition (2% galactose) and after treating with 5-OH-3,7-DMF the cells showed normal bud morphology. % elongated cell = number of elongated cells in 100 cells.

### **4.3 Mck1, human ortholog GSK3, a potential molecular target of 5-OH-3,7-DMF in the Ca<sup>2+</sup>-signaling pathways.**

Mizunuma et al. (2001) used genetic analyses of yeast mutants Ca<sup>2+</sup>-signaling pathways and found that Mck1, a component in the pathways, functions downstream of the Mpk1. To see whether 5-OH-3,7-DMF inhibited the Ca<sup>2+</sup>-signals at the step of Mck1 or not, phenotype of  $\Delta zds1$  cells overexpressed *MCK1* (NSC2 strain) was observed. The calcium hyperactivation caused growth defect (G2/M delay) in  $\Delta zds1$  cells (Mizunuma et al. 1998). The  $\Delta zds1$  overexpressed *MCK1* cells should show the similar phenotypes when cultivated under induced condition. If 5-OH-3,7-DMF could inhibit overexpressed Mck1 activity, then the growth defect phenotypes should be alleviated. To see the effect of 5-OH-3,7-DMF on the overexpressed *MCK1* cells, the yeast transformants were prior grown in SR-Ura at 30 °C then, cultivated in SG-Ura broth either in the presence or absence of 500, 250 or 125  $\mu\text{M}$  5-OH-3,7-DMF while 10  $\mu\text{M}$  GSK-3 $\beta$  inhibitor I was used as positive control. The growth of  $\Delta zds1$  overexpressed *MCK1* cells was monitored. It was found that the growth of the yeast transformants overexpressed *MCK1* showed severe defect when cultivated under induced condition (2% galactose). However, in the presence of 500, 250 or 125  $\mu\text{M}$  5-OH-3,7-DMF even cultivated in the induced condition, the growth defect could be restored to somewhat similar extent as that of control (uninduced condition) in dose dependent manner (Figure 4.4 (a.) and (b.)). It was able to note that 5-OH-3,7-DMF up to 500  $\mu\text{M}$  showed no toxicity to the mutant yeast cells (Figure 4.4 (a.)). The results suggested that Mck1 is a possible molecular target of 5-OH-3,7-DMF.



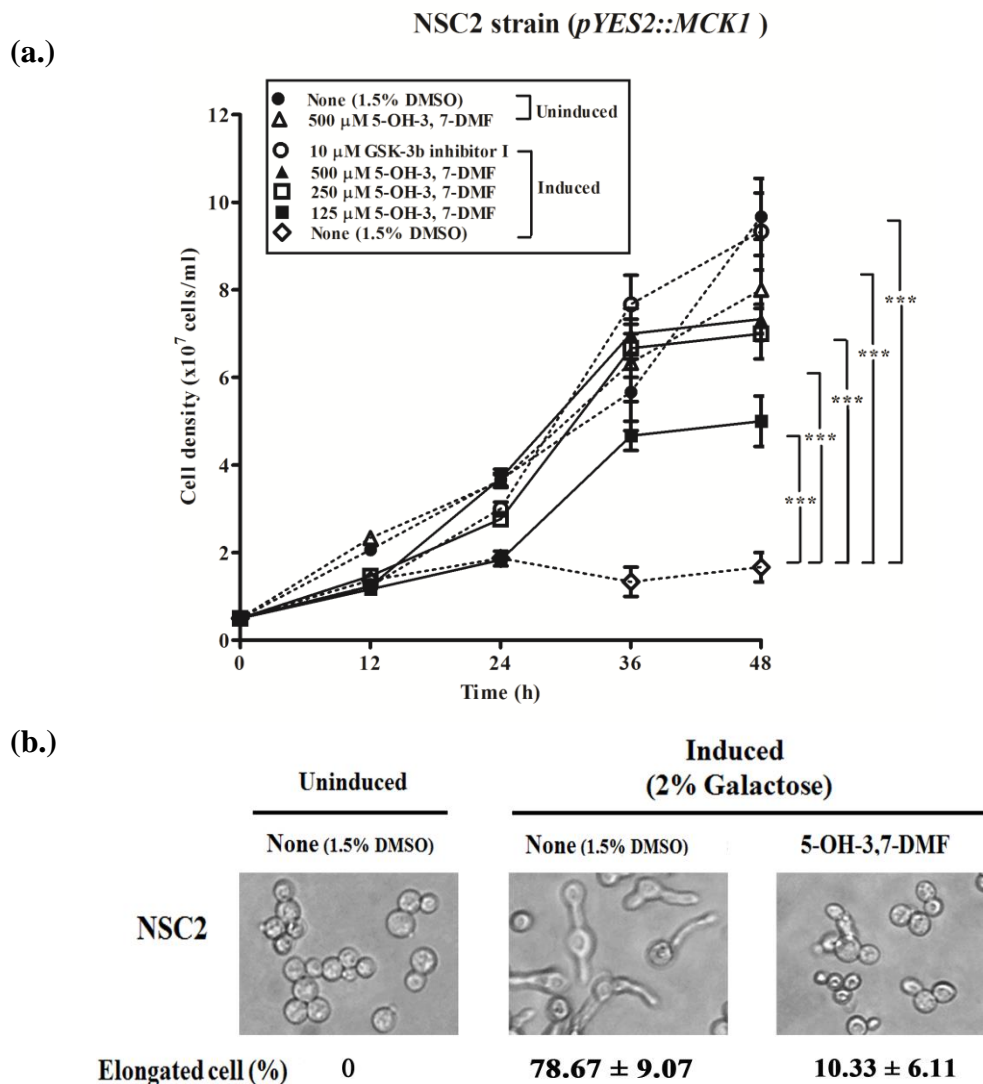


**Figure 4.4** The effect of 5-OH-3,7-DMF on the growth of  $\Delta zds1$  cells overexpressed *MCK1*. **(a.)**; The NSC2 strain bearing *pYES2::MCK1* of  $5 \times 10^6$  cells/mL were cultivated under induced condition in SR-Ura + 2% galactose medium in either presence or absence of 5-OH-3,7-DMF at 30°C with shaking at 200 rpm. The cell density was measured using hemocytometer every 12 h until 48 h. The data showed values of mean  $\pm$  SD from the triplicate experiments. \*\*\*Significant differences at  $p$ -value < 0.001 as compared with the control group using Tukey's multiple comparison test. **(b.)**; The cell morphology of mutant yeast cells under microscope (X400). The mutant yeast showed normal bud morphology after treating with 5-OH-3,7-DMF under induced condition (2% galactose). % elongated cell = number of elongated cells in 100 cells.

#### **4.4 5-OH-3,7-DMF could not restore the growth defect of $\Delta zds1$ cells overexpressed *SWE1* of the $\text{Ca}^{2+}$ -signaling pathway.**

In *S. cerevisiae*, Swe1 kinase, the kinase downstream of Calcineurin and MPK1 MAPK cascades in  $\text{Ca}^{2+}$ -signaling pathways, specifically inhibits a G2 phase form of Cdc28 by phosphorylating it at Tyr19 (Booher et al. 1993) and delays the onset of mitosis. To see the effect of 5-OH-3,7-DMF on Swe1, the growth of cells overexpressed *SWE1* (the YCR2 strain) was observed in either presence or absence of 5-OH-3,7-DMF. To induce expression of *SWE1* under control of *GALI* promoter, the YCR2 strain was cultivated in YPR medium containing 2% galactose either in the presence or absence of 500, 250 or 125  $\mu\text{M}$  5-OH-3,7-DMF or 10  $\mu\text{M}$  radicicol, an inhibitor of Swe1 (as a positive control) (Chanklan et al. 2008). The growths of the cultures were monitored for 48 h. The results showed that in the presence of 10  $\mu\text{M}$  radicicol, the growth defect could be partially alleviated. However, either in the absence or presence of 5-OH-3,7-DMF, the mutant cells showed severe growth defect. In addition, 5-OH-3,7-DMF could not restore abnormal bud morphology (Figure 4.5 (a.) and (b.)). These results suggested that Swe1 was not the molecular target of 5-OH-3,7-DMF in the  $\text{Ca}^{2+}$ -signaling pathways in yeast.



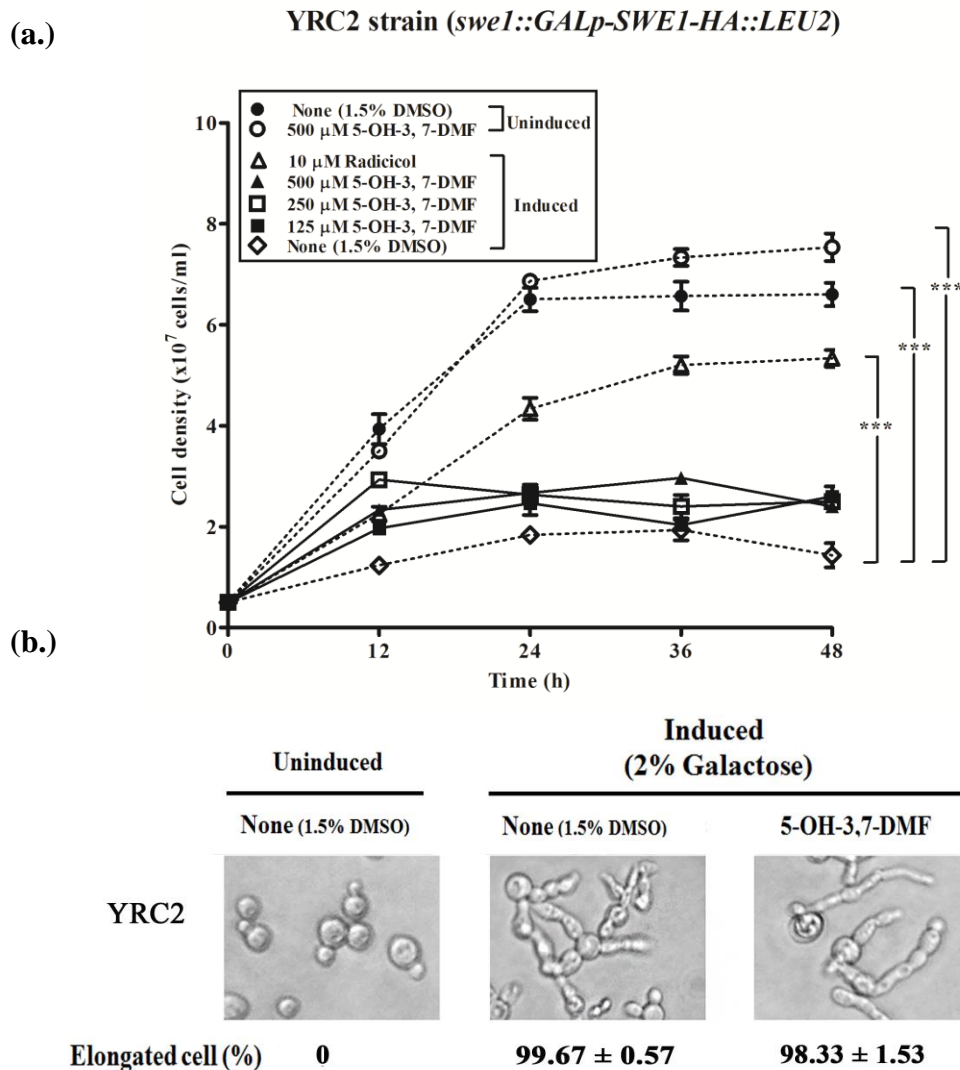


**Figure 4.5** The effect of 5-OH-3,7-DMF on the growth of  $\Delta zds1$  cells overexpressed *SWE1*. (a.);  $5 \times 10^6$  cells/mL of the YRC2 strain (*swe1::GALp-SWE1-HA::LEU2*) were cultivated under induced condition in YPR+2% galactose medium in either presence or absence of 5-OH-3,7-DMF at 30°C with shaking at 200 rpm. The cell density was measured using hemocytometer every 12 h until 48 h. The data showed values of mean  $\pm$  SD from the triplicate experiments. \*\*\*Significant differences at  $p$ -value  $<$  0.001 as compared with the control group using Tukey's multiple comparison test. (b.); The cell morphology of the mutant yeast cells under microscope (X400). The mutant yeast cells showed abnormal elongated bud morphology after treating with 5-

OH-3,7-DMF under induced condition (2% galactose). % elongated cell = number of elongated cells in 100 cells.

#### 4.5 Kinase-Glo<sup>®</sup> Luminescent Kinase Assay Platform

From the result of the  $\Delta zds1$  yeast - based assay suggested that the likely molecule target of the bioactive compound 5-OH-3,7-DMF from *K. parviflora* Wall. Ex. Baker was *MCK1*, ortholog gene with human *GSK-3 $\beta$* . Then, to investigate the *in vitro* inhibitory activity of 5-OH-3,7-DMF on GSK-3 $\beta$  activity, the Kinase Glo<sup>®</sup> Plus luminescent kinase assay platform was employed, using recombinant human GSK-3 $\beta$  as an enzyme and phosphopeptide as an *in vitro* substrate. GSK-3 $\beta$  assays were performed using the Kinase Glo<sup>®</sup> Plus luminescent kinase assay platform. To learn more on the mechanism between kinase enzyme and inhibitor or 5-OH-3,7-DMF and to find out the inhibition pattern either ATP-competitive inhibition, or non-ATP-competitive inhibition or substrate-competitive inhibition, GSK-3 $\beta$  assays were performed using the Kinase Glo<sup>®</sup> Plus luminescent kinase assay platform in a white flat bottom 96-well plate. Optimized concentration of peptide kinase substrate (100  $\mu$ M) was mixed with recombinant human GSK-3 $\beta$  (0.011 unit) in a total volume of 50  $\mu$ l of assay buffer. To set up the assay, several parameter were optimized (Figure 4.6-4.10). From a curve of Michaelis-Menten and Lineweaver-Burk, the enzyme kinase reaction showed maximum reaction velocity ( $V_{max}$ ) = 0.003218  $\mu$ M/min and the Michaelis constant ( $K_m$ ) = 17.60  $\mu$ M (Figure 4.11).

#### 4.5.1 Optimizing kinase reaction conditions

##### ATP standard curve

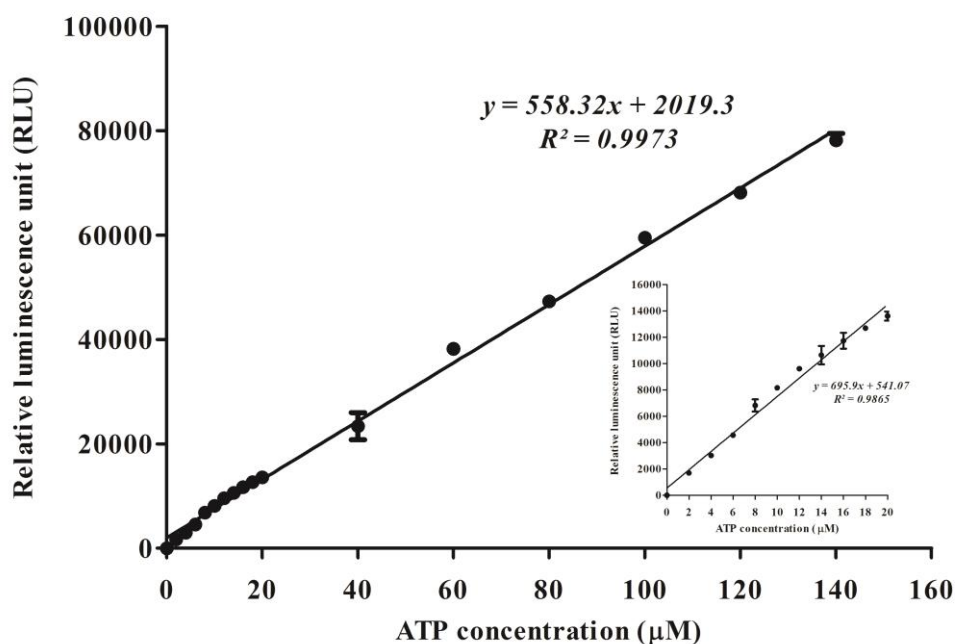


**Figure 4.6** A linear relationship exists between the luminescent signal measured and the ATP concentration in the reaction buffer up to 0 - 140  $\mu\text{M}$ . The lower ATP concentrations between 0 and 20  $\mu\text{M}$  were also presented in the inset graph and the correlation coefficient ( $R^2$ ) was 0.9908 for this range. The luminescent signal was recorded 10 min after addition of an equal volume of Kinase-Glo<sup>®</sup> reagent. The data presented were means standard error of the mean of triplicate wells ( $n = 3$ ). The slope was the rate of relative luminescence unit (RLU) per 1 $\mu\text{M}$  ATP (RLU/1  $\mu\text{M}$  ATP) = 619.3. Curve fitting was performed using GraphPad Prism5<sup>®</sup> linear regression software.

### Optimized substrate concentration

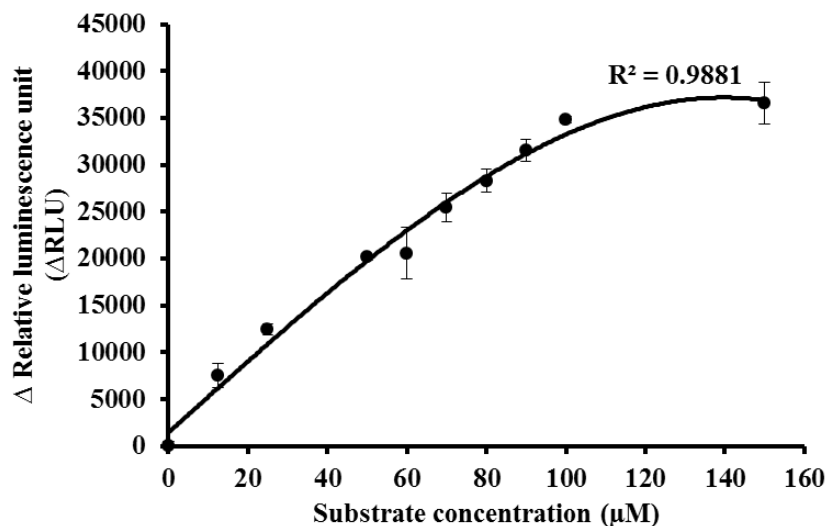


**Figure 4.7** A curve of enzyme activity relationship exists between the relative luminescent signal measured and the peptide kinase substrate concentration in the reaction buffer 0 - 150 µM and reaction solution were incubated at room temperature for 180 min. The optimal kinase substrate concentration at the early stationary phase was 100 µM. The correlation coefficient ( $R^2$ ) was 0.9881 for this range. The luminescent signal was recorded at 10 min after addition of an equal volume of Kinase-Glo<sup>®</sup> reagent. The data presented was means  $\pm$  standard error of the mean of triplicate wells ( $n = 3$ ). Curve fitting was performed using GraphPad Prism5<sup>®</sup> enzyme kinetic software.

### Optimized amount of kinase

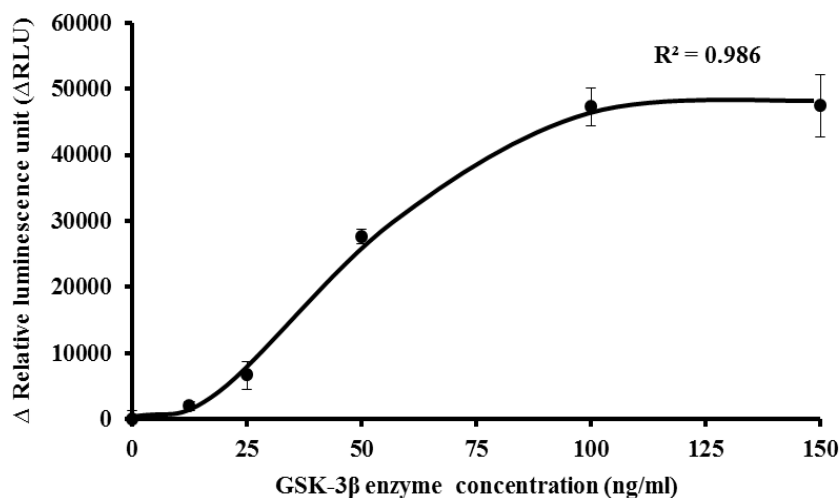


**Figure 4.8** A curve of enzyme activity relationship exists between the relative luminescent signal measured and the human GSK-3β active enzyme concentration in the reaction buffer 0 - 150 μM and reaction solution were incubated at room temperature for 180 min. The optimal kinase enzyme concentration was at the early stationary phase 100 μM. The correlation coefficient ( $R^2$ ) was 0.9860 for this range. The luminescent signal was recorded at 10 min after addition of an equal volume of Kinase-Glo<sup>®</sup> reagent. The data presented were means ± standard error of the mean of triplicate wells (n = 3). Curve fitting was performed using GraphPad Prism5<sup>®</sup> enzyme kinetic software.

### Determining the enzyme activity

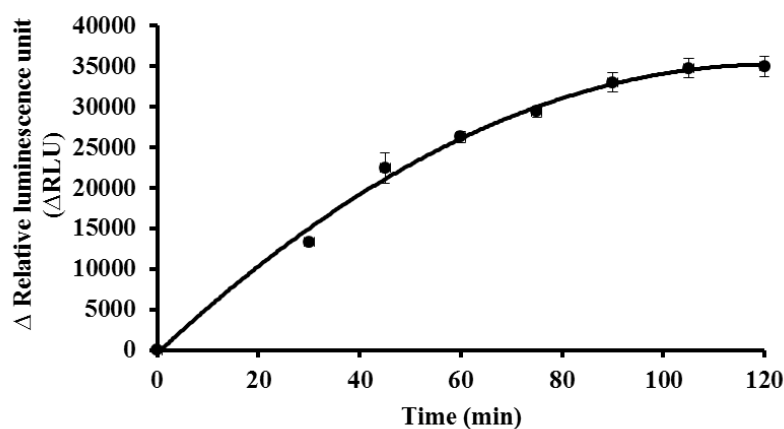


**Figure 4.9** A curve of enzyme activity relationship exists between the relative luminescent signals measured and times in the reaction buffer were incubated at room temperature for 120 min. The luminescent signal was recorded at 10 min after addition of an equal volume of Kinase-Glo<sup>®</sup> reagent. The data presented were means  $\pm$  standard error of the mean of triplicate wells ( $n = 3$ ). Curve fitting was performed using GraphPad Prism5<sup>®</sup> enzyme kinetic software.

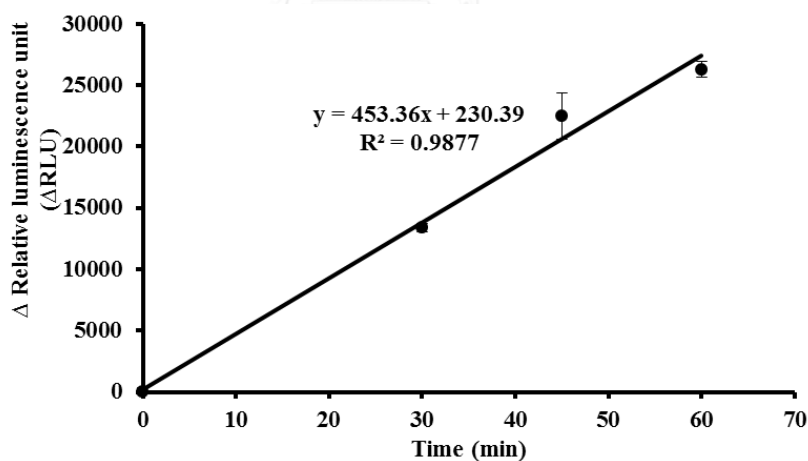


**Figure 4.10** A linear curve fitted from figure 4.9 of enzyme activity relationship exists between the relative luminescent signals. The data presented were means  $\pm$  standard error of the mean of triplicate wells ( $n = 3$ ). The correlation coefficient ( $R^2$ ) was 0.9860 for this range and the slope of exponential phase was the initial rate of enzyme kinase reaction  $\Delta\text{RLU}/\text{min} = 453.36$  and reversal of initial rate of enzyme kinase reaction to unit of enzyme =  $0.01098\mu\text{M ATP}/\text{min}$  and specific activity of enzyme kinase =  $7320.539 \mu\text{M ATP}/\text{min}/\text{mg protein}$ . Curve fitting was performed using GraphPad Prism5<sup>®</sup> linear regression software.



### The $K_m$ and $V_{max}$ of enzyme kinase

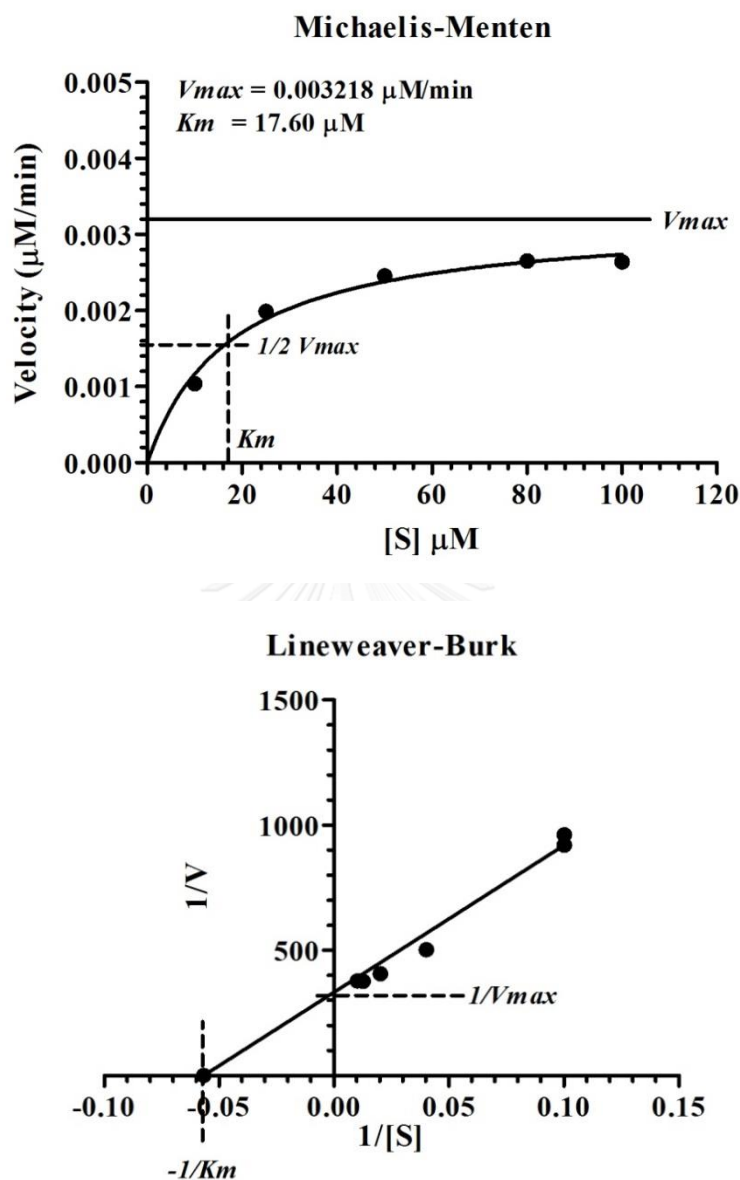


**Figure 4.11** A curve of Michaelis-Menten and Lineweaver-Burk relationship exists between the velocity of enzyme activity and peptide kinase substrate concentration [S] in the reaction buffer was incubated at room temperature for 120 min. The luminescent signal was recorded at 10 min after addition of an equal volume of Kinase-Glo<sup>®</sup> reagent. The maximum reaction velocity ( $V_{max}$ ) = 0.003218  $\mu\text{M}/\text{min}$  and the Michaelis constant ( $K_m$ ) = 17.60  $\mu\text{M}$ . Curve fitting was performed using GraphPad Prism5<sup>®</sup> enzyme kinetic (Michaelis-Menten) software.

#### 4.5.2 *In vitro* GSK-3 $\beta$ activity assay of 5-OH-3,7-DMF

GSK-3 $\beta$  assays were performed using the Kinase Glo<sup>®</sup> Plus luminescent kinase assay platform in a white flat bottom 96-well plate with optimized concentration of peptide kinase substrate (100  $\mu$ M) was mixed with recombinant human GSK-3 $\beta$  (0.011 unit) in a total volume of 50  $\mu$ l of assay buffer. 5-OH-3,7-DMF inhibited GSK-3 $\beta$  with an IC<sub>50</sub> values of  $9.72 \pm 0.15$   $\mu$ M (Figure 4.12 (a.)) and showed  $85.6 \pm 7.41$  % of inhibition (Figure 4.13) while GSK-3 $\beta$  inhibitor I with an IC<sub>50</sub> values of  $9.98 \pm 0.09$   $\mu$ M (Figure 4.12 (b.)) and  $82.7 \pm 11.55$  % inhibition (Figure 4.13) in this study. Interestingly, these results indicated that 5-OH-3,7-DMF is a high potential GSK-3 $\beta$  inhibitor comparable to the commercial GSK-3 $\beta$  inhibitor I.

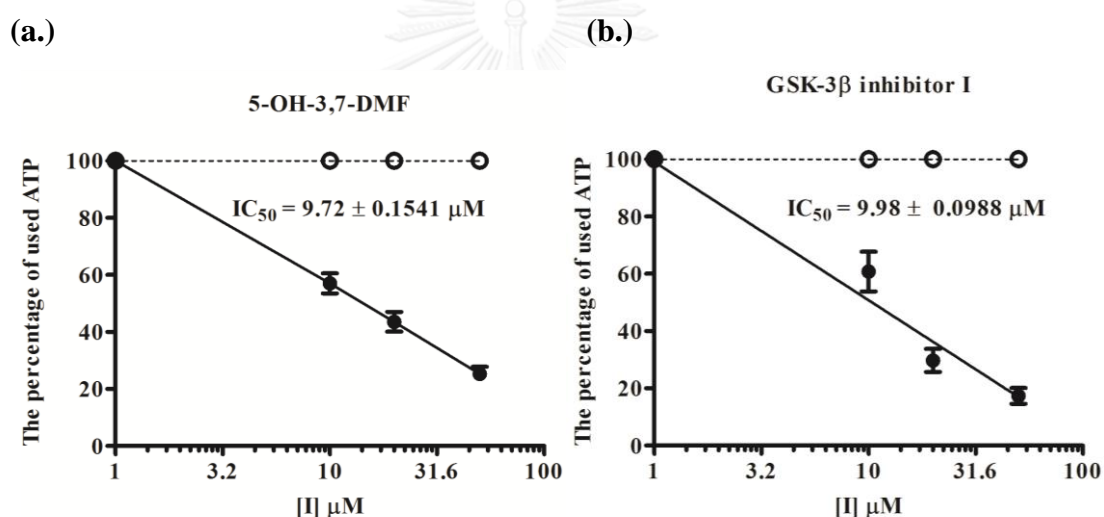


**Figure 4.12** IC<sub>50</sub> determination of *in vitro* GSK-3 $\beta$  activity inhibition of 5-OH-3,7-DMF and GSK-3 $\beta$  inhibitor I (as a positive control) using the Kinase-Glo<sup>®</sup> Plus Assay were varying concentration 0, 10, 20, 50  $\mu$ M in the reaction buffer containing 100  $\mu$ M ATP. Curve fitting was performed using GraphPad Prism5<sup>®</sup> sigmoidal dose-response (normalized response) software.

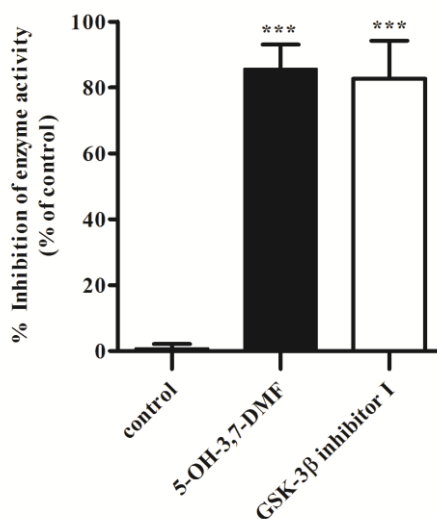
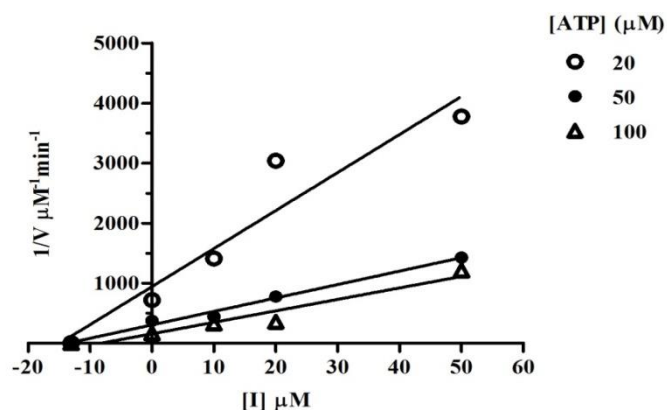


**Figure 4.13** Percentage inhibition of GSK-3 $\beta$  enzyme activity by 5-OH-3,7-DMF. A column relationship exists between the percentage of inhibitory enzyme activity related with luminescence signal remaining after stopping the enzyme reaction. GSK-3 $\beta$  inhibitors including  100  $\mu$ M 5-OH-3,7-DMF,  100  $\mu$ M GSK-3 $\beta$  inhibitor I and  control treatment (DMSO). The luminescent signal was recorded at 10 min after addition of an equal volume of Kinase-Glo<sup>®</sup> reagent. The data showed values of mean  $\pm$  SD from the triplicate experiments. \*\*\* Significant differences at  $p$ -value  $<$  0.001 as compared with the control group using Dunnett's Multiple Comparison test.

#### 4.5.3 5-OH-3,7-DMF is an ATP non-competitive but substrate competitive GSK-3 $\beta$ inhibitor.

From the previous experiment 5-OH-3,7-DMF and the GSK-3 $\beta$  inhibitor I inhibited GSK-3 $\beta$  with an  $IC_{50}$  values of 10.12  $\mu$ M and 10.19  $\mu$ M, respectively (Figure 4.12). From Dixon plotting analysis, 5-OH-3,7-DMF exhibited an ATP non-competitive binding mode to GSK-3 $\beta$  ( $K_i = 13.04$   $\mu$ M, Figure 4.14 (a.)) and showed a substrate competitive binding mode to GSK-3 $\beta$  by Dixon plot ( $K_i = 53.92$   $\mu$ M, Figure 4.14 (b.)). These results confirmed that 5-OH-3,7-DMF is a novel ATP non-competitive GSK-3 $\beta$  inhibitor but substrate competitive GSK-3 $\beta$  inhibitor that might be a useful functional compound for treatment of diseases with high level of GSK-3 $\beta$  activity such as type-2 diabetes, Alzheimer's disease and inflammation.

(a.)



(b.)

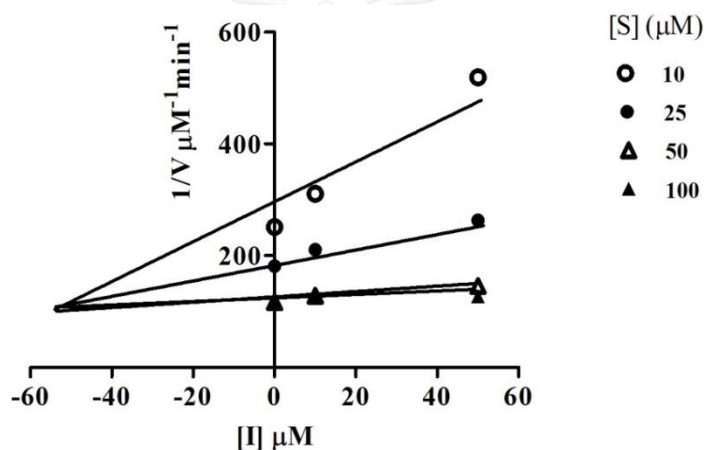
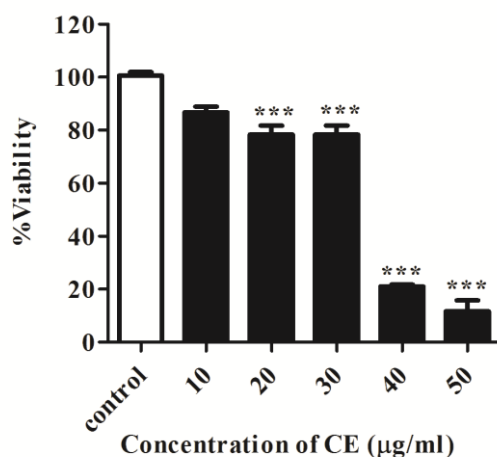


**Figure 4.14** Dixon plot of 5-OH-3,7-DMF against human GSK-3 $\beta$  activity. **(a.)**; Double-reciprocal plot of Kinetic analyses was performed using three ATP concentrations (20 ( $\circ$ ), 50 ( $\bullet$ ), 100 ( $\Delta$ )  $\mu\text{M}$ ) and four concentrations (0, 10, 20, 50  $\mu\text{M}$ ) of 5-OH-3,7-DMF. The GSK-3 $\beta$  activity reaction was performed with a constant concentration of peptide kinase substrate (100 $\mu\text{M}$ ). **(b.)**; Double-reciprocal plots of kinetic analyses were performed using four peptide kinase substrate concentrations (10 ( $\circ$ ), 25 ( $\bullet$ ), 50 ( $\Delta$ ), 100( $\blacktriangle$ )  $\mu\text{M}$ ) and three concentrations (0, 10, 50  $\mu\text{M}$ ) of 5-OH-3,7-DMF with a constant concentration of ATP (100  $\mu\text{M}$ ). The GSK-3 $\beta$  reaction was performed in the reaction buffer for 120 min. Curve fitting was performed using GraphPad Prism<sup>®</sup> (linear regression) software.

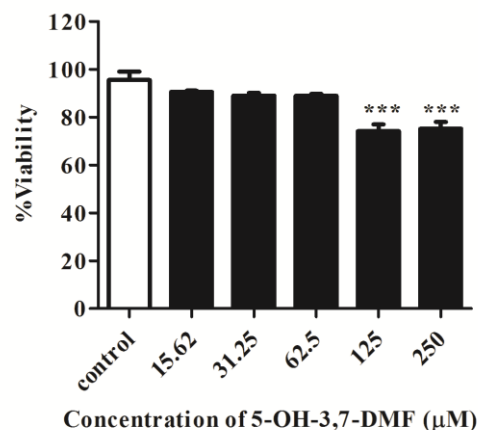
#### **4.6 Study of cytotoxic effect of crude extracted of *K. parviflora* and 5-OH-3,7-DMF in HepG2 cell lines.**

Anti-type 2 diabetes effect of 5-OH-3,7-DMF on a human hepatic cell line (HepG2) will be used in the insulin resistance model. Since 5-OH-3,7-DMF was isolated from crude extract of *K. parviflora* (CE), the cytotoxicity studies in HepG2 cells will evaluate the biological effect of CE and 5-OH-3,7-DMF in parallel. HepG2 cells were exposed to various concentrations of crude extract of *K. parviflora* (CE) (50, 40, 30, 20, 10  $\mu\text{g}/\text{mL}$ ), 5-OH-3,7-DMF (250, 125, 62.5, 31.25, 15.63  $\mu\text{M}$ ), GSK-3 $\beta$  Inhibitor I (100, 80, 60, 40, 20, 10  $\mu\text{M}$ ) and LiCl (10, 20, 30, 40, 50 mM) as positive controls and 0.5% DMSO (normal control) in RPMI complete medium. Then the cells were incubated at 37°C in humidified condition with 5% CO<sub>2</sub> for 1 d before subjected to MTT assay. The results showed that HepG2 cell viability reduced to >30% at 20-30  $\mu\text{g}/\text{mL}$  of CE and also showed acute cytotoxic effect at concentration higher than 40  $\mu\text{g}/\text{mL}$  as the % viability sharply declined compared to that of control (0.5% DMSO) after 1 d of treatment (Figure 4.15 (a.)). Cell viability was reduced to about 30% when treated with  $\geq 125 \mu\text{M}$  5-OH-3,7-DMF (Figure 4.15 (b.)). While, cell viability of HepG2 treated with GSK-3 $\beta$  Inhibitor I reduced around 30% at concentration 40  $\mu\text{M}$  compared to that of control (0.5% DMSO) (Figure 4.15 (c.)). On the other hand, cell viability of HepG2 treated with LiCl (another positive control) was reduced around 20% at 40 mM. Further experiments on investigating of anti-type 2 diabetes effect in HepG2 insulin resistant cell model, the following concentrations of each compounds were chosen; CE (15, 10, 5  $\mu\text{g}/\text{mL}$ ), 5-OH-3,7-DMF (62.5, 31.25, 15.625  $\mu\text{M}$ ), GSK-3 $\beta$  Inhibitor I (20, 10  $\mu\text{M}$ ) and LiCl (10, 1, 0.5 mM), respectively.

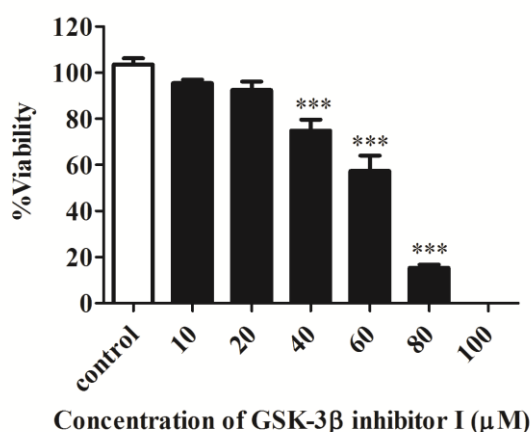
(a.) Crude extracted of KP (CE)



(b.) 5-OH-3,7-DMF



(c.) GSK-3β Inhibitor I



(d.) LiCl

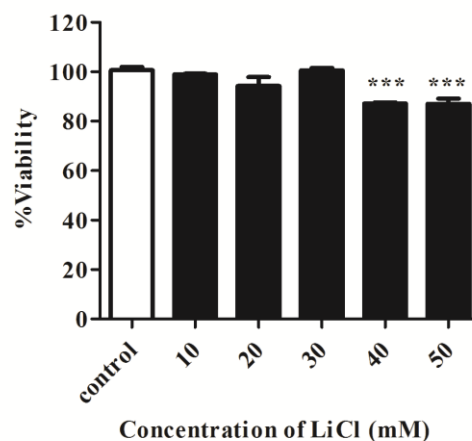


**Figure 4.15** Cytotoxicity of CE, 5-OH-3,7-DMF, GSK-3β Inhibitor I and LiCl on human hepatoma HepG2 cell lines. The cell viability was measured by MTT assay. Cells were treated with either varying concentrations of CE (a.) or 5-OH-3,7-DMF (b.) or GSK-3β Inhibitor I (c.) or LiCl (d.) and 0.5% DMSO (for control treatment) in RPMI complete medium containing 0.5% DMSO incubated at 37°C in humidified conditions with 5% CO<sub>2</sub> for 1 d. The data showed values of mean ± SD from the triplicate experiments. \*\*\* Significant differences at  $p$ -value < 0.001 as compared with that of the control group with Dunnett's Multiple Comparison test.

#### **4.7 Study on insulin-resistant condition induced hepatic gluconeogenesis on the expression of Glucose-6-phosphatase.**

In the hepatocyte, in a situation of insulin resistance, alterations of insulin signaling stimulates Glucose-6-phosphatase (G6Pase) levels, as a key mechanism for controlling glucose production (gluconeogenesis) in hepatocyte, as well as restrains the synthesis of glycogen (Klover and Mooney 2004). CE and/or 5-OH-3,7-DMF was hypothesized to have protective effects on *G6Pase* levels in cells incubated with high glucose (25 mM glucose) and high insulin (500 nM insulin) (HGHI) condition. To see whether both substances were able to modulate the expression of G6Pase, a major enzyme responsible for the regulation of gluconeogenesis, as well as the production of the glycogen content, the following experiments were performed. HepG2 cells were pre-treated with CE (15, 10 or 5 µg/mL), 5-OH-3,7-DMF (62.5, 31.25 or 15.63 µM) compared to the both of positive controls, GSK-3β Inhibitor I (20 or 10 µM) and LiCl (10, 1 or 0.5 mM) for 24 h in high glucose medium. Then, later exposed to HGHI medium for 24 h. Another experiment, the HepG2 cells were post-treated with CE (15µg/mL), 5-OH-3,7-DMF (62.5 µM), GSK-3β Inhibitor I (20 µM) and LiCl (10 mM) at the changing the medium to HGHI step. Then, total RNAs were isolated from the treated HepG2 cells to measure the expression level of G6Pase. It was found that when HpeG2 cells were incubated in HGHI medium, G6Pase was induced rapidly compared to that of the controls (0.5% DMSO and low glucose (5 mM glucose) with high insulin (LGHI) medium), which was a normal glucose metabolism condition. Pre-treatment of HepG2 cells with CE or 5-OH-3,7-DMF led to a comparable decrease G6Pase gene expression in a dose-dependent manner compared to those of both positive controls even reduced G6Pase expression at high dose (GSK-3β Inhibitor I (20 µM) and LiCl (10 mM)) (Figure 4.16). Interestingly, both CE (as low as 15 µg/mL) and 5-OH-3,7-DMF (as low as 15.63 µM) showed higher effect on reduction gluconeogenesis (G6Pase) gene expression at low concentration in insulin-resistant HepG2 cell model than LiCl or GSK-3β Inhibitor I in pre-treatment. The result demonstrated that LiCl, a GSK-3 inhibitor on clinical trial (Cole et al. 2014) showed low protective effect on G6Pase level in HepG2 cells. These results suggested that 5-OH-3,7-DMF is a novel bioactive compound for modulating glucose homeostasis in type 2 diabetes disease.

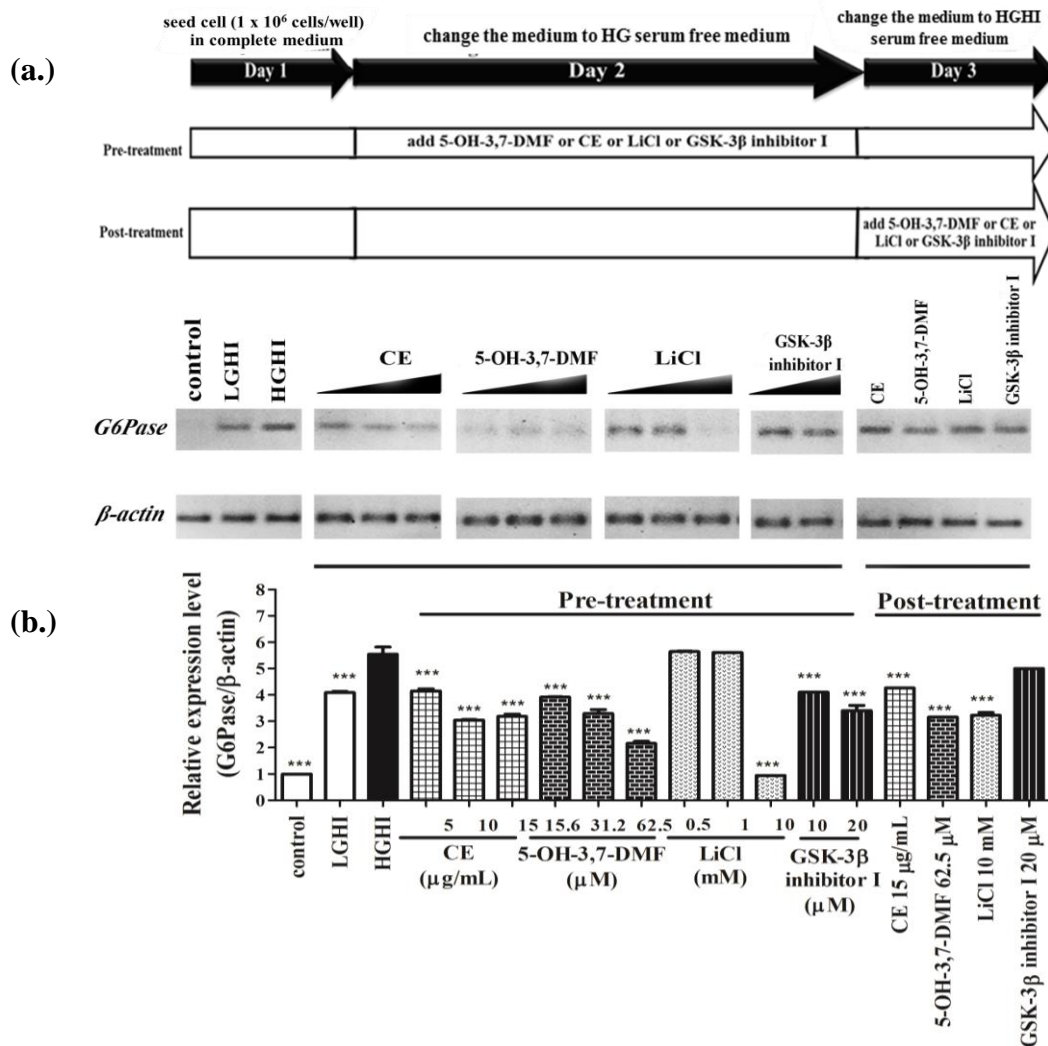
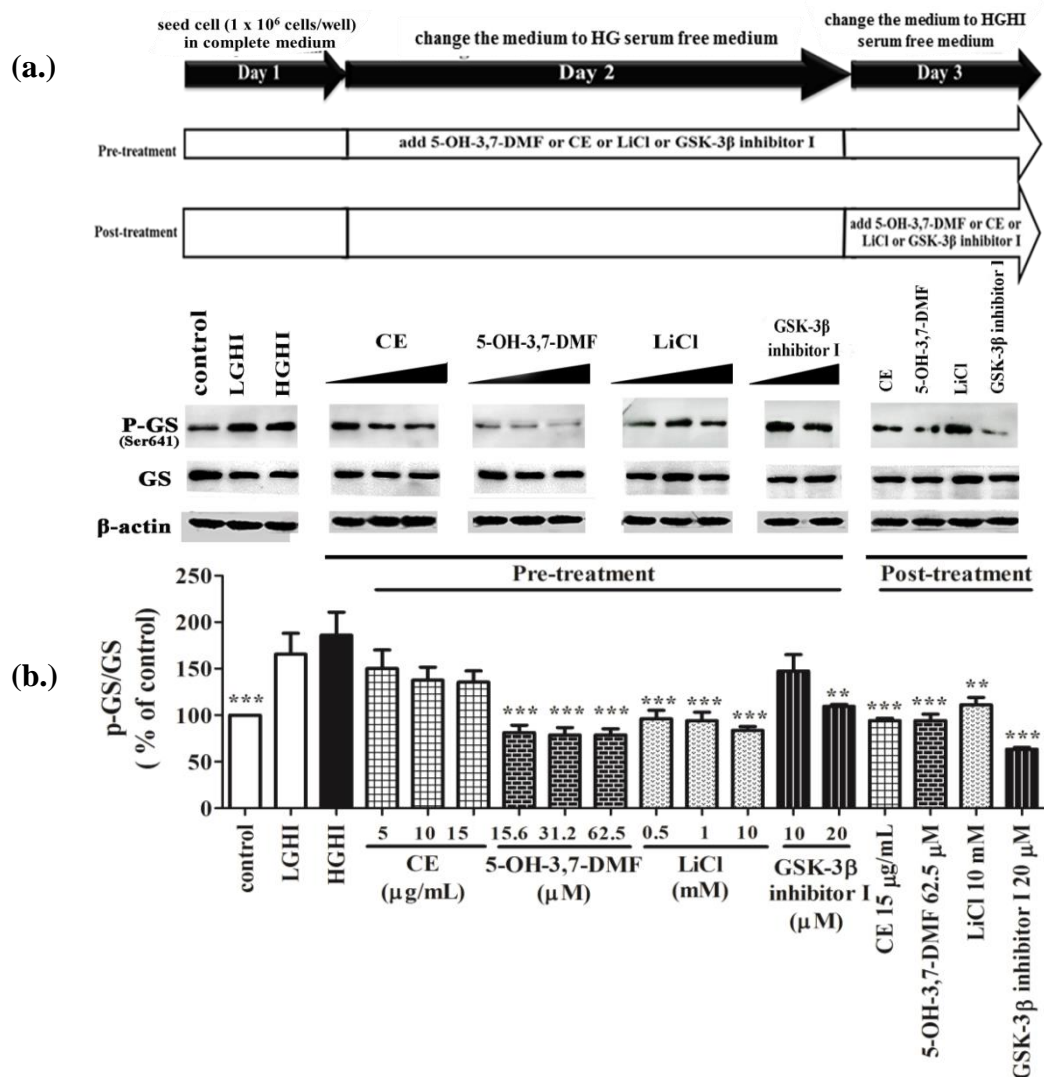


**Figure 4.16** Effect of CE and 5-OH-3,7-DMF on the expression of *G6Pase*. HepG2 cells were cultured in HGHI medium contained various concentrations of CE (15, 10 or 5  $\mu\text{g/mL}$ ), 5-OH-3,7-DMF (62.5, 31.25 or 15.63  $\mu\text{M}$ ) compared to the both of positive controls, GSK-3 $\beta$  Inhibitor I (20 or 10  $\mu\text{M}$ ) and LiCl (10, 1 or 0.5 mM) in pre-treatment or post-treatment for 24 - 48 h. Total RNA were extracted and the expression of *G6Pase* was assessed by one-step RT-PCR (a.); bands of representative experiments. (b.); Relative expression level of *G6Pase* normalize by  $\beta$ -actin. The data showed values of mean  $\pm$  SD from the triplicate experiments. \*\*\* Significant differences at  $p$ -value  $< 0.05$  and  $< 0.0001$  respectively as compared to the HGHI group with Dunnett's Multiple Comparison test. Control: untreated cells, LGHI: low glucose (5 mM) high insulin (500 nM), HGHI: high glucose (25 mM) high insulin (500 nM).

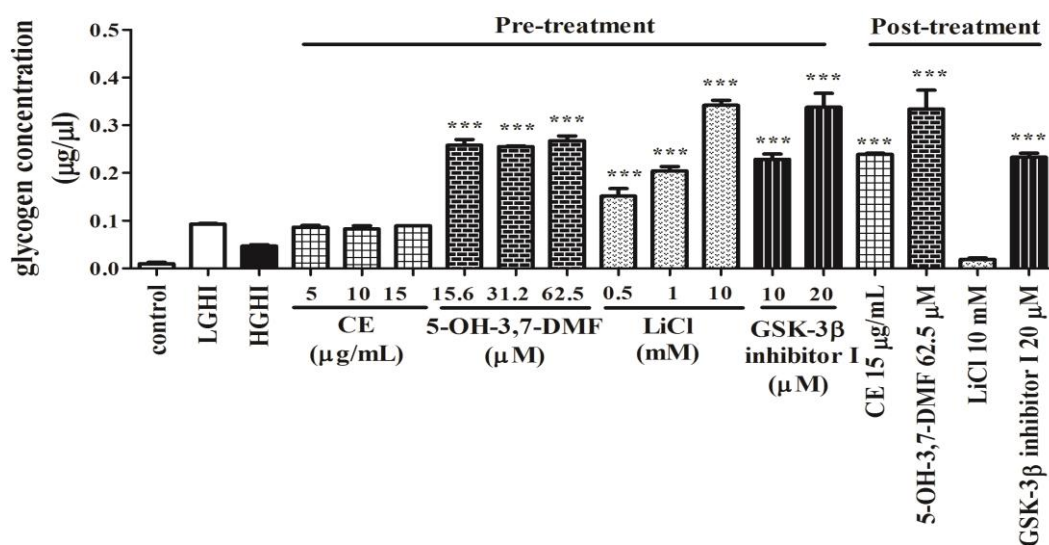


#### **4.8 5-OH-3,7-DMF could recover glycogen level in insulin-resistant HepG2 cells through inhibition phosphorylation of glycogen synthase protein (GS).**

According to insulin induces the inhibition of GSK-3, small molecules that inhibit this protein Kinase possibly expected to mimic some of the actions of insulin, such as its ability to activate glycogen synthase and stimulate the conversion of glucose to glycogen that lead to lower blood glucose by inhibiting the production of glucose by the liver (Norman 2001). Elevation level of GSK-3 has been observed in diabetic and obese strains of mice (Eldar-Finkelman et al. 1999a). In addition, GSK-3 has a role in negative regulation of glycogen synthesis via phosphorylation of glycogen synthase (GS). In this study, insulin-resistant HepG2 cells were pre-treated with CE (15, 10 or 5  $\mu\text{g/mL}$ ), 5-OH-3,7-DMF (62.5, 31.25 or 15.63  $\mu\text{M}$ ) compared to both of positive controls, GSK-3 $\beta$  Inhibitor I (20 or 10  $\mu\text{M}$ ) and LiCl (10, 1 or 0.5 mM), respectively, for 24 h in high glucose medium and then exposed to HGHI medium for 24 h. Another experiment, the HepG2 cells were post-treated with CE (15 $\mu\text{g/mL}$ ), 5-OH-3,7-DMF (62.5  $\mu\text{M}$ ), GSK-3 $\beta$  Inhibitor I (20  $\mu\text{M}$ ) and LiCl (10 mM) at the changing the medium to HGHI step. Then, cell lysates were prepared and used for measuring glycogen content by glycogen assay kit. The extracted proteins were used to determine GS protein level by Western blotting analysis. In previous experiments, HGHI incubation increased the levels of G6Pase expression but was totally decreased in cells pre-treated or post-treated with CE or 5-OH-3,7-DMF. In addition, HepG2 cells in HGHI treatment increased GS phosphorylation at Ser641 (Figure 4.17 (a.) and (b.)) leading to lack of glycogen activity or reducing glycogen synthesis (Figure 4.18). However, when cells were pre-treated or post-treated with 5-OH-3,7-DMF cause both reduction of GS phosphorylation and increased in glycogen content as same as those in the positive controls, LiCl (20mM) and GSK-3 $\beta$  Inhibitor I (20  $\mu\text{M}$ ). In the CE treatment showed slightly decreased in GS phosphorylation and recovered of glycogen content only in the post-treatment (Figure 4.17 and 4.18).



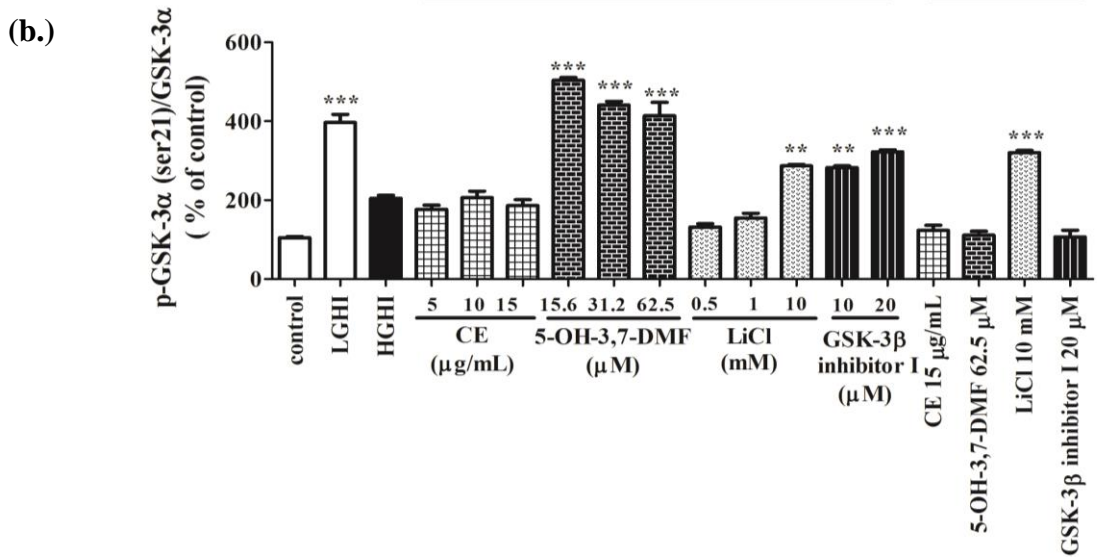
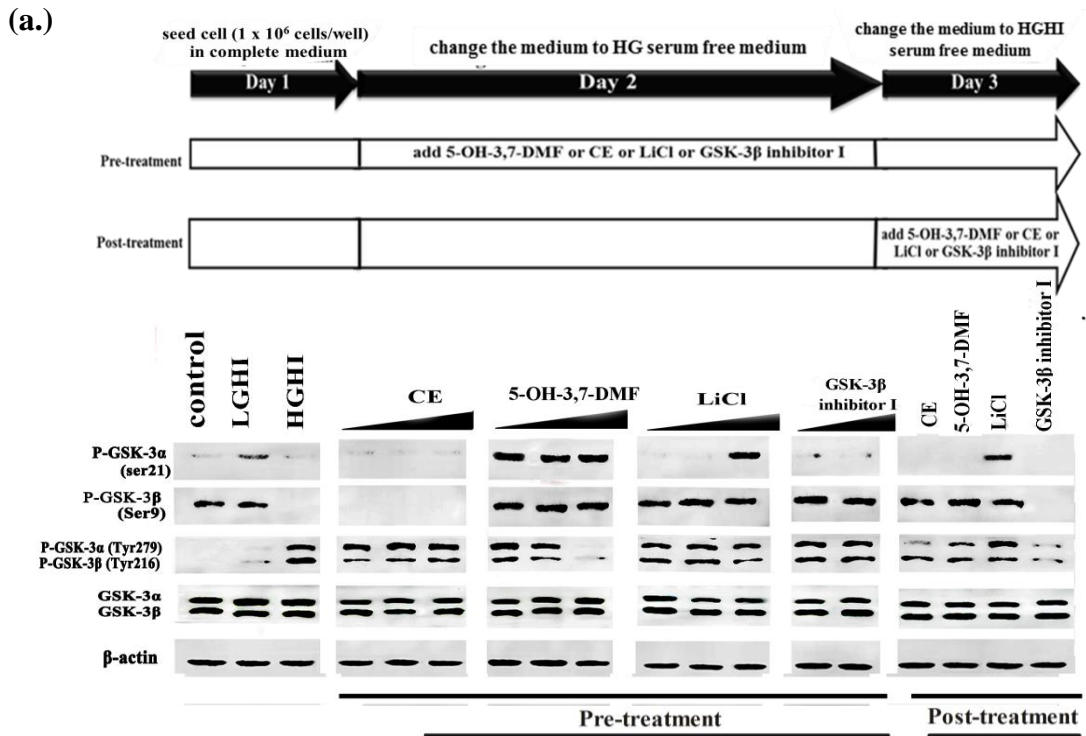
**Figure 4.17** Effect of CE and 5-OH-3,7-DMF on the expression of Glycogen synthase (GS). HepG2 cells were cultured in HGHI medium contained various concentrations of CE (15, 10 or 5  $\mu\text{g/mL}$ ) and 5-OH-3,7-DMF (62.5, 31.25 or 15.63  $\mu\text{M}$ ) in pre-treatment or post-treatment for 24 - 48 h. Protein extract samples were prepared and subjected to Western blotting analysis using anti-GS and anti-p-GS (Ser641) primary antibodies.  $\beta$ -actin was used as a loading control. **(a.)**; bands of representative experiments. **(b.)**; Percentage of p-GS/GS band intensity normalize by  $\beta$ -actin band intensity. The data showed values of mean  $\pm$  SD from the triplicate experiments. \*\*, \*\*\* Significant differences at  $p$ -value  $< 0.05$  and  $< 0.0001$ , respectively as compared to the HGHI group using Dunnett's Multiple Comparison test. Control: untreated cells, LGHI: low glucose (5 mM) high insulin (500 nM), HGHI: high glucose (25 mM) high insulin (500 nM).

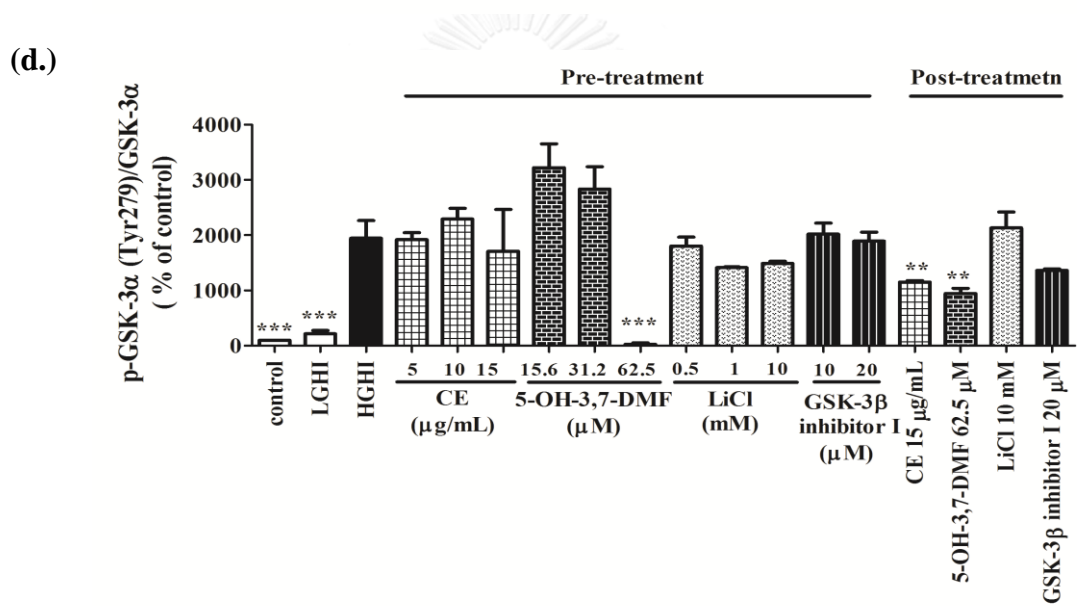
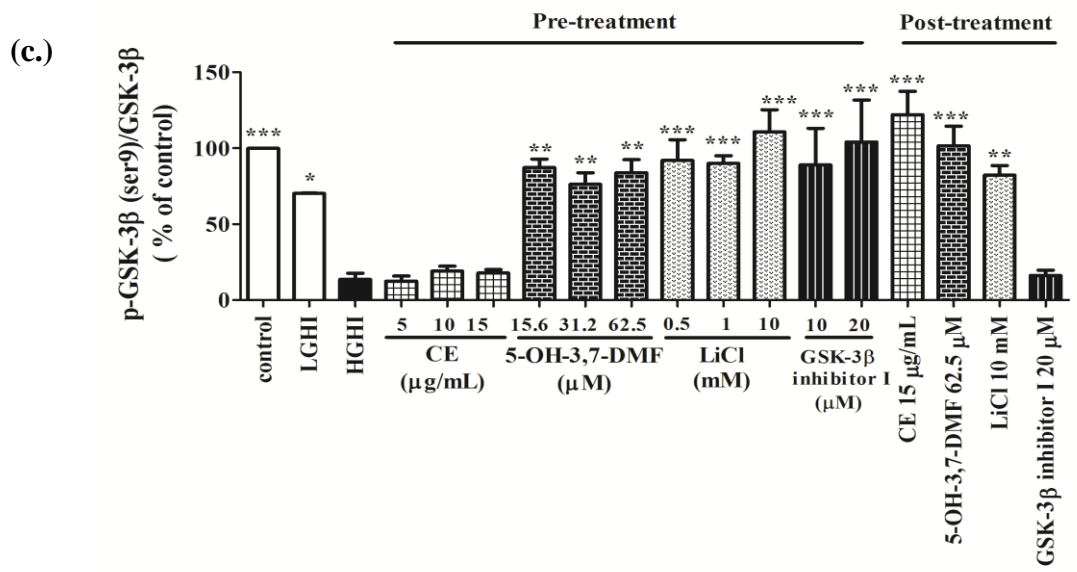


**Figure 4.18** Effect of CE and 5-OH-3,7-DMF on recovery of glycogen synthesis. HepG2 cells were cultured in HGHI medium contained various concentrations of CE (15, 10 or 5 µg/mL) and 5-OH-3,7-DMF (62.5, 31.25 or 15.63 µM) in pre-treatment or post-treatment for 24 - 48 h. Cell lysates were prepared and subjected to glycogen content analysis. Glycogen content expressed as concentration (µg/µl) as calculating with glycogen standard curve (appendix C). The data showed values of mean ± SD from the triplicate experiments. \*\*\* Significant differences at  $p$ -value < 0.0001 as compared to the HGHI group with Dunnett's Multiple Comparison test. Control: untreated cells, LGHI: low glucose (5 mM) high insulin (500 nM), HGHI: high glucose (25 mM) high insulin (500 nM).

#### **4.9 5-OH-3,7-DMF abolished the impairment of insulin signaling in insulin-resistant HepG2 cells model via down regulation of GSK-3.**

GSK-3, locates at downstream of insulin signaling pathways, facilitates glycogen synthesis in the liver, and directly contributes to the activity of GS, which is the key molecular mediator for metabolic effects of insulin signaling (Whiteman et al., 2002). Insulin inhibits Ser21 and Ser9 phosphorylation of glycogen synthase Kinase-3 (GSK3)  $\alpha$  and  $\beta$ , respectively, through PI3K and AKT signaling. To evaluate the potential protective effect of CE and 5-OH-3,7-DMF against the alterations of glycogen synthesis caused elevate GSK-3 by a HGHI concentration, phosphorylation of GSK-3 $\alpha$  and - $\beta$  were detected by Western blotting analysis using specific antibodies against p-GSK-3 $\beta$  (ser9), p-GSK-3 $\alpha$  (ser21) and p-GSK-3 $\alpha/\beta$  (Tyr279/Tyr216). Treatment of HepG2 cells with HGHI medium during 48 h activated a significant decrease in the phosphorylated levels of P-Ser-GSK-3 $\alpha/\beta$  and increased the phosphorylated level of P-Tyr-GSK-3 $\alpha/\beta$  (Figure 4.19), indicated that insulin signaling was impaired as compared to those controls (0.5% DMSO (control treatment or LGHI). Interestingly, pre-treatment of HepG2 cells with 5-OH-3,7-DMF showed increase in the level of p-Ser-9 (Figure 4.19 (a.) and (c.)) and p-Ser-21 (Figure 4.19 (a.) and (b.)) and decrease in the level of p-Tyr-279/216 (Figure 4.19 (a.), (d.) and (e.)) in the insulin-resistant cells. Post-treatment, 5-OH-3,7-DMF showed increase in the level of p-Ser-9 (Figure 4.19 (a.) and (c.)) and decrease in P-Tyr-279 (Figure 4.19 (a.) and (d.)). CE did not show the effect on P-GSK-3 in pre-treatment however, in post-treatment CE showed increase in the level of p-Ser-9 (Figure 4.19 (a.) and (c.)) and decrease in the level of p-Tyr-279 (Figure 4.19 (a.) and (d.)). The pre-treatment with LiCl caused increase in the phosphorylation level of p-Ser-21 (Figure 4.19 (a.) and (b.)) and p-Tyr-279/216 only at very high concentration (10 mM) (Figure 4.19 (a.), (d.) and (e.)) and showed increase in the level of p-Ser-9 (Figure 4.19 (a.) and (c.)). In post-treatment with LiCl showed increase in both of the level of p-Ser-9/21 (Figure 4.19 (a.), (b.) and (c.)) but not those of p-Tyr-279/216 level (Figure 4.19 (a.), (d.) and (e.)). GSK-3 $\beta$  Inhibitor I, one of the positive controls, only increased the phosphorylation level of p-Ser-9 in pre-treatment (Figure 4.19 (a.) and (c.)) and decreased p-Tyr-216 in post-treatment (Figure 4.19 (a.) and (e.)).





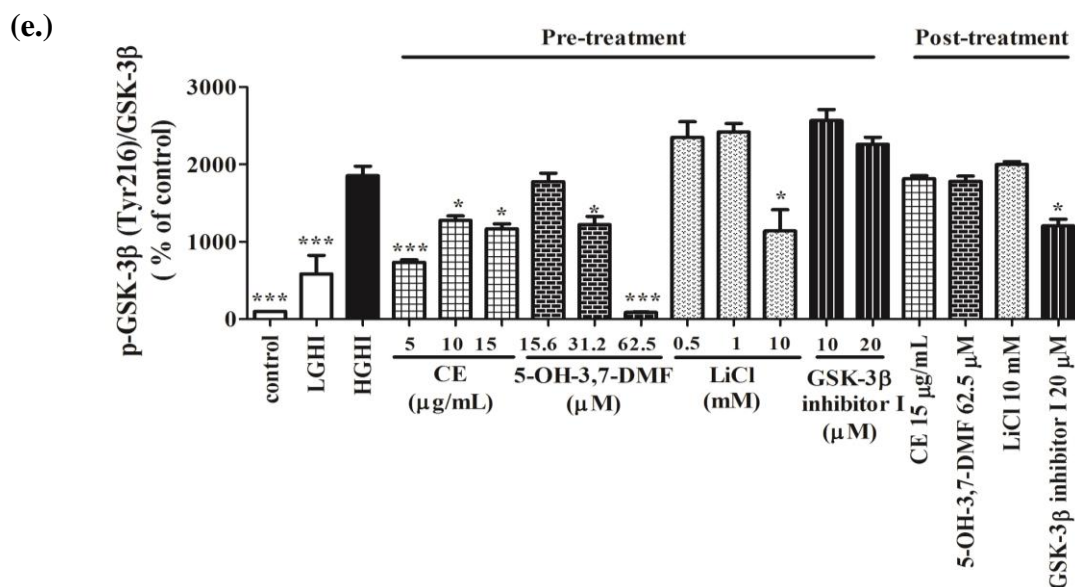


**Figure 4.19** Effect of CE and 5-OH-3,7-DMF on the phosphorylation of GSK-3. HepG2 cells were cultured in HGHI medium containing various concentrations of CE (15, 10 or 5  $\mu\text{g/mL}$ ) and 5-OH-3,7-DMF (62.5, 31.25 or 15.63  $\mu\text{M}$ ) in pre-treatment or post-treatment for 24 - 48 h. Protein samples were prepared and subjected to Western blotting analysis using anti-p-GSK-3 $\beta$  (ser9), anti-p-GSK-3 $\alpha$  (ser21), anti-p-GSK-3 $\alpha/\beta$  (Tyr279/Tyr216) and anti-GSK-3 $\alpha/\beta$  primary antibodies.  $\beta$ -actin was used as a loading control. (a.); bands of representative experiment. (b.); Percentage relating band intensity of p-GSK-3 $\alpha$  (Ser21)/GSK-3 $\alpha$ , (c.); p-GSK-3 $\beta$  (Ser9)/GSK-3 $\beta$ , (d.); p-GSK-3 $\alpha$  (Tyr279)/GSK-3 $\alpha$ , (f.) p-GSK-3 $\beta$  (Tyr216)/GSK-3 $\beta$ , normalized by those of  $\beta$ -actin band intensity. The data showed values of mean  $\pm$  SD from the triplicate experiments. \*, \*\*, \*\*\* Significant differences at  $p$ -value  $< 0.05$ ,  $< 0.01$  and  $< 0.0001$  respectively as compared to the HGHI group using Dunnett's Multiple Comparison test. Control: untreated cells, LGHI: low glucose (5 mM) high insulin (500 nM), HGHI: high glucose (25 mM) high insulin (500 nM).

## CHAPTER V

### DISCUSSION AND CONCLUSION

#### 5.1 Discussion

A  $\Delta zds1$ -proliferation procedure assay is a drug screening for small molecules targeting toward a wide range of the signaling molecules in the  $Ca^{2+}$ -mediated cell-cycle regulatory pathways (Shitamukai et al. 2000). This procedure seems to cover a set of wide range of well conserved, pharmacological interesting molecules as potential targets (Mizunuma et al. 1998). Hyperactivation of a signaling pathway often confers deleterious physiological effects including growth defect. Thus, for example the consequence of MAP Kinase cascades, such as those mediated by Hog1, Fus3 and Mpk1, is poor growth or lethality (Mager and De Kruijff 1995). This type of inhibitors of the signaling pathways will be selectable as the compounds enable the cells with the activated signal to adapt to stress condition otherwise prohibiting growth. The activation of a signaling pathway can be achieved by various procedures. Additional  $CaCl_2$  to the medium as one of a convenient and inexpensive mean of the  $Ca^{2+}$ -signal activation. Genetically, the signal activation in yeast can be done by various conditional mutations that hyperactivate the signaling pathway or by using an overexpression system with a regulable promoter, such as *GALI-10p* (Shitamukai et al. 2000). From these procedure Boonkerd et al. (2014) examined the biological activity of 5-OH-3,7-DMF from *K. parviflora* by addition of  $CaCl_2$  to hyperactivate  $Ca^{2+}$ -signaling in the *zds1* null mutant of *S. cerevisiae*. They demonstrated that 5-OH-3,7-DMF alleviated the G2/M cell-cycle delay in the  $\Delta zds1$  yeast (YNS17 strain).

The molecular target of 5-OH-3,7-DMF that acts on this pathways was determined in this study by hyperactivation of the pathway using an overexpression system under control of *GALI1p* caused growth defect (G2/M delay) in  $\Delta zds1$  cells and also caused abnormal bud morphology (Mizunuma et al. 1998). Results from the overexpression of each gene involved in the pathways suggested that 5-OH-3,7-DMF did not inhibit at *Calcineruin* and *SWE1* step (Figure 4.2 and 4.5). On the other hand, the mutant cells overexpressed *MPK1* or *MCK1* (the NSC1 and NSC2 strain) showed dose dependent effect of 5-OH-3,7-DMF on restoration of the growth defect and the



elongated buds in these strains to the similar extent as that of the control (uninduced condition) (Figure 4.3 and 4.4). Taken together, all of the results suggested that *MCK1* locates at downstream of *MPK1* MAPK cascade was a likely molecular target of 5-OH-3,7-DMF in the  $\text{Ca}^{2+}$ -signaling pathways in yeast. The *MCK1* gene was genetically defined as a signaling component that acts in the downstream of the Mpk1 MAPK pathway. According to this pathway, all of the known  $\text{Ca}^{2+}$ -related phenotypes exhibited by the  $\Delta zds1$  strain were alleviated by the  $\Delta mck1$  mutation (Mizunuma et al. 2001) seemingly the inhibition of overexpressed *MCK1* by 5-OH-3,7-DMF.

The *MCK1* gene in yeast encodes a human glycogen synthase Kinase-3 (GSK-3) family protein Kinase (Andoh et al., 2000). Four of GSK-3 family protein Kinase homologs identified in the yeast genome, the other Kinases of this family (*MDS1*, *YGK3*, and *MRK1*) appear to contribute only trivially to this signaling pathway (Neugeborn and Mitchell 1991). Shitamukai et al. (2000) demonstrated that Mck1 protein promotes the  $\text{Ca}^{2+}$ -induced degradation of Hsl1 protein, an inhibitory Kinase of Swe1 protein. Hsl1 contains several potential phosphorylation sites known as the consensus sequence for the GSK-3 $\beta$  phosphorylation sites (Plyte et al. 1992). The GSK-3 functions by phosphorylating a serine or threonine residue on its target substrate. GSK-3 has been implicated in a number of diseases, including type 2 diabetes mellitus (T2DM). Moreover, the activity of GSK-3 has also been associated with both pathological features of Alzheimer's disease, namely the buildup of Amyloid- $\beta$  ( $\text{A}\beta$ ) deposits and the formation of neurofibrillary tangles by hyperphosphorylation of tau proteins (Jope et al. 2007). In addition, GSK-3 also involves in inflammation, cancer, and bipolar disorder. Hence, 5-OH-3,7-DMF might be a useful functional bioactive compound for future drug development. Several bioactive compounds have been reported in effectiveness as a potential GSK-3 $\beta$  inhibitor. Yoshida et al. (2013) identified an active compound as falcarindiol from some Apiaceae vegetables, especially Japanese parsley (*Oenanthe javanica*) using the mutant yeast YNS17 strain (*zds1 $\Delta$  erg3 $\Delta$  pdr1 $\Delta$  pdr3 $\Delta$* ) was discovered as an inhibitor of glycogen synthase Kinase-3 $\beta$  (GSK-3 $\beta$ ). Falcarindiol inhibited GSK-3 $\beta$  in an ATP non-competitive manner with a  $K_i$  value of 86.9  $\mu\text{M}$  and also suppressed gene expression of glucose-6-phosphatase (G6Pase) in rat hepatoma H42E (Yoshida et al. 2013).

Due to the fact that human *GSK-3 $\beta$*  is an ortholog gene of yeast *MCK1*, this study characterized the enzyme inhibitory activity (*in vitro*) on recombinant GSK-3 $\beta$  of 5-OH-3,7-DMF using the Kinase Glo<sup>®</sup> Plus luminescent Kinase assay platform. 5-OH-3,7-DMF strongly inhibited GSK-3 $\beta$  activity with an IC<sub>50</sub> value of 9.72  $\pm$  0.15  $\mu$ M (Figure 4.12 (a.)) with an ATP-noncompetitive binding mode by Dixon plot (K<sub>i</sub> = 13.04  $\mu$ M) (figure 4.14 (a.)), but a substrate competitive binding mode to GSK-3 $\beta$  with by Dixon plot (K<sub>i</sub> = 53.92  $\mu$ M) (figure 4.14 (b.)). These results demonstrated that 5-OH-3,7-DMF is a novel ATP-noncompetitive GSK-3 $\beta$  inhibitor dose not interacts with the ATP-binding pocket instead with the substrate binding site. The substrate competitive inhibitors are expected to be more specific and safer and resulting in less toxic effects than ATP-competitive inhibitors. Thus, the 5-OH-3,7-DMF might be a useful functional compound which exists in *K. parviflora*, Thai herbs, expected to prevent type 2 diabetes (T2DM), Alzheimer's disease and inflammation.

In addition to GSK-3 which have a role in regulating glycogen synthase, GSK-3 has also been implicated in other aspects of glucose homeostasis, including the phosphorylation of insulin receptor (IRS1), as one of potential inhibitory mechanism for insulin resistance in T2DM (Lieberman and Eldar-Finkelman 2005) and involved in activation of the hepatic gluconeogenesis through the modulation of the gluconeogenic enzymes, phosphoenolpyruvate carboxykinase (PEPCK) and glucose 6 phosphatase (G6Pase) (Lochhead et al. 2001). According to insulin induces the inhibition of GSK-3, small molecules that inhibit this protein kinase possibly expected to mimic some of the actions of insulin, such as its ability to activate glycogen synthase and stimulate the conversion of glucose to glycogen leading to lowering blood glucose by inhibiting the production of glucose by the liver (Cohen and Goedert 2004).

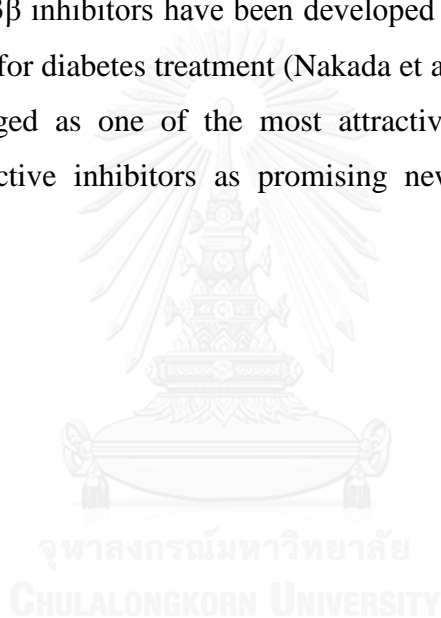
The result from this study, treatment of insulin-resistant HepG2 cells model with either CE or 5-OH-3,7-DMF led to a comparable decrease in G6Pase gene expression in a dose-dependent manner as compared to both of positive controls; GSK-3 $\beta$  Inhibitor I and LiCl, GSK-3 inhibitor on clinical trials (Cole et al. 2014). LiCl reduced G6Pase expression at 10 mM (Figure 4.16). Interestingly, CE (as low as 15  $\mu$ g/mL) and 5-OH-3,7-DMF (as low as 15.3  $\mu$ M) showed high effectiveness on the reduction of gluconeogenesis gene expression G6Pase than the LiCl (10 mM) and

GSK-3 $\beta$  Inhibitor I (20  $\mu$ M), positive controls either pre-treatment or post-treatment. Moreover 5-OH-3,7-DMF could restore glycogen levels (Figure 4.17) in insulin-resistant HepG2 cells through impairing phosphorylation of glycogen synthase protein (GS) (Figure 4.18). According to the normal insulin signaling state, insulin receptor substrate-1/-2 (IRS-1/-2) are readily in tyrosine phosphorylated by insulin receptor (IR) depend on stimulation of insulin (Klover and Mooney 2004). Although, it has been reported that the involvement of serine phosphorylation of IRS-1 in the desensitization of insulin caused elevation of GSK-3 by chronic high glucose treatment (Nakajima et al. 2000). In this regard, 5-OH-3,7-DMF treatment might prevented the increase in P-(Ser636/639) IRS-1 induced by elevation of GSK-3 in HGHI medium. Then, subsequently activation AKT pathways leading to activation of phosphorylation of 5' adenosine monophosphate-activated protein kinase (AMPK), the regulator of PEPCK and G6Pase expression. Likewise, Cordero-Herrera et al. (2014) reported that pre-treatment of HepG2 cells, evoked by the high glucose incubation, with cocoa extract and cocoa polyphenolic extract (its main flavonoids) repressed levels of PEPCK, one of gluconeogenesis and enhanced glucose production via activated p-AMPK leading to recovere glycogen content. Therefore, CE containing 11 flavonoid compounds that some of them might be enhance in inhibition of *G6Pase* expression. It have been reported that after type 2 diabetic mice administrated with CE showed the lowering blood glucose level (Akase et al. 2011; Promson and Puntheeranurak 2014; Toda et al. 2016). Thus, these results suggested that CE and 5-OH-3,7-DMF might be a novel compound for modulating the glucose homeostasis in type 2 diabetes disease (Figure 4.16 - 4.18).

In a situation of hepatic insulin resistance phosphorylation of AKT and its downstream effectors, GSK-3, decreased and leading to increase in phosphorylation levels of GS (Klover and Mooney 2004). The involvement of GSK-3 in diabetes was further demonstrated in two model systems: in fat tissue of obese diabetic mice, where GSK-3 activity was found to be two fold higher than in control mice (Eldar-Finkelman et al. 1999a) and in skeletal muscle of patients with T2DM, where GSK-3 activity and expression levels were significantly higher than in healthy individuals (Nikoulina et al. 2000). Thus, in insulin-sensitive tissue directly involved in the pathogenesis of T2DM, phosphorylation of GSK-3 was abolished when cells

were treated with 5-OH-37-DMF to the same extent comparable values to those of controls when cells were incubated with HGHI medium (Figure 4.19). However, the CE showed slightly enhances this impairment only at post-treatment.

Taken together, all of the results indicated that 5-OH-3,7-DMF might be a potential GSK-3 inhibitor (Figure 4.14) that possibly mimic some of the actions of insulin signaling, such as its ability to activate glycogen synthase (Figure 4.17) and stimulate the conversion of glucose to glycogen (Figure 4.18) that lead to lower blood glucose by inhibiting the production of glucose by the liver. Some GSK-3 inhibitors have recently been reported to lower blood glucose levels *in vivo* (Norman 2001). Several potent GSK-3 $\beta$  inhibitors have been developed by pharmaceutical companies in preclinical models for diabetes treatment (Nakada et al. 2011). Consequently, GSK-3 has recently emerged as one of the most attractive therapeutic targets for the development of selective inhibitors as promising new drugs for type 2 diabetes diseases.



## 5.2 Conclusion

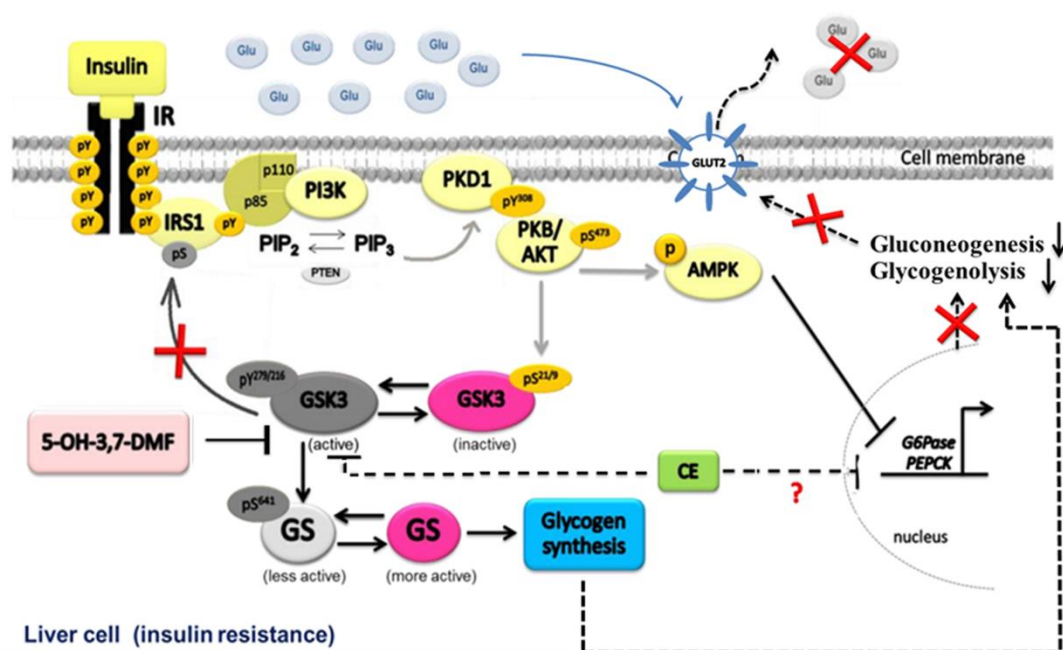


**Figure 5.1** Proposed model on mechanism of 5-OH-3,7-DMF on inhibitory activity of GSK-3 in insulin-resistant HepG2 cell model. The symbols as follow;  $\perp$  represent inhibition,  $\uparrow$  represent activation and  $\times$  represent interception.

In this study 5-OH-3,7-DMF from *K. parviflora* Well ex. Baker alleviated the G2/M cell-cycle delay in the  $\Delta zds1$  yeast-based assay (Boonkerd et al. 2014). This study further characterized the biological activity of the 5-OH-3,7-DMF on  $\Delta zds1$  yeast-based assay to investigating the molecular target in  $Ca^{2+}$ -signaling pathways and characterize the biochemical activity of 5-OH-3,7-DMF in inhibition of GSK-3 $\beta$  activity *in vitro* and investigate the role of 5-OH-3,7-DMF and *K. parviflora* crude extract (CE) against insulin restraint HepG2 cell line as a type 2 diabetes cell model. The results could be concluded as follows;

1) *MCK1* a molecule downstream of *MPK1* was a likely molecular target of 5-OH-3,7-DMF in the  $Ca^{2+}$ -signaling pathways in yeast.

2) 5-OH-3,7-DMF strongly inhibited GSK-3 $\beta$  (a human ortholog of yeast *Mck1*) activity *in vitro* with an  $IC_{50}$  value of  $9.72 \pm 0.15 \mu M$  in an ATP-noncompetitive binding mode but substrate competitive binding mode. The substrate competitive inhibitor is expected to be more specific and safer and resulting in less

toxic effects than the ATP-competitive inhibitors thus, might be a useful functional compound for T2DM drug development.

3) 5-OH-3,7-DMF exhibited no cytotoxic to yeast cells with highest concentration of (500  $\mu$ M; Figure 4.1 (a.) and (b.)) and up to 62.5  $\mu$ M in the HepG2 (Fig 4.15 (b.)).

4) In the study on the effect of 5-OH-3,7-DMF in insulin-resistance HepG2 cell model, 5-OH-DMF decreased the level of *G6Pase* expression (Figure 4.16). This might be through the inhibition of p-Ser-IRS and resulting in activation of the AKT pathway (Eldar-Finkelman et al. 1999b). Moreover 5-OH-3,7-DMF could recovered glycogen content to the same level as that of the two known GSK-3 inhibitors (LiCl and GSK-3 $\beta$  inhibitor I) through GSK-3 inhibition (Figure 4.18). CE could decrease in the level of *G6Pase* expression but did not recover glycogen content. Besides, 5-OH-3,7-DMF, the CE contained at least 11 flavonoid compounds that some of them might also enhance in the inhibition of G6Pase expression. The effect of CE on anti-T2DM in the HepG2 model was supported by the reports that after type 2 diabetic mice administrated with CE showed the lowering blood glucose level (Akase et al. 2011; Promson and Puntheeranurak 2014; Toda et al. 2016). Thus, CE could possibly be used as food supplement for modulating glucose homeostasis.

5) The phosphorylation of GSK-3 were abolished in 5-OH-3,7-DMF treated HepG2 cells cultivated in HGHI condition to the same extent comparable to those of the known GSK3 inhibitors, LiCl and GSK3 $\beta$  inhibitor I in both pre- and post-treatments. On the other hand, CE which contained approximately 2% of 5-OH-3,7-DMF, slightly enhanced this impairment and the effect could only be observed at post-treatment.

The mechanism of action of 5-OH-3,7-DMF and CE were proposed on figure 5.1. Taken together, all of these results indicated that 5-OH-3,7-DMF might be a potential GSK-3 inhibitor that possibly mimic some of the actions of insulin signaling and might be useful for future development of GSK3 $\beta$  selective inhibitors as a promising new drugs for type 2 diabetes.

## REFERENCES

- Akase, T., Shimada, T., Terabayashi, S., Ikeya, Y., Sanada, H., and Aburada, M. (2011). "Antiobesity effects of *Kaempferia parviflora* in spontaneously obese type II diabetic mice." *Journal of Natural Medicines*, 65(1), 73-80.
- Andoh, T., Hirata, Y., and Kikuchi, A. (2000). "Yeast glycogen synthase kinase 3 is involved in protein degradation in cooperation with Bul1, Bul2, and Rsp5." *Molecular and Cellular Biology*, 20(18), 6712-20.
- Azuma, T., Kayano, S.-i., Matsumura, Y., Konishi, Y., Tanaka, Y., and Kikuzaki, H. (2011). "Antimutagenic and  $\alpha$ -glucosidase inhibitory effects of constituents from *Kaempferia parviflora*." *Food chemistry*, 125(2), 471-475.
- Banjerdpongchai, R., Suwannachot, K., Rattanapanone, V., and Sripanidkulchai, B. (2008). "Ethanollic rhizome extract from *Kaempferia parviflora* Wall. ex. Baker induces apoptosis in HL-60 cells." *Asian Pacific Journal of Cancer Prevention*, 9(4), 595-600.
- Barral, Y., Parra, M., Bidlingmaier, S., and Snyder, M. (1999). "Nim1-related kinases coordinate cell cycle progression with the organization of the peripheral cytoskeleton in yeast." *Genes & Development*, 13(2), 176-187.
- Beurel, E., and Jope, R. S. (2010). "Glycogen synthase kinase-3 regulates inflammatory tolerance in astrocytes." *Neuroscience*, 169(3), 1063-1070.
- Bi, E., and Pringle, J. R. (1996). "ZDS1 and ZDS2, genes whose products may regulate Cdc42p in *Saccharomyces cerevisiae*." *Molecular and Cellular Biology*, 16(10), 5264-5275.
- Bogoyevitch, M. A. (2005). "Therapeutic promise of JNK ATP-noncompetitive inhibitors." *Trends in Molecular Medicine*, 11(5), 232-239.
- Booher, R. N., Deshaies, R. J., and Kirschner, M. W. (1993). "Properties of *Saccharomyces cerevisiae* wee1 and its differential regulation of p34CDC28 in response to G1 and G2 cyclins." *The EMBO journal*, 12(9), 3417.
- Boonkerd, S., Yompakdee, C., Miyakawa, T., and Chavasiri, W. (2011). "Screening of Thai medicinal plants for inhibitor of  $Ca^{2+}$ -signaling using a yeast cell growth-based assay." *Research Journal of Pharmaceutical, Biological and Chemical Sciences*, 2, 549-557.

- Boonkerd, S., Yompakdee, C., Miyakawa, T., and Chavasiri, W. (2014). "A flavonoid, 5-hydroxy-3, 7-dimethoxyflavone, from *Kaempferia parviflora* Wall. Ex. Baker as an inhibitor of Ca<sup>2+</sup> signal-mediated cell-cycle regulation in yeast." *Annals of Microbiology*, 64(3), 1049-1054.
- Chanklan, R., Aihara, E., Koga, S., Takahashi, H., Mizunuma, M., and Miyakawa, T. (2008). "Inhibition of Ca<sup>2+</sup>-signal-dependent growth regulation by radicicol in budding yeast." *Bioscience, Biotechnology, and Biochemistry*, 72(1), 132-138.
- Chen, E. Y., DeRan, M. T., Ignatius, M. S., Grandinetti, K. B., Clagg, R., McCarthy, K. M., Lobbardi, R. M., Brockmann, J., Keller, C., and Wu, X. (2014). "Glycogen synthase kinase 3 inhibitors induce the canonical WNT/ $\beta$ -catenin pathway to suppress growth and self-renewal in embryonal rhabdomyosarcoma." *Proceedings of the National Academy of Sciences*, 111(14), 5349-5354.
- Cheng, K., Creacy, S., and Lerner, J. (1983). "'Insulin-like' effects of lithium ion on isolated rat adipocytes II. Specific activation of glycogen synthase." *Molecular and Cellular Biochemistry*, 56(2), 183-189.
- Chomchalow, N., Bansiddhi, J., and MacBaine, C. (2003). *Amazing Thai medicinal plants*, Horticultural Research Institute (HRI), Bangkok: Department of Agricultural, and Horticultural Science Society of Thailand (HSST).
- Clapham, D. E. (1995). "Calcium signaling." *Cell*, 80(2), 259-68.
- Coghlan, M. P., Culbert, A. A., Cross, D. A., Corcoran, S. L., Yates, J. W., Pearce, N. J., Rausch, O. L., Murphy, G. J., Carter, P. S., and Cox, L. R. (2000). "Selective small molecule inhibitors of glycogen synthase kinase-3 modulate glycogen metabolism and gene transcription." *Chemistry & Biology*, 7(10), 793-803.
- Cohen, P., and Frame, S. (2001). "The renaissance of GSK3." *Nature Reviews Molecular Cell Biology*, 2(10), 769-76.
- Cohen, P., and Goedert, M. (2004). "GSK3 inhibitors: development and therapeutic potential." *Nature Reviews Drug Discovery*, 3(6), 479-487.



- Cole, E. L., Shao, X., Sherman, P., Quesada, C., Fawaz, M. V., Desmond, T. J., and Scott, P. J. (2014). "Synthesis and evaluation of [11 C] PyrATP-1, a novel radiotracer for PET imaging of glycogen synthase kinase-3 $\beta$  (GSK-3 $\beta$ )." *Nuclear Medicine and Biology*, 41(6), 507-512.
- Cordero-Herrera, I., Martin, M. A., Goya, L., and Ramos, S. (2014). "Cocoa flavonoids attenuate high glucose-induced insulin signalling blockade and modulate glucose uptake and production in human HepG2 cells." *Food and Chemical Toxicology*, 64, 10-9.
- Davies, S. P., Reddy, H., Caivano, M., and Cohen, P. (2000). "Specificity and mechanism of action of some commonly used protein kinase inhibitors." *Biochemical Journal*, 351(1), 95-105.
- DeFronzo, R. A., Ferrannini, E., Groop, L., Henry, R. R., Herman, W. H., Holst, J. J., Hu, F. B., Kahn, C. R., Raz, I., and Shulman, G. I. (2014). "Type 2 diabetes mellitus." *Nature Reviews. Disease Primers*, 1, 15019-15019.
- Dewhurst, S., Maggirwar, S. B., Schifitto, G., Gendelman, H. E., and Gelbard, H. A. (2007). "Glycogen synthase kinase 3 beta (GSK-3 $\beta$ ) as a therapeutic target in neuroAIDS." *Journal of Neuroimmune Pharmacology*, 2(1), 93-96.
- Doble, B. W., and Woodgett, J. R. (2003). "GSK-3: tricks of the trade for a multi-tasking kinase." *Journal of Cell Science*, 116(7), 1175-1186.
- Eldar-Finkelman, H., and Martinez, A. (2011). "GSK-3 Inhibitors: Preclinical and Clinical Focus on CNS." *Frontiers in Molecular Neuroscience*, 4, 32.
- Eldar-Finkelman, H., Schreyer, S. A., Shinohara, M. M., LeBoeuf, R. C., and Krebs, E. G. (1999a). "Increased glycogen synthase kinase-3 activity in diabetes- and obesity-prone C57BL/6J mice." *Diabetes*, 48(8), 1662-6.
- Eldar-Finkelman, H., Schreyer, S. A., Shinohara, M. M., LeBoeuf, R. C., and Krebs, E. G. (1999b). "Increased glycogen synthase kinase-3 activity in diabetes- and obesity-prone C57BL/6J mice." *Diabetes*, 48(8), 1662-1666.
- Embi, N., Rylatt, D. B., and Cohen, P. (1980). "Glycogen synthase kinase-3 from rabbit skeletal muscle. Separation from cyclic-AMP-dependent protein kinase and phosphorylase kinase." *European Journal of Biochemistry*, 107(2), 519-27.

- Espinal, M. A., Laszlo, A., Simonsen, L., Boulahbal, F., Kim, S. J., Reniero, A., Hoffner, S., Rieder, H. L., Binkin, N., and Dye, C. (2001). "Global trends in resistance to antituberculosis drugs." *New England Journal of Medicine*, 344(17), 1294-1303.
- Foskett, J. K., White, C., Cheung, K. H., and Mak, D. O. (2007). "Inositol trisphosphate receptor  $Ca^{2+}$  release channels." *Physiological Reviews*, 87(2), 593-658.
- García, I., Fall, Y., Gómez, G., and González-Díaz, H. (2011). "First computational chemistry multi-target model for anti-Alzheimer, anti-parasitic, anti-fungi, and anti-bacterial activity of GSK-3 inhibitors *in vitro*, *in vivo*, and in different cellular lines." *Molecular Diversity*, 15(2), 561-567.
- Gardner, T. B., Coelho-Prabhu, N., Gordon, S. R., Gelrud, A., Maple, J. T., Papachristou, G. I., Freeman, M. L., Topazian, M. D., Attam, R., Mackenzie, T. A., and Baron, T. H. (2011). "Direct endoscopic necrosectomy for the treatment of walled-off pancreatic necrosis: results from a multicenter U.S. series." *Gastrointest Endosc*, 73(4), 718-26.
- Garrett-Engele, P., Moilanen, B., and Cyert, M. S. (1995). "Calcineurin, the  $Ca^{2+}$ /calmodulin-dependent protein phosphatase, is essential in yeast mutants with cell integrity defects and in mutants that lack a functional vacuolar H (+)-ATPase." *Molecular and Cellular Biology*, 15(8), 4103-4114.
- Ginsberg, H. N. (2000). "Insulin resistance and cardiovascular disease." *The Journal of Clinical Investigation*, 106(4), 453-8.
- Guariguata, L., Linnenkamp, U., Beagley, J., Whiting, D. R., and Cho, N. H. (2014). "Global estimates of the prevalence of hyperglycaemia in pregnancy." *Diabetes Research and Clinical Practice*, 103(2), 176-85.
- Hicks, J. W., VanBrocklin, H. F., Wilson, A. A., Houle, S., and Vasdev, N. (2010). "Radiolabeled small molecule protein kinase inhibitors for imaging with PET or SPECT." *Molecules*, 15(11), 8260-8278.
- Hoeflich, K. P., Luo, J., Rubie, E. A., Tsao, M.-S., Jin, O., and Woodgett, J. R. (2000). "Requirement for glycogen synthase kinase-3 $\beta$  in cell survival and NF- $\kappa$ B activation." *Nature*, 406(6791), 86-90.

- International, F. D. (2015). *the IDF Diabetes Atlas 7<sup>th</sup> edition*, Brussels, Belgium: International Diabetes Federation, 2015.
- Jope, R. S., Yuskaitis, C. J., and Beurel, E. (2007). "Glycogen synthase kinase-3 (GSK3): inflammation, diseases, and therapeutics." *Neurochemical Research*, 32(4-5), 577-95.
- Kang, L. J., Lee, H. B., Bae, H. J., and Lee, S. G. (2010). "Antidiabetic effect of propolis: reduction of expression of glucose-6-phosphatase through inhibition of Y279 and Y216 autophosphorylation of GSK-3 $\alpha/\beta$  in HepG2 cells." *Phytotherapy research*, 24(10), 1554-1561.
- Klein, P. S., and Melton, D. A. (1996). "A molecular mechanism for the effect of lithium on development." *Proceedings of the National Academy of Sciences*, 93(16), 8455-8459.
- Klover, P. J., and Mooney, R. A. (2004). "Hepatocytes: critical for glucose homeostasis." *The International Journal of Biochemistry & Cell Biology*, 36(5), 753-8.
- Kuemmerle, J. F. (2005). "Endogenous IGF-I protects human intestinal smooth muscle cells from apoptosis by regulation of GSK-3 $\beta$  activity." *American Journal of Physiology-Gastrointestinal and Liver Physiology*, 288(1), G101-G110.
- Kummee, S., Tewtrakul, S., and Subhadhirasakul, S. (2008). "Antimicrobial activity of the ethanol extract and compounds from the rhizomes of *Kaempferia parviflora*." *Songklanakarinn Journal of Science & Technology*, 30(4).
- Laemmli, U., Amos, L., and Klug, A. (1976). "Correlation between structural transformation and cleavage of the major head protein of T4 bacteriophage." *Cell*, 7(2), 191-203.
- Leardkamolkarn, V., Tiomyuyen, S., and Sripanidkulchai, B.-o. (2009). "Pharmacological activity of *Kaempferia parviflora* extract against human bile duct cancer cell lines." *Asian Pacific Journal of Cancer Prevention*, 10, 695-698.

- Leclerc, S., Garnier, M., Hoessel, R., Marko, D., Bibb, J. A., Snyder, G. L., Greengard, P., Biernat, J., Wu, Y.-Z., and Mandelkow, E.-M. (2001). "Indirubins inhibit glycogen synthase kinase-3 $\beta$  and CDK5/p25, two protein kinases involved in abnormal tau phosphorylation in Alzheimer's disease a property common to most cyclin-dependent kinase inhibitors." *Journal of Biological Chemistry*, 276(1), 251-260.
- Leost, M., Schultz, C., Link, A., Wu, Y. Z., Biernat, J., Mandelkow, E. M., Bibb, J. A., Snyder, G. L., Greengard, P., and Zaharevitz, D. W. (2000). "Paullones are potent inhibitors of glycogen synthase kinase-3 $\beta$  and cyclin-dependent kinase 5/p25." *European Journal of Biochemistry*, 267(19), 5983-5994.
- Li, D. W., Liu, Z. Q., Chen, W., Yao, M., and Li, G. R. (2014). "Association of glycogen synthase kinase-3 $\beta$  with Parkinson's disease (Review)." *Molecular Medicine Reports*, 9(6), 2043-2050.
- Liberman, Z., and Eldar-Finkelman, H. (2005). "Serine 332 phosphorylation of insulin receptor substrate-1 by glycogen synthase kinase-3 attenuates insulin signaling." *The Journal of Biological Chemistry*, 280(6), 4422-8.
- Lim, N. K., Hung, L. W., Pang, T. Y., Mclean, C. A., Liddell, J. R., Hilton, J. B., Li, Q.-X., White, A. R., Hannan, A. J., and Crouch, P. J. (2014). "Localized changes to glycogen synthase kinase-3 and collapsin response mediator protein-2 in the Huntington's disease affected brain." *Human Molecular Genetics*, 23(15), 4051-4063.
- Llorens-Marín, M., Jurado, J., Hernández, F., and Ávila, J. (2014). "GSK-3 $\beta$ , a pivotal kinase in Alzheimer disease." *Frontiers in Molecular Neuroscience*, 7, 46.
- Lochhead, J., and Thompson, G. M. (2001). "Bilateral papilloedema with concomitant neuroretinitis in a 7-year-old girl with Lyme disease." *Eye (Lond)*, 15(Pt 6), 799-801.
- Lochhead, P. A., Coghlan, M., Rice, S. Q., and Sutherland, C. (2001). "Inhibition of GSK-3 selectively reduces glucose-6-phosphatase and phosphatase and phosphoenolpyruvate carboxykinase gene expression." *Diabetes*, 50(5), 937-46.

- Ma, X.-J., Lu, Q., and Grunstein, M. (1996). "A search for proteins that interact genetically with histone H3 and H4 amino termini uncovers novel regulators of the Swe1 kinase in *Saccharomyces cerevisiae*." *Genes & Development*, 10(11), 1327-1340.
- Mager, W. H., and De Kruijff, A. J. (1995). "Stress-induced transcriptional activation." *Microbiological Reviews*, 59(3), 506-31.
- Mager, W. H., and Winderickx, J. (2005). "Yeast as a model for medical and medicinal research." *Trends in Pharmacological Sciences*, 26(5), 265-73.
- Malakul, W., Thirawarapan, S., Ingkaninan, K., and Sawasdee, P. (2011). "Effects of *Kaempferia parviflora* Wall. Ex Baker on endothelial dysfunction in streptozotocin-induced diabetic rats." *Journal of Ethnopharmacology*, 133(2), 371-377.
- Manning, G., Whyte, D. B., Martinez, R., Hunter, T., and Sudarsanam, S. (2002). "The protein kinase complement of the human genome." *Science*, 298(5600), 1912-1934.
- McQueen, J., van Dyk, D., Young, B., Loewen, C., and Measday, V. (2012). "The Mck1 GSK-3 kinase inhibits the activity of Clb2-Cdk1 post-nuclear division." *Cell Cycle*, 11(18), 3421-3432.
- Meijer, L., Skaltsounis, A.-L., Magiatis, P., Polychronopoulos, P., Knockaert, M., Leost, M., Ryan, X. P., Vonica, C. A., Brivanlou, A., and Dajani, R. (2003). "GSK-3-selective inhibitors derived from Tyrian purple indirubins." *Chemistry & Biology*, 10(12), 1255-1266.
- Meijer, L., Thunnissen, A.-M., White, A., Garnier, M., Nikolic, M., Tsai, L., Walter, J., Cleverley, K., Salinas, P., and Wu, Y. (2000). "Inhibition of cyclin-dependent kinases, GSK-3 $\beta$  and CK1 by hymenialdisine, a marine sponge constituent." *Chemistry & Biology*, 7(1), 51-63.
- Miyakawa, T., and Mizunuma, M. (2007). "Physiological roles of calcineurin in *Saccharomyces cerevisiae* with special emphasis on its roles in G2/M cell-cycle regulation." *Bioscience, Biotechnology, and Biochemistry*, 71(3), 633-45.

- Mizunuma, M., Hirata, D., Miyahara, K., Tsuchiya, E., and Miyakawa, T. (1998). "Role of calcineurin and Mpk1 in regulating the onset of mitosis in budding yeast." *Nature*, 392(6673), 303-6.
- Mizunuma, M., Hirata, D., Miyaoka, R., and Miyakawa, T. (2001). "GSK-3 kinase Mck1 and calcineurin coordinately mediate Hsl1 down-regulation by Ca<sup>2+</sup> in budding yeast." *The EMBO Journal*, 20(5), 1074-85.
- Mizunuma, M., Miyamura, K., Hirata, D., Yokoyama, H., and Miyakawa, T. (2004). "Involvement of S-adenosylmethionine in G1 cell-cycle regulation in *Saccharomyces cerevisiae*." *Proceedings of the National Academy of Sciences of the United States of America*, 101(16), 6086-6091.
- Nakada, M., Minamoto, T., Pyko, I. V., Hayashi, Y., and Hamada, J. (2011). "The pivotal roles of GSK3 $\beta$  in glioma biology", *Molecular Targets of CNS Tumors*. InTech.
- Nakajima, K., Yamauchi, K., Shigematsu, S., Ikeo, S., Komatsu, M., Aizawa, T., and Hashizume, K. (2000). "Selective attenuation of metabolic branch of insulin receptor down-signaling by high glucose in a hepatoma cell line, HepG2 cells." *Journal of Biological Chemistry*, 275(27), 20880-20886.
- Nakamura, T., Ohmoto, T., Hirata, D., Tsuchiya, E., and Miyakawa, T. (1996). "Genetic evidence for the functional redundancy of the calcineurin-and Mpk1-mediated pathways in the regulation of cellular events important for growth in *Saccharomyces cerevisiae*." *Molecular and General Genetics MGG*, 251(2), 211-219.
- Nakamura, T., Ohmoto, T., Hirata, D., Tsuchiya, E., and Miyakawa, T. (1997). "Yeast Crv4/Ttp1, a predicted type II membrane protein, is involved in an event important for growth, functionally overlapping with the event regulated by calcineurin-and Mpk1-mediated pathways." *Molecular and General Genetics MGG*, 256(5), 481-487.
- Nanditha, A., Ma, R. C., Ramachandran, A., Snehalatha, C., Chan, J. C., Chia, K. S., Shaw, J. E., and Zimmet, P. Z. (2016). "Diabetes in Asia and the Pacific: implications for the global epidemic." *Diabetes Care*, 39(3), 472-485.

- Neigeborn, L., and Mitchell, A. P. (1991). "The yeast MCK1 gene encodes a protein kinase homolog that activates early meiotic gene expression." *Genes & Development*, 5(4), 533-48.
- Nikoulina, S. E., Ciaraldi, T. P., Mudaliar, S., Mohideen, P., Carter, L., and Henry, R. R. (2000). "Potential role of glycogen synthase kinase-3 in skeletal muscle insulin resistance of type 2 diabetes." *Diabetes*, 49(2), 263-71.
- Norman, P. (2001). "Emerging fundamental themes in modern medicinal chemistry." *Drug News Perspect*, 14(4), 242.
- Pandey, M. K., and DeGrado, T. R. (2016). "Glycogen synthase kinase-3 (GSK-3)-targeted therapy and imaging." *Theranostics*, 6(4), 571.
- Paquet, D., Bhat, R., Sydow, A., Mandelkow, E.-M., Berg, S., Hellberg, S., Fälting, J., Distel, M., Köster, R. W., and Schmid, B. (2009). "A zebrafish model of tauopathy allows in vivo imaging of neuronal cell death and drug evaluation." *The Journal of Clinical Investigation*, 119(5), 1382-1395.
- Patanasethanont, D., Nagai, J., Matsuura, C., Fukui, K., Sutthanut, K., Sripanidkulchai, B.-o., Yumoto, R., and Takano, M. (2007). "Modulation of function of multidrug resistance associated-proteins by *Kaempferia parviflora* extracts and their components." *European Journal of Pharmacology*, 566(1), 67-74.
- Peat, A. J., Boucheron, J. A., Dickerson, S. H., Garrido, D., Mills, W., Peckham, J., Preugschat, F., Smalley, T., Schweiker, S. L., and Wilson, J. R. (2004). "Novel pyrazolopyrimidine derivatives as GSK-3 inhibitors." *Bioorganic & Medicinal Chemistry Letters*, 14(9), 2121-2125.
- Phiel, C. J., and Klein, P. S. (2001). "Molecular targets of lithium action." *Annual Review of Pharmacology and Toxicology*, 41(1), 789-813.
- Plyte, S. E., Hughes, K., Nikolakaki, E., Pulverer, B. J., and Woodgett, J. R. (1992). "Glycogen synthase kinase-3: functions in oncogenesis and development." *Biochimica et Biophysica Acta* 1114(2-3), 147-62.

- Polychronopoulos, P., Magiatis, P., Skaltsounis, A.-L., Myrianthopoulos, V., Mikros, E., Tarricone, A., Musacchio, A., Roe, S. M., Pearl, L., and Leost, M. (2004). "Structural basis for the synthesis of indirubins as potent and selective inhibitors of glycogen synthase kinase-3 and cyclin-dependent kinases." *Journal of Medicinal Chemistry*, 47(4), 935-946.
- Promson, N., and Puntheeranurak, S. (2014). "*Kaempferia parviflora* extract diminishes hyperglycemia and visceral fat accumulation in mice fed with high fat and high sucrose diet." *The Journal of Physiology*, 27(1), 13-19.
- Putiyanan, S., Chansakaow, S., Phrutivorapongkul, A., and Charoensup, W. (2008). "Standard pharmacognostic characteristic of some Thai herbal medicine." *Chiang Mai University Journal of Natural of Sciences*, 7(2), 239-55.
- Roy, N., and Runge, K. W. (2000). "Two paralogs involved in transcriptional silencing that antagonistically control yeast life span." *Current Biology*, 10(2), 111-114.
- Sae-wong, C., Tansakul, P., and Tewtrakul, S. (2009). "Anti-inflammatory mechanism of *Kaempferia parviflora* in murine macrophage cells (RAW 264.7) and in experimental animals." *Journal of Ethnopharmacology*, 124(3), 576-580.
- Sawasdee, P., Sabphon, C., Sitthiwongwanit, D., and Kokpol, U. (2009). "Anticholinesterase activity of 7-methoxyflavones isolated from *Kaempferia parviflora*." *Phytotherapy Research*, 23(12), 1792-1794.
- Schwer, B., Linder, P., and Shuman, S. (1998). "Effects of deletion mutations in the yeast Ces1 protein on cell growth and morphology and on high copy suppression of mutations in mRNA capping enzyme and translation initiation factor 4A." *Nucleic Acids Research*, 26(3), 803-809.
- Sekiya-Kawasaki, M., Abe, M., Saka, A., Watanabe, D., Kono, K., Minemura-Asakawa, M., Ishihara, S., Watanabe, T., and Ohya, Y. (2002). "Dissection of upstream regulatory components of the Rho1p effector, 1, 3- $\beta$ -glucan synthase, in *Saccharomyces cerevisiae*." *Genetics*, 162(2), 663-676.
- Shero, J. H., and Hieter, P. (1991). "A suppressor of a centromere DNA mutation encodes a putative protein kinase (MCK1)." *Genes & Development*, 5(4), 549-60.



- Shitamukai, A., Mizunuma, M., Hirata, D., Takahashi, H., and Miyakawa, T. (2000). "A positive screening for drugs that specifically inhibit the Ca<sup>2+</sup>-signaling activity on the basis of the growth promoting effect on a yeast mutant with a peculiar phenotype." *Bioscience, Biotechnology, and Biochemistry*, 64(9), 1942-6.
- Stambolic, V., Ruel, L., and Woodgett, J. R. (1996). "Lithium inhibits glycogen synthase kinase-3 activity and mimics wingless signalling in intact cells." *Current Biology*, 6(12), 1664-1669.
- Sudwan, P., Saenphet, K., Saenphet, S., and Suwansirikul, S. (2005). "Effect of *Kaempferia parviflora* Wall. ex. Baker on sexual activity of male rats and its toxicity." *The Southeast Asian Journal of Tropical Medicine and Public Health*, 37, 210-215.
- Sutthanut, K., Sripanidkulchai, B., Yenjai, C., and Jay, M. (2007). "Simultaneous identification and quantitation of 11 flavonoid constituents in *Kaempferia parviflora* by gas chromatography." *Journal of Chromatography A*, 1143(1), 227-233.
- Tanaka, S., and Nojima, H. (1996). "Nik1: a Nim1-like protein kinase of *S. cerevisiae* interacts with the Cdc28 complex and regulates cell cycle progression." *Genes to Cells*, 1(10), 905-921.
- Tanti, J.-F., Gremeaux, T., Van Obberghen, E., and Le Marchand-Brustel, Y. (1994). "Serine/threonine phosphorylation of insulin receptor substrate 1 modulates insulin receptor signaling." *Journal of Biological Chemistry*, 269(8), 6051-6057.
- Tep-areenan, P., Sawasdee, P., and Randall, M. (2010). "Possible mechanisms of vasorelaxation for 5, 7-dimethoxyflavone from *Kaempferia parviflora* in the rat aorta." *Phytotherapy Research*, 24(10), 1520-1525.
- Ter Haar, E., Coll, J. T., Austen, D. A., Hsiao, H.-M., Swenson, L., and Jain, J. (2001). "Structure of GSK3 $\beta$  reveals a primed phosphorylation mechanism." *Nature Structural & Molecular Biology*, 8(7), 593-596.
- Tewtrakul, S., Subhadhirasakul, S., Karalai, C., Ponglimanont, C., and Cheenpracha, S. (2009). "Anti-inflammatory effects of compounds from *Kaempferia parviflora* and *Boesenbergia pandurata*." *Food Chemistry*, 115(2), 534-538.

- Toda, K., Takeda, S., Hitoe, S., Nakamura, S., Matsuda, H., and Shimoda, H. (2016). "Enhancement of energy production by black ginger extract containing polymethoxy flavonoids in myocytes through improving glucose, lactic acid and lipid metabolism." *Journal of Natural Medicines*, 70(2), 163-172.
- Tsuchiya, E., Matsuzaki, G., Kurano, K., Fukuchi, T., Tsukao, A., and Miyakawa, T. (1996). "The *Saccharomyces cerevisiae* SSD1 gene is involved in the tolerance to high concentration of Ca<sup>2+</sup> with the participation of HST1/NRC1/BFR1." *Gene*, 176(1), 35-38.
- Vasdev, N., Garcia, A., Stableford, W. T., Young, A. B., Meyer, J. H., Houle, S., and Wilson, A. A. (2005). "Synthesis and ex vivo evaluation of carbon-11 labelled N-(4-methoxybenzyl)-N'-(5-nitro-1,3-thiazol-2-yl) urea ([<sup>11</sup>C] AR-A014418): a radiolabelled glycogen synthase kinase-3 $\beta$  specific inhibitor for PET studies." *Bioorganic & Medicinal Chemistry Letters*, 15(23), 5270-5273.
- Viollet, B., Guigas, B., Garcia, N. S., Leclerc, J., Foretz, M., and Andreelli, F. (2012). "Cellular and molecular mechanisms of metformin: an overview." *Clinical Science*, 122(6), 253-270.
- Wangkangwan, W. (2007). *Positive screening and preliminary characterization of calcium signal inhibitor from plant extracts using Saccharomyces cerevisiae mutant.*, Thesis, Chulalongkorn University.
- Wangkangwan, W., Boonkerd, S., Chavasiri, W., Sukapirom, K., Pattanapanyasat, K., Kongkathip, N., Miyakawa, T., and Yompakdee, C. (2009). "Pinostrobin from *Boesenbergia pandurata* is an inhibitor of Ca<sup>2+</sup>-Signal-Mediated Cell-Cycle regulation in the Yeast *Saccharomyces cerevisiae*." *Bioscience, Biotechnology, and Biochemistry*, 73(7), 1679-1682.
- Wattanapitayakul, S. K., Suwatronnakorn, M., Chularojmontri, L., Herunsalee, A., Niumsakul, S., Charuchongkolwongse, S., and Chansuvanich, N. (2007). "*Kaempferia parviflora* ethanolic extract promoted nitric oxide production in human umbilical vein endothelial cells." *Journal of Ethnopharmacology*, 110(3), 559-562.

- Wattanathorn, J., Pangpookiew, P., Sripanidkulchai, K., Muchimapura, S., and Sripanidkuchai, B. (2007). "Evaluation of the anxiolytic and antidepressant effects of alcoholic extract of *Kaempferia parviflora* in aged rats." *American Journal of Agricultural and Biological Science*, 2(2), 94-98.
- Wen, X., Walle, U. K., and Walle, T. (2005). "5, 7-Dimethoxyflavone downregulates CYP1A1 expression and benzo [a] pyrene-induced DNA binding in Hep G2 cells." *Carcinogenesis*, 26(4), 803-809.
- Woodgett, J. R. (1990). "Molecular cloning and expression of glycogen synthase kinase-3/factor A." *The EMBO Journal*, 9(8), 2431-8.
- Woodgett, J. R. (2001). "Judging a protein by more than its name: GSK-3." *Science's STKE : signal transduction knowledge environment*, 100(12), 8-12.
- Woodgett, J. R., and Cohen, P. (1984). "Multisite phosphorylation of glycogen synthase: Molecular basis for the substrate specificity of glycogen synthase kinase-3 and casein kinase-II (glycogen synthase kinase-5)." *Biochimica et Biophysica Acta (BBA)-Protein Structure and Molecular Enzymology*, 788(3), 339-347.
- Wudtiwai, B., Sripanidkulchai, B., Kongtawelert, P., and Banjerdpongchai, R. (2011). "Methoxyflavone derivatives modulate the effect of TRAIL-induced apoptosis in human leukemic cell lines." *Journal of Hematology & Oncology*, 4(1), 52.
- Yenjai, C., Prasanphen, K., Daodee, S., Wongpanich, V., and Kittakoop, P. (2004). "Bioactive flavonoids from *Kaempferia parviflora*." *Fitoterapia*, 75(1), 89-92.
- Yenjai, C., Sutthanut, K., Sripanidkulchai, B., Mungkhun, N., Wongma, C., Mukdasai, S., and Kongkaew, T. (2007). "Further studies of bioactive flavonoids from *Kaempferia parviflora*." *Warasan Witthayasat Mo Kho*, 82-87.
- Yoshida, J., Seino, H., Ito, Y., Nakano, T., Satoh, T., Ogane, Y., Suwa, S., Koshino, H., and Kimura, K. (2013). "Inhibition of glycogen synthase kinase-3beta by faltarindiol isolated from Japanese Parsley (*Oenanthe javanica*)." *Journal of Agricultural and Food Chemistry*, 61(31), 7515-21.

- Yu, Y., Jiang, Y. W., Wellinger, R. J., Carlson, K., Roberts, J. M., and Stillman, D. J. (1996). "Mutations in the homologous ZDS1 and ZDS2 genes affect cell cycle progression." *Molecular and Cellular Biology*, 16(10), 5254-5263.
- Zhou, F., Xue, M., Qin, D., Zhu, X., Wang, C., Zhu, J., Hao, T., Cheng, L., Chen, X., and Bai, Z. (2013). "HIV-1 Tat promotes Kaposi's sarcoma-associated herpesvirus (KSHV) vIL-6-induced angiogenesis and tumorigenesis by regulating PI3K/PTEN/AKT/GSK-3 $\beta$  signaling pathway." *PloS One*, 8(1), e53145.



**APPENDIX**



จุฬาลงกรณ์มหาวิทยาลัย  
CHULALONGKORN UNIVERSITY

**APPENDIX A**  
**Media preparation**

**Yeast peptone dextrose (YPD)**

Yeast extract	10 g
Peptone	20 g
Glucose	20 g

Dissolved in distilled water up to 1000 mL and autoclaved at 121°C, 15 psi for 20 min.

**Yeast peptone adenine uracil dextrose broth (YPAUD broth)**

Yeast extract	10 g
Peptone	20 g
Glucose	20 g
Adenine	400 mg
Uracil	200 mg

Dissolved in distilled water up to 1000 mL and autoclaved at 121°C, 15 psi for 20 min.

**Yeast peptone adenine uracil dextrose agar (YPAUD agar)**

Yeast extract	10 g
Peptone	20 g
Glucose	20 g
Adenine	400 mg
Uracil	200 mg
Agar	20 g

Dissolved in distilled water up to 1000 mL and autoclaved at 121°C, 15 psi for 20 min.

**Synthetic complete medium (SC medium)**

Yeast nitrogen base without amino acid	6.7 g
Glucose	20 g

Distilled water 1000 mL then adjusted pH up to 4.5 with 1 N NaOH and autoclaved at 121°C, 15 psi for 20 min, then supplemented with 100 mL 10 x amino acid without uracil.

**Synthetic complete medium agar (SC medium agar)**

Yeast nitrogen base without amino acid	6.7 g
Glucose	20 g
Agar	20 g

Distilled water 1000 mL then adjusted pH up to 4.5 with 1 N NaOH and autoclaved at 121°C, 15 psi for 20 min, then supplemented with 100 mL 10 x amino acid without uracil.

**1% Raffinose YP medium**

Yeast extract	10 g
Peptone	20 g
Raffinone	10 g

Dissolved in distilled water up to 1000 mL and autoclaved at 121°C, 15 psi for 20 min.

**1% Raffinose SC medium**

Yeast nitrogen base without amino acid	6.7 g
Raffinone	10 g

Distilled water 1000 mL then adjusted pH up to 4.5 with 1 N NaOH and autoclaved at 121°C, 15 psi for 20 min, then supplemented with 100 mL 10 x amino acid without uracil.

**10% Galactose**

Galactose	10 g
ddH <sub>2</sub> O	90 mL

Autoclaved at 121°C, 15 psi for 20 min

**10 x amino acid without uracil**

Adenine sulfate	200 mg
L-Tryptophan	200 mg
L-Histidine HCl	200 mg
L-Arginine HCl	200 mg
L-Methionine	200 mg
L-Tyrosine	300 mg
L-Leucine	1,000 mg
L-Isoleucine	300 mg
L-Lysine HCl	300 mg
L-Phenylalanine	500 mg
L-Glutamic acid	1000 mg
L-Aspartic acid	1,000 mg
L-valine	1,500 mg
L-Threonine	2000 mg
L-Serine	4,000 mg

Dissolved in distilled water up to 1000 mL and autoclaved at 121°C, 15 psi for 20 min.

**RPMI-1640 medium (1X) + 2.05 mM L-Glutamine (Complete media)**

RPMI-1640 medium	90 mL
Fetal bovine serum	10 mL
Penicillin G (106 U/mL)	0.01 mL
Streptomycin (500 mg/mL)	0.05 mL
Sodium pyruvate	1 mL
HEPES	1 mL

**RPMI-1640 medium (1X) + 2.05 mM L-Glutamine (Free serum media)**

RPMI-1640 medium	90 mL
Penicillin G (106 U/mL)	0.01 mL
Streptomycin (500 mg/mL)	0.05 mL
Sodium pyruvate	1 mL
HEPES	1 mL



**RPMI freezing media**

RPMI complete media	9 mL
DMSO	1 mL

**Fetal bovine serum activation**

Fetal bovine serum (FBS) must be activated at 56°C for 30 min in water bath before use.



## APPENDIX B

### The chemical preparation

#### Enzyme Kinase assay reaction buffer

1 M Tris pH 7.5	0.4 mL
1 M MgCl <sub>2</sub>	0.2 mL
2 mg/mL BSA	0.5 mL
ddH <sub>2</sub> O	8.9 mL

#### 2% Agarose gel

Agarose (electrophoresis grade)	1 g
1X TAE	50 mL

Heated on hot plate until all agarose is dissolved (approximately 10 mins).

Reheat for several mins if necessary.

#### Ethidium Bromide Staining Solution

5 mg/mL ethidium bromide	0.1 mL
dH <sub>2</sub> O	500 mL

Stored in dark container or wrapped container in aluminum foil

#### 50X TAE buffer

Trisma base	242 g
Acetic acid	57.1 mL

Dissolve Trisma base and acetic acid in 0.5 M pH 8.0 100 mL and adjust to 1000 mL by ddH<sub>2</sub>O. Autoclaved at 121°C, 15 psi for 15 min.

#### 10% SDS

Dissolve sodium dodecyl sulfate 10 g in distilled water up to 100 mL and autoclaved at 121°C, 15 psi for 20 min.

#### 10% Ammonium persulfate (APS)

Dissolve the 0.5 g of ammonium persulfate in sterile ddH<sub>2</sub>O 5 mL. Aliquot and kept at 4°C.

**Ethanol 70%**

Ethanol 99%	700 mL
ddH <sub>2</sub> O	300 mL

**5% Stacking gel**

ddH <sub>2</sub> O	2.975 mL
40% Acrylamide	0.67 mL
1 M Tris pH 6.8	1.25 mL
10% SDS	0.05 mL
10% APS	0.05 mL
TEMED	0.005 mL

**10% Separating gel**

ddH <sub>2</sub> O	3.8 mL
40% Acrylamide	3.4 mL
1 M Tris pH 8.8	2.6 mL
10% SDS	0.1 mL
10% APS	0.1 mL
TEMED	0.01 mL

**10X Phosphate buffer saline (PBS, Ca<sup>2+</sup>, Mg<sup>2+</sup> free) pH 7.4**

NaCl	80 g
KCl	2 g
Na <sub>2</sub> HPO <sub>4</sub>	14.4 g
KH <sub>2</sub> PO <sub>4</sub>	2.4 g

Dissolve in ddH<sub>2</sub>O up to 1 l and adjusted pH up to 7.4 with 1N HCl or 1 N NaOH and autoclaved at 121°C, 15 psi for 15 min.

**MTT solution (5mg/mL)**

MTT	50 mg
ddH <sub>2</sub> O	10 mL

Dissolve MTT in ddH<sub>2</sub>O and filter by syringe filter pore size 0.45 µM. Aliquot 1 mL in microcentrifuge tube and store at 4°C.

**0.04 N HCl in isopropanol**

Add HCl 0.331 mL in 80 mL isopropanol and adjust volume to 100 mL by isopropanol.

**RIPA solution**

1 M Tris-HCl pH 7.4	0.05 mL
0.5 M NaCl	0.3 mL
20% NP-40	0.05 mL
10% Sodium deoxycholate	0.05 mL
20% SDS	0.005 mL
Phosphatase inhibitor	0.01 mL
Protease inhibitor (100X)	0.01 mL
ddH <sub>2</sub> O	525 mL

**BCA<sup>TM</sup> protein assay solution**

BCA Reagent A	50 part
BCA Reagent B	1 part

**1 M Tris pH 6.8 solution**

Dissolve trisma base 12.11 g in ddH<sub>2</sub>O 80 mL. Adjusted pH up to 6.8 with 1N HCl or 1 N NaOH and adjust volume to 100 mL. Autoclaved at 121°C, 15 psi for 15 min.

**1 M Tris pH 7.5 solution**

Dissolve trisma base 12.11 g in ddH<sub>2</sub>O 80 mL. Adjusted pH up to 7.5 with 1N HCl or 1 N NaOH and adjust volume to 100 mL. Autoclaved at 121°C, 15 psi for 15 min.

**1 M Tris pH 8.8 solution**

Dissolve trisma base 90.85 g in ddH<sub>2</sub>O 400 mL. Adjusted pH up to 8.8 with 1N HCl or 1 N NaOH and adjust volume to 500 mL. Autoclaved at 121°C, 15 psi for 15 min.

**5X Running buffer**

Trisma base	15.1 g
Glycine	94 g
SDS	5 g

Dissolve trisma base, glycine and SDS in ddH<sub>2</sub>O 800 mL and adjust to 1000 mL. Autoclaved at 121°C, 15 psi for 15 min.

**Transfer buffer**

Trisma base	15.1 g
Glycine	2.9 g
SDS	0.37 g

Dissolve trisma base, glycine and SDS in ddH<sub>2</sub>O 800 mL and autoclaved at 121°C, 15 psi for 15 min. Add absolute methanol 200 mL up to 1000 mL.

**2X loading buffer**

10% SDS	4 mL
Glycerol 87%	2.29 mL
1.0 M Tris pH 6.8	1 mL
ddH <sub>2</sub> O	2.71 mL
Bromphenol blue	0.001 g

**Staining buffer**

β-mercapto-ethanol	0.1 mL
2X loading buffer	0.9 mL

**Phosphate buffer saline tween 20 (PBST)**

1X Phosphate buffer saline	1000 mL
Tween 20	0.5 mL

**Developer and Fixer**

Developer	1 part : H <sub>2</sub> O 4 part
Fixer	1 part : H <sub>2</sub> O 4 part

**Blocking solution (5% sKim milk in PBST)**

PBST	100 mL
SKim milk	5 g

**ECL Western blot reagent**

Solution 1	2 mL
Solution 2	2 mL

**DEPC Water**

Add 0.01 mL of diethylpyrocarbonate (DEPC) in ddH<sub>2</sub>O and mix thoroughly. Let the DEPC-mixed water incubate for overnight at room temperature. Autoclave at 121°C, 15 psi for 15 min.

**70% Ethanol in DEPC water**

Absolute ethanol	70 mL
DEPC water	30 mL

**2% Agarose gel**

1X TAE buffer	20 mL
Agarose gel	0.4 g

**Ethidiumbromide solution**

Dissolve ethidiumbromide in 1X TAE buffer at final concentration 10 µg/mL and store in dark container or wrap container in aluminum foil.

**Penicillin G and streptomycin solution**

Pencillin G and streptomycin were prepared at final concentration 106 U/mL and 500 mg/mL in sterile deionized water. The solution were sterilized by filtrating passed 0.45 µm filter, aliquoted and kept at -20°C.

## APPENDIX C

### THE GLYCOGEN STANDARD CURVE

#### Glycogen Standards for Colorimetric Detection

Glycogen Standard (2.0 mg/mL) was diluted with ultrapure water to prepare a 0.2 mg/mL standard solution. Standard solution 0, 2, 4, 6, 8, and 10  $\mu\text{L}$  of the 0.2 mg/mL was added into a 96 well plate, generating 0 (assay blank), 0.4, 0.8, 1.2, 1.6, and 2.0  $\mu\text{g}/\text{well}$  of glycogen standards. The hydrolysis buffer was added to each well to bring the volume to 50  $\mu\text{L}$ . The hydrolysis enzyme mix was added 2  $\mu\text{L}$  and mixed well, incubated for 30 min at room temperature. Subsequently, the Master Reaction Mix (Development Buffer 46  $\mu\text{l}$ , Development Enzyme Mix 2  $\mu\text{l}$ , Fluorescent Peroxidase Substrate 2  $\mu\text{l}$ ) was added in volume of 50  $\mu\text{l}$  to each of the wells. Mixing well using a horizontal shaker or by pipetting and incubated the reaction for 30 min at room temperature in dark. The absorbance was measured at 570 nm.

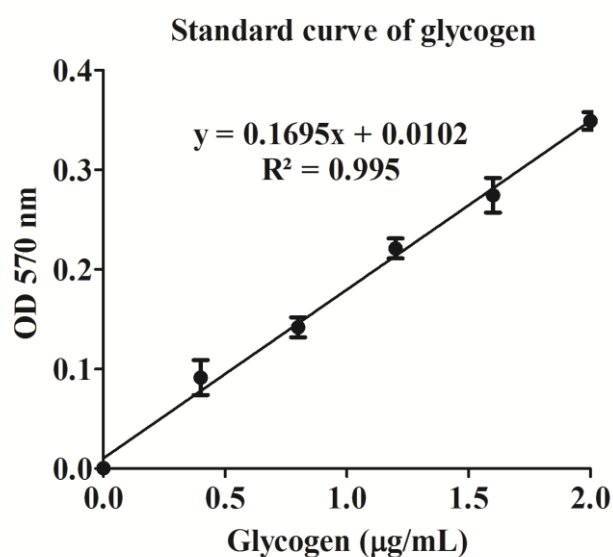


**Figure C.1** Typical glycogen standard calibration curve using colorimetric reading at OD 570 (a new standard curve must be generated for each assay performed). Curve fitting was performed using GraphPad Prism<sup>®</sup> 5 (linear regression) software.

## VITA

My name is Miss Nattanich Suanmali was born in Lumpang, Thailand on December 15, 1991. After graduation with Bachelor's degree of Science from Department of Industrial Microbiology, Faculty of Science at King Mongkut's Institute of Technology Ladkrabang in 2014, I enrolled in the Master's degree of Program in Microbiology and Microbial technology, Faculty of Science at Chulalongkorn University in 2014.

### Academic presentation

Suanmali<sup>1</sup>, N., Chavasiri, W. and Yompakdee, C. A likely molecular target of a flavonoid 5-hydroxy-3,7-dimethoxyflavone in the yeast Ca<sup>2+</sup>-signaling pathways from *Kempferia parviflora* Wall. ex. Baker. Proceeding in the 28th Annual Meeting of the Thai Society for Biotechnology and International, Chiang Mai University, Chiang Mai, Thailand 28-30 November, 2016.

Preparing the manuscript in “Identification and characterization of molecular target of a flavonoid 5-hydroxy-3,7-dimethoxyflavone from *Kempferia parviflora* Wall. ex. Baker in the yeast Ca<sup>2+</sup>-signaling pathways” and “Inhibition of GSK-3 by flavonoid compound, 5-hydroxy-3,7-dimethoxyflavone from *Kempferia parviflora* Wall. ex. Baker attenuate insulin signaling blockade and modulate glycogen production in insulin-resistance human HepG2 cells”